# “REDUCED SCALE MODEL TESTING OF COMPOSITE STRUCTURES”

Dissertation submitted as part requirement

for the Degree of Master of Science in

Structural Engineering

By

Burak Kaan CIRPICI

Supervisor:

Dr Buick DAVISON

The University of Sheffield

Department of Civil and Structural Engineering

3 September 2010

## Declaration statement

Burak Kaan CIRPICI certifies that all material contained within this dissertation is his own work except where it is clearly referenced to others.

______________________

(Signature)

Date __________________

# Abstract

The purpose of this project is to investigate a strategy for the fire testing of reduced scale structural models which will help engineers design safer structures and reduce the loss from fires. The concept of this project is how composite frame floor arrangements, beam-column connections might be modelled at a small scale suitable for fire testing.

Testing full-scale is expensive, besides the testing of scaled model produces reasonable results which help us to understand the failure mechanism and all significant thermo-structural responses involved in a fire. Thermal effects within a structural element generate fire curve, thermal input and structural displacement output, in other words cause and impact. Dimensional analysis, which is a condition for dynamic similarity between prototype and model, can be achieved when all the dimensionless groups are set equal for both model and prototype. On the other hand, scaling rules are used to decide how much insulating material will be used on a structure.

Finally, it is clear that the reduced scale model fire test method would be advantageous for the provision of statistically meaningful many demonstrator test data with determined reference to parametric investigations.

## Acknowledgements

With grateful thanks

All lecturers of the University of Sheffield, especially to my supervisor **Dr Buick Davison** for his time and effort in providing advice during instructive meetings on my dissertation. This project would not have been possible without his help.

For the generous help of **my mother (Lütfiye Çırpıcı)** who bravely agreed to take part in my whole life and also in this study; without your encouragement and support I wouldn't be where I am now.

All my friends in Sheffield but especially **Daqian Zhang** for helping too much in this MSc year and for his tireless support during this dissertation, I hope our paths will cross somewhere again in the future.

Finally special thanks to all my Turkish friends in UK and Turkey but especially **Ebru Çetin** for her endless encouragement and attention.

--- oOo ---

# Table of Contents

## List of Figures

# List of Tables

# CHAPTER – 1 Introduction

Structural models in other words reduced-scale structures sometimes called replica models have usually had an important role in structural engineering in terms of education, research and design. The physical modelling of a structure is an individual sample in which the model stands for a complete structure or some part of a structure. In other words, it is defined as any physical representation of a structure or assembly of structural elements which is built by small scale compared with full size structures is to be tested and the laws of resemblance must be applied to explain test results. Many reduced scale structural model studies on prototype (full–size) structures such as buildings, bridges, towers, shells, dams, aerospace and mechanical engineering structures and also undersea structures, etc. are used in research studies. However, it should be pointed out that the material of prototype can be used for the reduced–size structure. When these materials cannot be used for reduced–size structure, appropriate model materials must be taken place instead of prototype material and then the reduced–size structure is properly constituted a "model".

In terms of fire tests on reduced scale models, as an alternative to the more traditional analysis methods, the use of reduced model tests analysis will be explored in this dissertation. Fire tests on small scale models offer considerable saving in costs and resources. Scaled experiments offer an economical alternative to full-scale tests. In other words, these tests are repetitive to find the parametric investigations really easily, and understanding the behaviour of structures and structural members of varying geometries, shapes and end conditions would be readily attainable. The meaningful many test data would then aid statistical analysis, which will be the most important providing the design formulae and methodologies.

Structural models might be classified in different ways. In other words, what we expect to get from test results. The type of models can be shown below.

*Elastic Model*: This kind of model is similar to the prototype but it contains elastic material which does not behave like the prototype material. The elastic model is limited to the elastic range of material and might not predict post cracking behaviour of concrete if the material is concrete or post yield behaviour of steel.

*Indirect Model*: An indirect model does not have a direct physical similarity to the prototype as an example, a frame, whose flexural stiffness properties (EI) determines its behaviour, can be modelled indirectly that produces the relative stiffness values.

In the past, indirect model applications have been done for non-uniform members in indeterminate frames.

*Direct Model*: A direct model is geometrically similar to the prototype in all situations, and applying the loads to it is the same as to the prototype. Deformations, strains, and stresses in the model have similar quantities in the prototype for all loading condition. Because of this reason, an elastic model can also be called a direct model.

*Strength Model*: This type of model can be called realistic or ultimate strength model, in other words replica model which is a direct model, the materials of model that is made are similar to the prototype materials.

*Wind Effects Model*: There are different kinds of ways to classify wind modelling. One of them is utilizing the shape or rigid models where total forces or wind pressures on the structure might be measured. The other way to model is shape and stiffness properties of prototype which is modelled to get the wind induced stresses and deformations.

*Dynamic Model*: Vibration and dynamic loading effects on structures has been studied on these models. A shaking table tests might be taken place to study earthquake loading effects or in a wind tunnel test is to determine the aero elastic effects on structure. On the other hand, internal or external blast effects on structures can be found by dynamic models.

*Other Models*: Other model classifications include thermal models which effects of temperature is pointed out. Thermally loaded models are usually elastic, direct models even though in some situations both mechanical loads and thermal loads are combined for strength models. (Harris & Sabnis, 1999)

## Aims and Objectives

Aim of this dissertation is to investigate how composite frame floor arrangements, beam-column connections might be modelled at a small scale for fire testing and suggest suitable model in terms of section sizes for structural members, floor construction and time. In order to achieve this aim, there are many objectives which should be considered as can be seen below.

i) A review of behaviour of

- composite floor frames in fire conditions
- steel and composite beams in fire conditions
- unrestrained columns in fire conditions
- restrained columns in fire conditions
- beam-column connections in fire conditions
- the 96$^{th}$ floor of World Trade Centre Tower 1

ii) An overview of scale modelling of

- wood crib fires
- compartment fires

iii) Proposing how to build a scale model suitable for fire testing

- Section sizes (model size)
- Floor construction
- Fire compartment
- Duration of test
- Instrumentation

# CHAPTER – 2 Literature Review

## 2.1 Choice of Geometric Scale

Every model has an optimum geometric scale factor however significantly small models need light loads. That’s why many difficulties such as fabrication and instrumentation are occurred on small scale models. Large models, which require heavier loads, are built really easy and also there will be several problems in smaller laboratory to test the large models. Typical scale factors might be shown below. (Harris & Sabnis, 1999)

| Type of Structure | Elastic Models | Strength Models |
|---|---|---|
| **Shell roof** | $\frac{1}{200}$ to $\frac{1}{50}$ | $\frac{1}{30}$ to $\frac{1}{10}$ |
| **Highway bridge** | $\frac{1}{25}$ | $\frac{1}{20}$ to $\frac{1}{4}$ |
| **Reactor vessel** | $\frac{1}{100}$ to $\frac{1}{50}$ | $\frac{1}{20}$ to $\frac{1}{4}$ |
| **Beam / slab structures** | $\frac{1}{25}$ | $\frac{1}{10}$ to $\frac{1}{4}$ |
| **Dams** | $\frac{1}{400}$ | $\frac{1}{75}$ |
| **Wind effects** | $\frac{1}{300}$ to $\frac{1}{50}$ | Not applicable |

Table 2.1: Typical scale factors for several classes of structures (Harris & Sabnis, 1999, p. 9)

It can be seen from this table that there are many practical dimensional limitations for strength models of concrete structures, such as bar spacing, cover, minimum feasible thickness, etc.

## 2.2 Advantages and Disadvantages of Model Analysis

The main advantage of a physical model is to show the behaviour of complete structure on the collapse stage which is loaded. Although great progress is made in computer based analysis, the failure capacity of three dimensional systems in complex loadings condition is not predicted by analytically. Another great advantage on structures for reduced scales is to reduce the cost. Cost reductions depend on two issues; one of them is reduction of loading equipment and the other is a reduction in cost of test structure fabrication, preparation and disposal after the tests have done.

Time and expense are the factors for limiting the using of structural models in a design environment. If reduced scale models are compared with the analytical models, computer based models are less expensive and faster but they cannot replace the behaviour of prototype structures because their procedure leads to acceptable definition of behaviour of the real structure. Hence, physical models are more adequate and feasible than analytical models. Another limiting factor is that when the prototypes design changes it will be resulted in changing the small scale model in other words it needs a second model to check the prototype. In terms of time, it usually adds another pressure because it is decided to go to a physical study at the last minute. That's why suitable efforts must be made very earlier in the design process that a model test is needed. This would depend on earlier planning and a correct approach to the model study. (Harris & Sabnis, 1999)

## 2.3 Reliable of Structural Models

The accuracy of the test results from a model study is probably the most important factor that is difficult to formulate, because two identical reinforced concrete elements normally show differences which is approximately 20 % or more. There are many factors to affect the model accuracy such as model material properties, fabrication, loading techniques, measurement methods and explanation of the test results. Elastic models usually give elastic response and thus they will have high accuracy (errors less than 5 – 10%) for structures including minimal cracking such as reinforced concrete. A number of factors that affect the strength of materials and also the structures which are constructed from these materials might also have an effect on accuracy of models. The main material strengths are usually measured from control specimens in prototype structures. However the size of the structure becomes more important since the experimenter will predict the strength of prototype from the eventual result of a model testing in scaled models. Moreover, the value of results is linked to the confidence that depends on the errors which will happen at various stages of the modelling process. These errors can be shown below in Figure 2.1. (Harris & Sabnis, 1999)

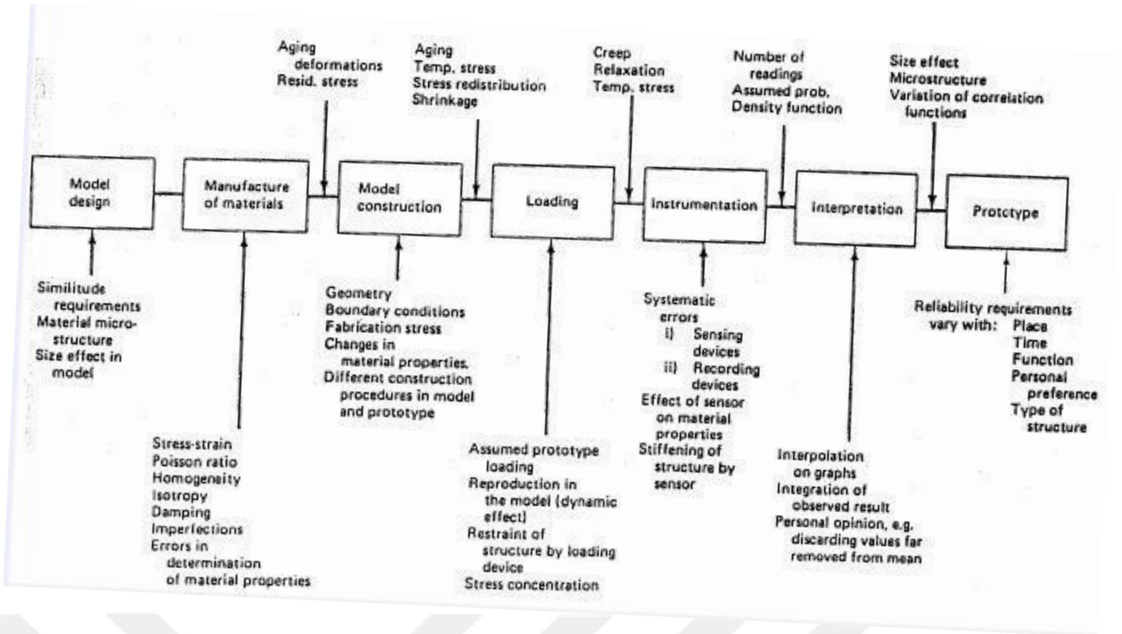


Figure 2.1: Parameters affecting the model confidence level. (After Pahl, P.J., 1963) (Harris & Sabnis, 1999, p. 413)

It might be shown that structural modelling process can be divided to the five steps, namely (1) planning, (2) fabrication, (3) loading, (4) data recording and (5) interpretation to the prototype. Any errors may come into each of these five steps and a list may be made for possible error sources. It is not comprehensive.

1. Planning
    a. Error from dimensional analysis
    b. Error from the model proportion
    c. Mistake to choose inadequate material
    d. Possible failure to recognize a relevant variable

Planning part is very important because all variables are put into the model must be accounted for as conveniently as possible at this stage. Some variables might be eliminated but after preliminary testing all considerations such as dimensional analysis should be made.

2. Fabrication
    a. Geometry of the model (e.g. thickness, length, etc.)
    b. Material properties
        i. Poisson's ratio (e.g. $\nu_{steel}$ = 0.25 – 0.30  $\nu_{concrete}$ = 0.15 – 0.20)
        ii. Modulus of elasticity
        iii. Stress–strain–time characteristics
        iv. Thermal expansions coefficient

v. Initial stresses

vi. The type of structure (e.g. microscopic or macroscopic structure)

In the fabrication step, material properties should be carefully involved and the behaviour of the structure should be decided such as if the duration of the experiment is short and the loads on the model do not exceeds the service loading conditions, the behaviour of the structure will be roughly elastic. Because of this reason material properties constitute highly important part in the process of the model.

3. Loading
   a. Boundary conditions
   b. Magnitude, direction, distribution of load
   c. Time history of load
   d. Effect of gravity loading

   The loading part of process is extremely important, because any errors for applying the load will affect the other parameters and also results. Hence, it will be reflected in the prediction of prototype behaviour.

4. Instrumentation and Data Recording
   a. Error in recording the data and readings
   b. Displacements
      i. Judgement errors in smallest division of instrument
      ii. Magnitude of displacements are not compatible with support system of recording device
      iii. Errors in calibration
      iv. Natural recording instrument error
   c. Pressure
      i. Meniscus corrections in a manometer
      ii. Reading and/or inconvenient calibration of pressure gages
5. Interpretation
   a. Wrong assumption of transformation of surface strains into stress, e.g. assumption of plane strain instead of plane stress
   b. Error in reduction of data

The above listing errors, which are seen in the process steps, are commonly referred to as experimental error. (Harris & Sabnis, 1999, p. 438-439)

## 2.4 Structural Fire Testing

The World Trade Center event, which happened in 11th September 1996, showed that the loading condition with the fire can be tragic for high storey buildings. The reasons of collapse of towers and possible collapse hypotheses have been studied and defined by many studies. The reason of collapse of the World Trade Center towers is the lateral torsional buckling of heated columns according to Bažant and Zhou (2002a,b). Many investigations, which have been conducted by The Federal Emergency Management Agency (FEMA) (2002), were about studying the buildings performance at the World Trade Center (WTC) and developing an idea of the response of every affected building. In order to design safer structures and reduce the loss from fires depend on understanding the mechanism of structural damage which is caused by fire.

The BRE Cardington tests have been known the best experiments which help to investigate the combined effects exposed to fire. An 8-storey composite steel framed structure was constructed as a platform, as shown in Figure 2.2, so that researchers can understand the behaviour of structures from full scale structural tests using different type of fires. (Lennon & Moore, 2003)

Figure 2.2: Cardington composite steel framed building (Wang, 2002, p.62)

Another full-scale fire test is the open car park which has been done by CTICM (France, the coordinator), ARBED (Luxembourg) and TNO (Netherlands). The performance and behaviour of structure were investigated by burning the cars in the car park as shown in Figure 2.3.

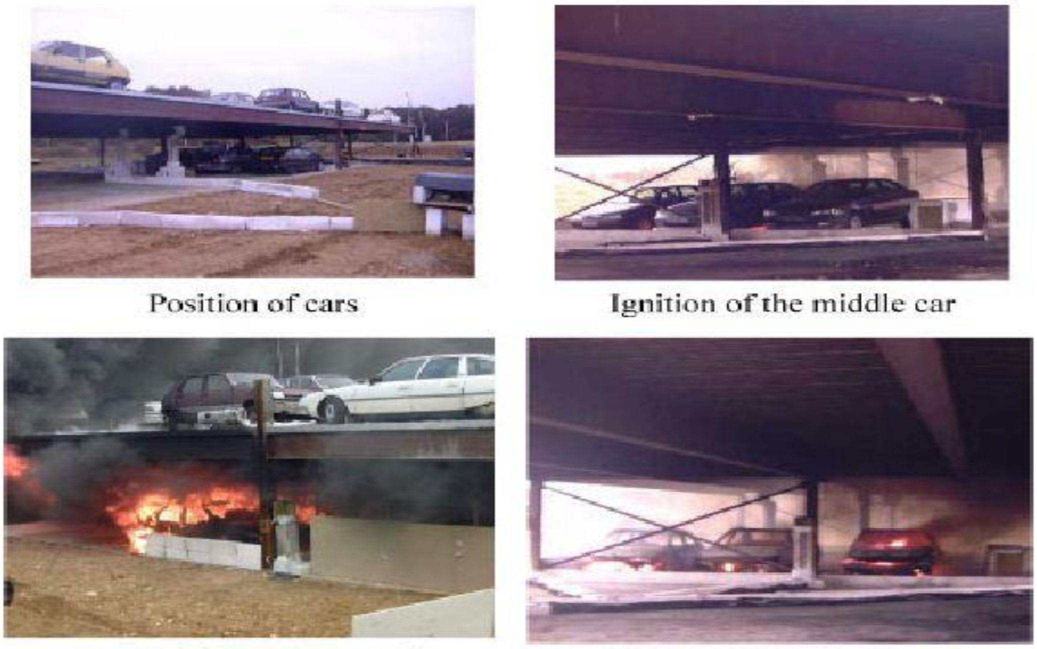


Figure 2.3: Summary of a fire test involving three cars(Zhao & Kruppa, 2004, p.273)

These full scale experiments shows that they can be confidential and accuracy providing that a real fire occurs in a building. However, in terms of size and cost of the full scale or large scale models are unable to test very often in fire. Moreover the number of study of the structural member's behaviour by themselves is limited instead of standard fire. Although standard fire test is able to provide information about the response of individual members of structure when they are subjected to a standard fire curve, it does not show the real performance of the whole structure in a real fire. Scaled models can be used to understand the behaviour of structures in real fire phenomenon. (Wang, 2002)

## 2.5 Structural Behaviour in Fire

### 2.5.1 Behaviour of Composite Floor

When the floor behaviour is discussed, the load carrying capacity depends on the flexural strength and also the support conditions of composite beam. The steel deck and concrete are the key factors to determine the strength of composite slab. Fire design methods are quite similar but any contribution from the steel deck is ignored in theoretical design method for composite slabs. However it has seen from many fires that the steel deck has deboned due to the release from the concrete during fire. The theoretical flexural strength of the slab is based on the mesh reinforcement, concrete and supporting composite beams since the steel deck is ignored in the design procedure.

Current design method is based on the load path mechanisms which are worked out at the ultimate and serviceability limit states. If the displacements experienced by floor system at normal temperature are small and vertical, these assumptions are acceptable. However, the true load path mechanisms are not considered because they are large vertical displacements which are actually happened during a fire. At ambient temperature, a composite floor slab is designed to carry the bending load only. Restraint at the slab edges is going to lead to significantly compressive forces which help to carry the load by compressive membrane action. In the beginning of a fire these forces will increase in the supporting steel beams which heat up faster than concrete slab. Finally the compressive forces in the beam will increase sufficiently that cause the buckling of the lower flange at the supports. (Bailey & Moore, 2000)

Composite construction, which involves concrete cast in situ on top of the steel decking, is usually used as a construction method for floor slabs. There are many standard tests have been carried out to prevent the requirements of fire regulations. A study of these fire tests is given by Cooke et al. (1988). According to Cooke et al., the reason of structural failure is due to plastic hinge formation; hence, plastic design method might be used to calculate the capacity of load of composite slab. In terms of temperature distribution of composite slabs, the temperatures in a composite slab near the steel sections were lower than away from the steel sections. If a uniformly loaded continuous composite slab is considered, it can be shown in Figure 2.4 that design is usually directed by the hogging bending moment capacity. When the hogging bending moment capacity decreases dramatically across the width of the supporting sections, benefit can be obtained if consideration is given to this distribution of temperatures in the composite slab near the steel sections.

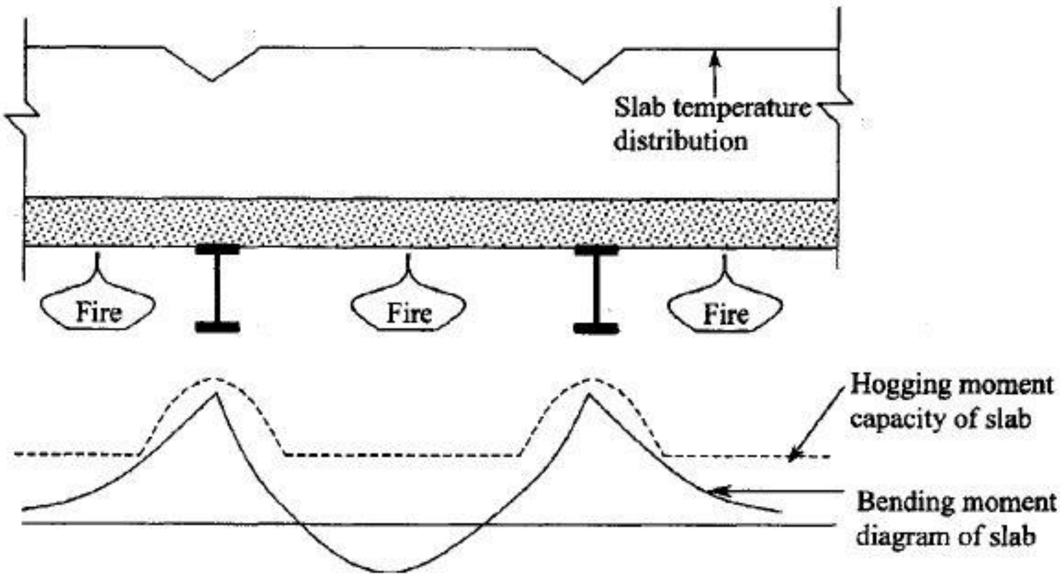


Figure 2.4: Effect of non-uniform longitudinal temperature distribution on the fire resistance of a continuous slab (Wang, 2002, p. 53)

It needs to ensure in designing a composite slab that the hogging bending moment capacity of the slab in the span is not less than the amount of reduction of hogging bending moment away from the supports.

*Simplified fire design method with membrane action*

Considering a floor slab which is a simply supported rectangular or square supported by steel composite beams, in order to calculate the load carrying capacity at a particular temperature the following energy equation can be used.

$$\omega_{p\theta} = e\left(\frac{\begin{array}{l}\text{Internal work done by the}\\ \text{composite slab in bending}\end{array}}{\begin{array}{l}\text{External work done by the}\\ \text{floor system / unit load}\end{array}}\right) + \frac{\begin{array}{l}\text{Internal work done by the}\\ \text{beam(s) in bending}\end{array}}{\begin{array}{l}\text{External work done by the}\\ \text{floor system / unit load}\end{array}} \qquad (2.1)$$

'e' is the enhancement because of the membrane action in the composite slab.

When a composite floor is subjected to fire, the shape of the yieldline pattern will be based on the behaviour of the support conditions from steel composite beams which always reduces in terms of strength. The mode behaviour of system with increasing temperature can be shown in Figure 2.5. The behaviour changes from one mode to another form due to the strength of the steel composite beam.

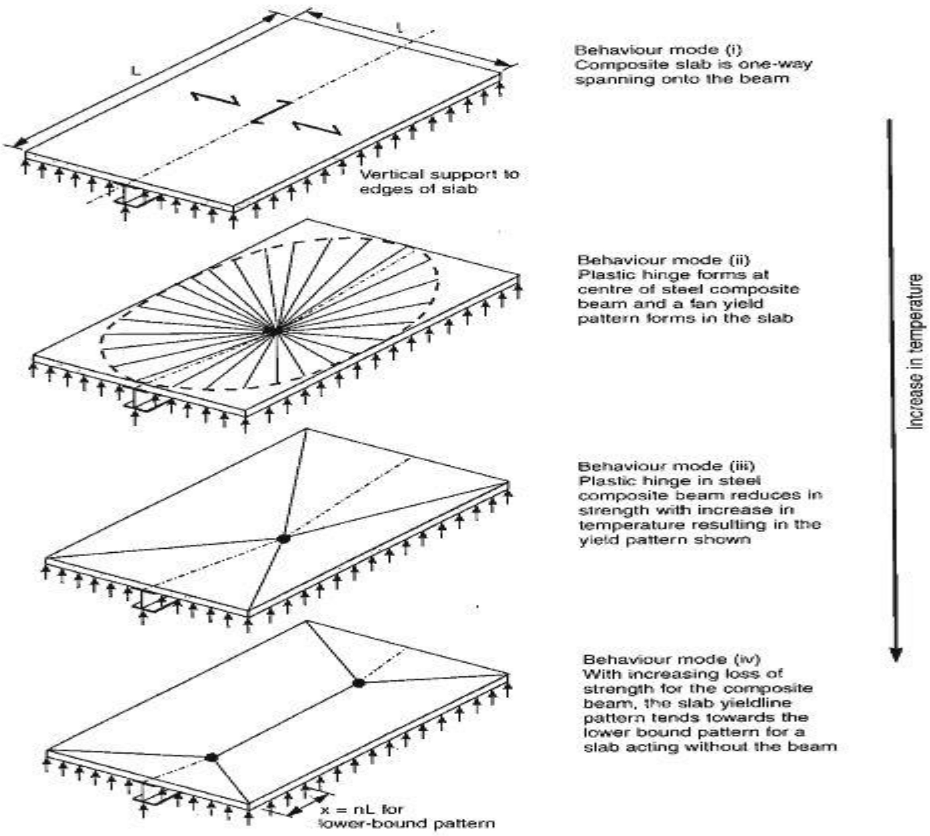


Figure 2.5: Slab and beam behaviour with increase in temperature
(Bailey & Moore, 2000, p. 21)

It can be seen from the figure that membrane action can occur and the increasing in temperature will result in a change in the mode of behaviour. In addition to this, it can be seen that although applying equation (2.1) to the simple example, can be complicated and time consuming.

However, if it is assumed that composite slabs affect the dominant load carrying capacity of the system, some assumptions can be applied to get a roughly estimate.

- The beams, which will fail first in a fire, are assumed to be simply supported. Because of this reason loaded area can be calculated.
- Assuming that the beams are unprotected the loads are supported by the flexural behaviour of the composite slab which is calculated from the lower-bound yieldline mechanism.
- The enhancement (e) in the equation (2.1) depends on the lower bound yieldline mechanism of the slab.

### 2.5.2 Behaviour of Composite Beam

When the behaviour of a beam in fire is discussed, it is important to determine type of support of the beam. For example if the beam is 'simple support', it means that the beam is statically determinate and there is no rotational and longitudinal restraint to the beam. In terms of flexural bending behaviour of a beam, there are two types of beam which are laterally restrained and laterally unrestrained. For a laterally unrestrained beam, if it is really long, bending of the beam about its major axis has an effect with the lateral movement in its weak axis and twist. This is called Lateral Torsional Buckling (LTB) which has similar effects with flexural buckling of a slender column. LTB does not occur in a laterally restrained beam while it occurs in beams with open profile because the compression flange of the beam is not restrained.

When a compartment in a building is subjected to fire, the heated zone is affected immediately by surrounding parts of the structure while outside of the compartment is cold enough and strong, does not loss its stiff. On the other hand, the heated zone starts to expand and loses its strength, besides several different effects that are really hard to explain happen after the fire starts. Finite element programs might describe the experimental observations. However, they cannot calculate such as internal forces and moments in a structural member.

Many fire tests have been done on composite beams (Wang, 2002). They are;

- Tests on unprotected, simply supported as usual composite beams (Wanman and Kirby, 1987, 1988)
- Tests on protected simply supported conventional composite beams (Newman and Lawson, 1991)
- Tests on partially encased steel section and partially encased steel section in composite action with concrete floor slabs (CEC 1987; Hosser *et al.*, 1994; Kordina, 1989).

It can be seen from results of all tests except tests of Zhao and Kruppa (1995), the structural behaviour of a composite beam is quite similar to a steel beam. The reason of failure of composite beam was because of the tensile yielding of the steel section, in other words the plastic bending moment capacity of the composite beam reaches. The other tests, which have been done by Newman and Lawson (1991), were about a comparison between the performance of composite beams with filled and unfilled voids and the protected steel beam and the profiled steel deck. The temperature of the upper flange increased in the unfilled voids while filled voids have been used the upper flange temperature would be 20% lower than lower flange.

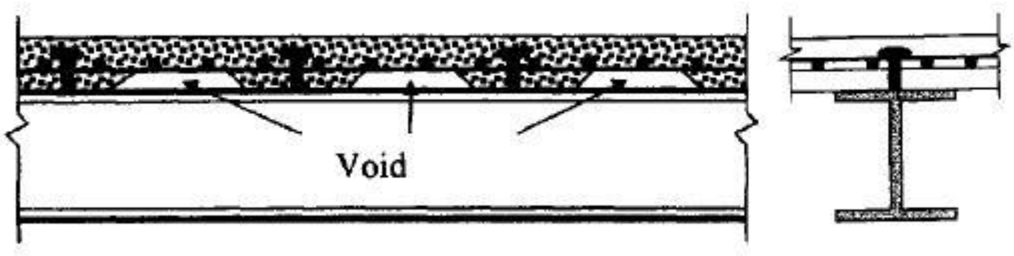


(Elevation) (Section)

Figure 2.6: Cross sections of a structural floor system (Wang, 2002, p. 51)

Many observations from Zhao and Kruppa (1995) fire tests may be listed below.

- One of failure type of composite beam was due to tensile yielding of the steel section as can be seen in other tests when the steel section was unprotected.
- Another failure is due to the fact that the temperature of the protected steel profile was lower than the concrete slab at the shear connector surface when a protected steel profile and partial shear connection were used and the slip ( > 10 mm) between the concrete slab and the steel profile at the ends of the beam.
- For testing the continuous beams with a cantilever span, local buckling in the web and lower flange of the steel section has been observed at the middle support.
- In terms of temperatures, the temperature in the steel section near the supports was much lower than in the span.
- If there was a concentrated load in the web near the centre support, fracture of shear connector has been observed in continuous composite beams.

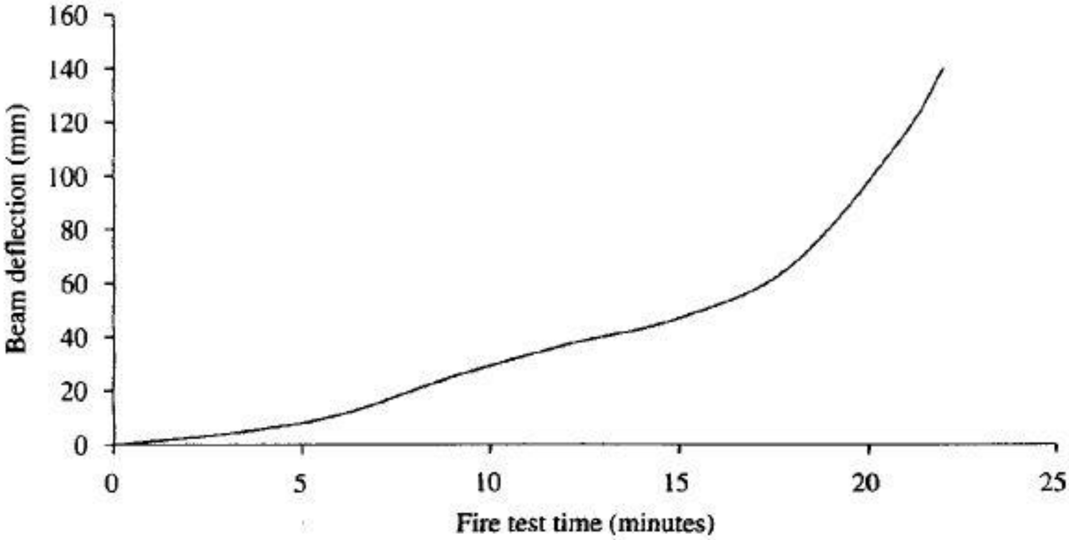


Figure 2.7: Typical behaviour of a simply supported beam under standard fire exposure (Wainman and Kirby, 1987). Reproduced with the permission of Corus. (Wang, 2002, p. 50)

It can be seen from Figure 2.7 that this line graph is about deflection-time relationship of a simply supported beam. The deflection of the beam rises up steadily until around 20 minutes, after this time beam deflection increases dramatically. In other words, failure of the beams runs quickly at nearly 25 minutes with very large deflections in the beam.

### 2.5.3 Behaviour of Beam-to-Column Connection

The conventional metal deck floor system involves concrete that is put on profiled metal decking on top of steel beams which are connected with shear connectors provided by through deck welded shear studs. There are many types of connections such as flush endplates, partial depth endplates, seating cleat with double web cleats and fin plate connections which can be shown in Figure 2.8, moreover there are some arrangements of composite connections for example cruciform type arrangement that is shown in Figure 2.9 and cantilever type arrangement can be shown in Figure 2.10.

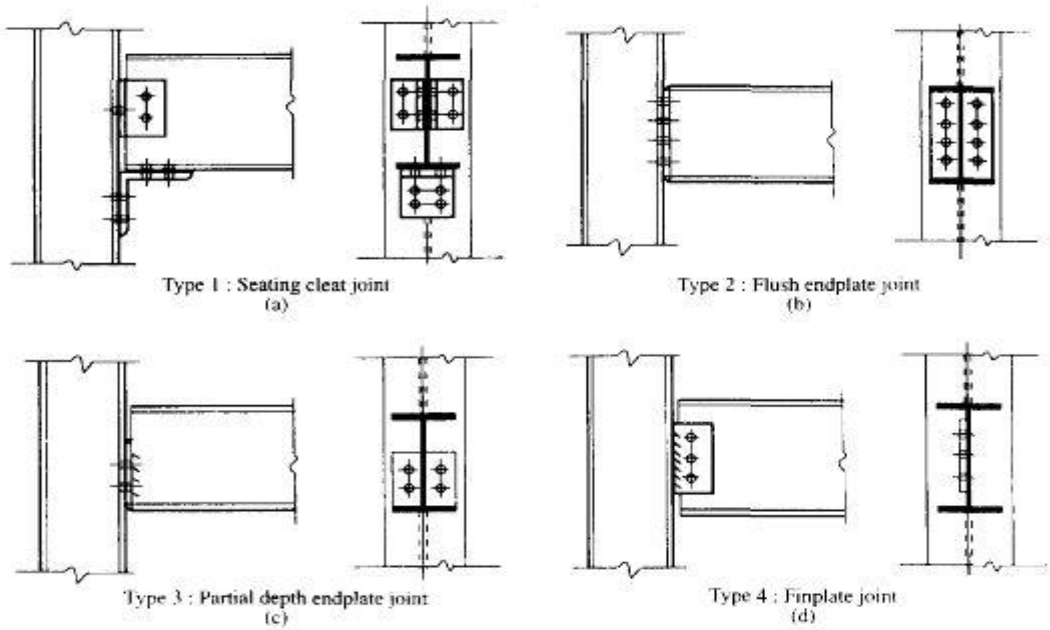


Figure 2.8: Four types of steel joint (Xiao et al., 1994, p. 5)

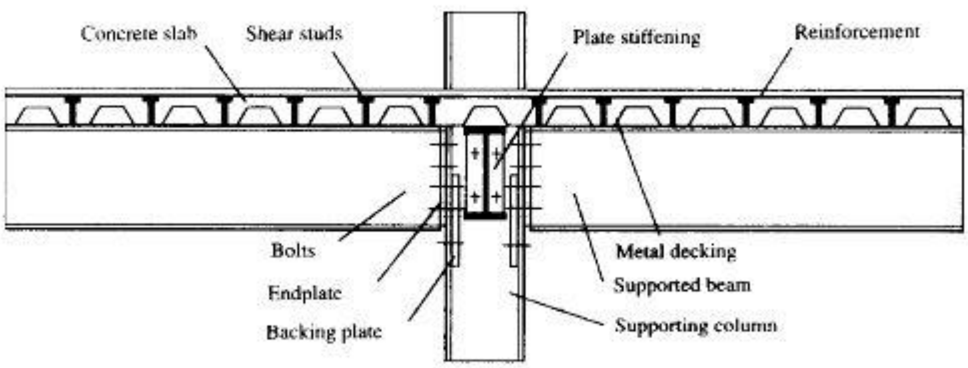


Figure 2.9: Cruciform arrangement of composite connection
(Xiao et al., 1994, p. 5)

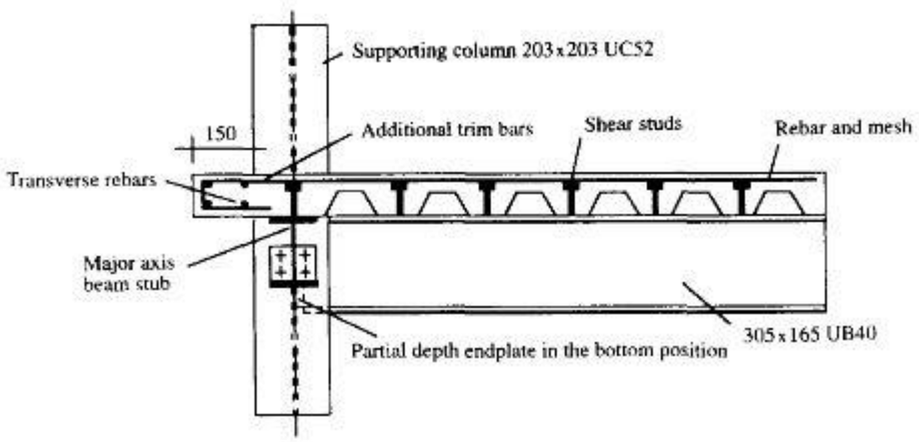


Figure 2.10: Cantilever arrangement of composite connection (Xiao et al., 1994, p. 5)

According to the report for fire test results on composite beam to column connections from Leston-Jones et al. (1997), connection behaviour at ambient temperature shows similarity with the behaviour at elevated temperature. Deformations were observed in the column web in the compression zone while very little deformations occurred in the beam and the end plate. For a composite connection, because of the stiffening effect of the reinforcement in the tension zone in which the temperature was low, hence the deformations were in the column web in the compression zone. Besides, if the steel connections compared with the composite connections, it can be seen that composite connections showed much less reductions in their bending moment resistance at high temperatures. On the other hand, the reinforcement in a composite connection helps to contribute to the bending moment resistance of connection. The temperature of reinforcement is law, so that its strength remains stable in other words the strength does not change significantly. (Wang, 2002)

### 2.5.4 Behaviour of Steel Column

The possible failures of unrestrained columns under compression load are local buckling, global buckling and cross sectional yield under fire conditions, and also they depend on the type of temperature distributions such as uniform and non-uniform. The behaviour of steel columns is simple when the temperature distribution is uniform. However, the behaviour is complicated with non-uniform temperature distributions since thermal bowing, additional bending moments and thermal stresses are occurred in column. (Wang, 2002)

**Local buckling**

In the design of steel columns when local buckling occurred, the load carrying capacity of steel column is evaluated by term of “effective width”. Effective width can be defined that the width of plate sustains the maximum stress in uniform compression. The effective width of steel plate depends on many factors like the ratio of width to thickness, the support condition and the stress distribution. If the stress distributions and temperature are non-uniform, the local buckling will be more complex. The effective width will change very barely when the realistic steel temperatures change in a wide range. (Wang, 2002)

**Global behaviour**

The column axial deformation with uniform temperature distribution is due to the thermal expansion at elevated temperatures. In other words, this deformation can be explained by reducing column stiffness at increasing temperatures. The thermal expansion causes the column to expand without any additional mechanical effects. When the applied stress exceeds the steel strength, column failure occurs due to yield of steel. As the global behaviour of steel column is explained briefly, the reduced strength and stiffness of steel at elevated temperatures should be considered.

If non-uniform temperature distribution in a column is considered, it can be obtained that this kind of temperature distribution causes non-linear thermal strain distribution. In addition to this, additional bending moments in the column occurred due to thermal bowing; hence it might reduce the column capacity (Wang, 2002). Different type of non-uniform temperature distribution can be shown below.

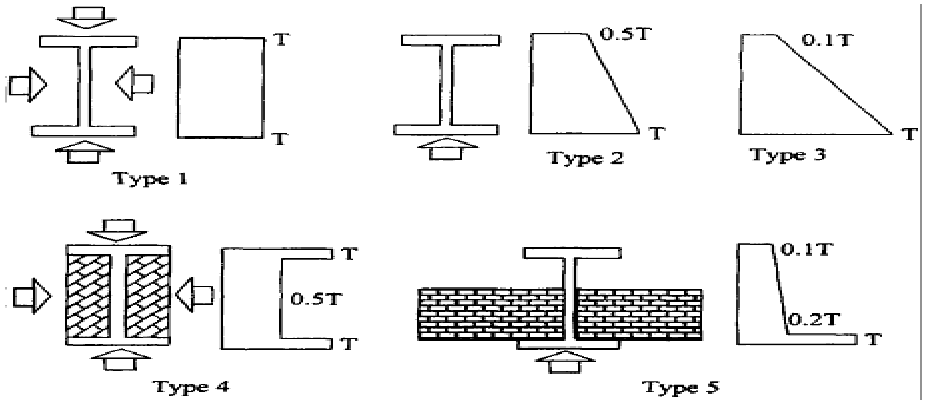


Figure 2.11: Different types of assumed non-uniform temperature distribution (from Wang et al. 1995) (Wang, 2002, p. 120)

Type 1 illustrates the basic uniform heating. Type 2 and 3 show the linear temperature distribution of a column heated from one side with different grades. Type 4 is a column with blocked in web while type 5 is constructed in a wall. It can be understood from Figure 2.11 that types 2, 3 and 5 are unsymmetrical temperature distributions, so thermal bowing and additional bending moments are produced in these types of columns. In type 4 there is no thermal bowing or additional bending moments occurred in the columns.

The behaviour of restrained columns in fire is quite different from unrestrained columns. Possible changes in the column under fire conditions are,

- Axial load changes due to axial restraint to its thermal expansion as shown in Figure 2.12,
- Buckling length changes due to variable rotational restraint,
- Bending moment changes due to variable bending stiffness of the column and also it changed due to lateral load of thermally restrained adjacent beam as shown in Figure 2.13,
- Bending moment also changes due to the column axial load acting on the thermal expansion of the adjacent beam as shown in Figure 2.14,

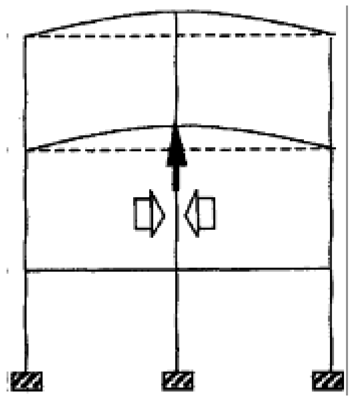

Figure 2.12: Effect of restrained thermal expansion

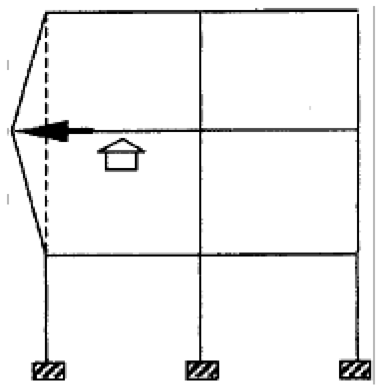

Figure 2.13: Effect of push over the adjacent beam

(Wang, 2002, p. 125)

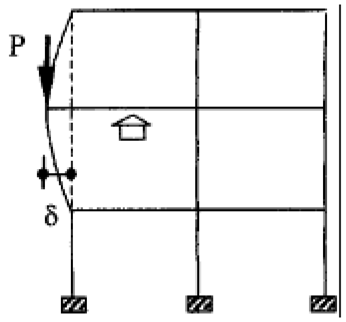


Figure 2.14: P-δ effect in column (Wang, 2002, p. 125)

## 2.6 Small-Scaled Fire Test of World Trade Center Tower 1 (WTC)

The study of collapse mechanism of WTC helped the designers to understand the mechanism of structure in fire from many tests and studied on the building. When the structure load effect combines the effect of fire, this situation can be really dangerous and disasterous. One of the possible collapse according to Bažant and

Zhou (2002a;b) is the buckling of heated columns at high temperatures. Besides, in the light of Quintiere et al. (2002) comments; they have concluded that inadequacy of insulation on the floor trusses causes the collapses after analyzing a single web member of the floor truss system. Usmani et al. (2003) concluded that the collapse mechanism of WTC depends on the instability of the structural systems because the thermal expansion is highly possible to occur at high temperatures.

When the fire is occured in the structural members, the steel temperatures of floor trusses and especially columns are highly important. According to the researches of FEMA 2002; Quintiere et al. 2002; Usmani et al. 2003 the steel temperatures have been evaluated from characterized fire conditions in terms of temperature and time curves, and also the effect of insulation and fire scenarious have been understood from these research results.

After Sebtember 11 event, a small scale model of 96th floor was built and demonstrated under fire conditions to find the structural response. The modeling rules have been applied in terms of fire loading, the structural and material similarity between the protoype and model and also the design and modeling of fire compartment. (Wang et al., 2007)

**Construction and Burning of Scaled Model**

The 96th floor of WTC1 was geometrically scaled as 1/20-scale model. The dimension of scaled model was 3m×3m×0.15m. The damage of airplane crash has been represented in the model. It can be shown in Figure 2.15.

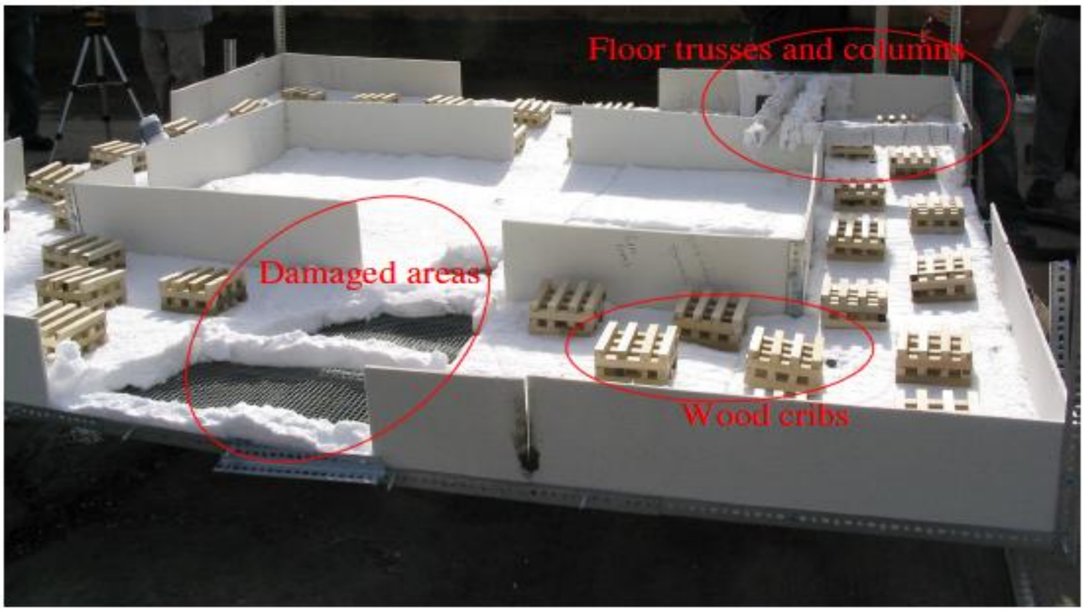


Figure 2.15: The 1/20-scale floor model of 96th floor (Wang, 2006, p. 104)

Wood cribs were used as the fuel to fire the model. 638 wood sticks with 19mm×19mm were used to built 40 wood cribs which can be shown in Figure 2.16. The burning time of WTC1 was assumed aproximately 120 minutes and this burning time was scaled ($t \sim s^{1/2}$) and was approximately 26.8 minutes.

Figure 2.16: Wood cribs as the fuel in the model (Wang, 2006, p. 106)

After design of the wood cribs, floor trusses were built according to rules of geometric scaling as can be shown in Figure 2.17. The insulation for structural members can be shown in Figure 2.18. “The fire was started by igniting the five pans of liquid fuel (mix of kerosene and heptanes) simultaneously”(Wang, 2006, p. 112). The burning of model is shown in Figure 2.19.

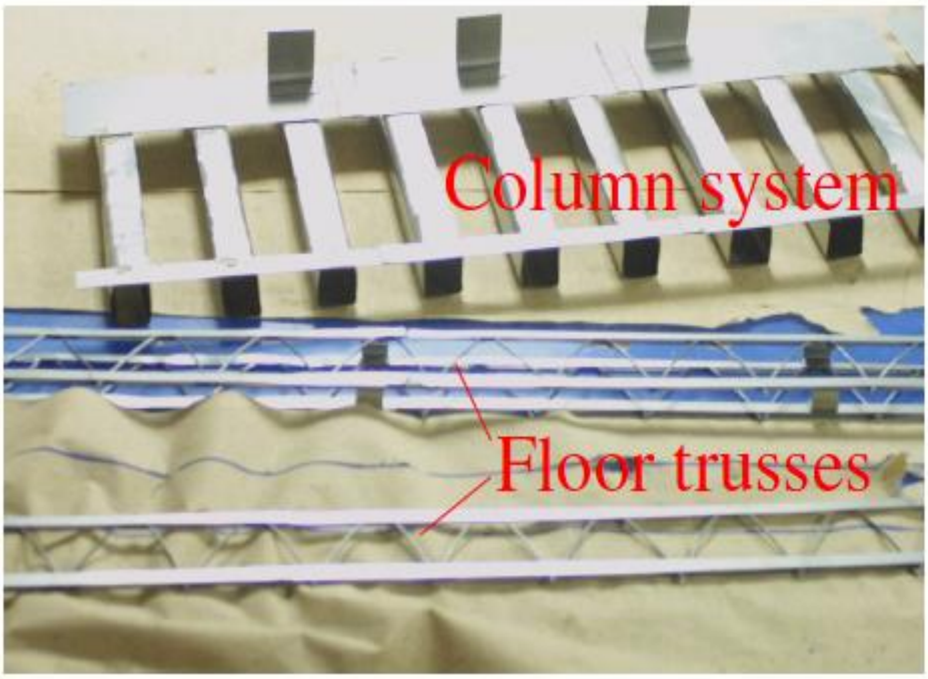


Figure 2.17: Scaled truss and column models (Wang, 2006, p. 112)


Figure 2.18: Insulated structural models (Wang, 2006, p. 113)

Figure 2.19: Burning of 1/20-scale model (Wang, 2006, p. 114)

Figure 2.20 shows the methodology to estimate the structural failure in fire. Firstly, prototype conditions need to be determined in terms of fire, insulation and structure. This determination based on the information of ventilation configuration and structural types. The ventilation changes during fire and the structural loading should be determined according to protoype loading condition. Secondly, small-scaled model can be designed and tested according to the scaling rules. After testing, fire behaviour and response of structure can be obtained. The test results should represent the behaviour of full-scaled structure. Lastly, the performance of the structure and the possible failure mechanism of it can be understood by a properly small-scaled model testing. (Wang, 2006)

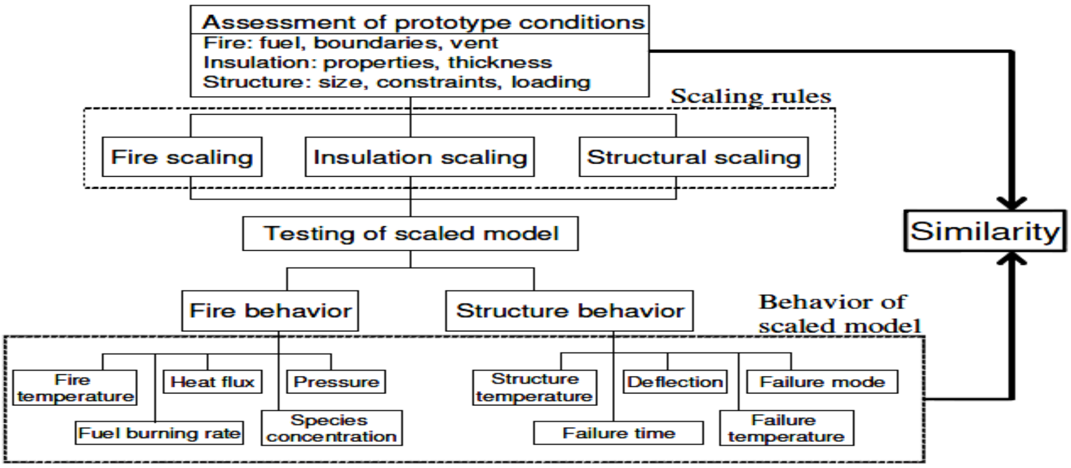


Figure 2.20: Schema of methodology for failure prediction (Wang, 2006, p. 95)

# CHAPTER – 3 Scale Modelling of Structures and Design

The development of structural scaling introduces simple scaling rules to design the structural geometry, structural loading and also boundary conditions. Every structural model must be designed due to the many similitude requirements that mean like connection between the model and the prototype structure. The theory of modelling relates to these similitude requirements which might be derived from a dimensional analysis.

## 3.1 Theoretical Development of Structural Scaling

Dimensional analysis will be used to develop the scale relations between important parameters which are involved in fire. In this dissertation, "~" will be used to define the dimensional equality and "^" will be used to define the dimensionless variables. In other words, dimensionless variables will be showed as a ratio of the variables e.g. $\hat{T} = \frac{T}{T_\propto}$, $\hat{\rho} = \frac{\rho}{\rho_w}$ and $\hat{t} = \frac{t}{t_r}$ show the dimensionless of temperature, density and time. "$s$" is the scale factor or called the geometric length scale. In this project (dissertation) the scale factor "$s$" is considered as 1/5. The all equations for structural scaling have been taken from (Wang, 2006).

If an object is subjected to a fire, the change of temperature can be related to the heat flux onto object;

$$mc\frac{dT}{dt} \sim \dot{q} \tag{3.1}$$

In this equation, m is the mass. m ~ $s^3$ which is related to density and volume of the object. As mentioned above, density is dimensionless factor i.e. $\rho \sim s^0$. Volume is scaled according to $V \sim s^3$ when the object is scaled by geometrically.

The heat generation rate and heat loss rate are scaled,

$$\dot{Q} \sim s^{5/2} \tag{3.2}$$

$$\dot{q} \sim s^{5/2} \tag{3.3}$$

In the equation 3.1, $c \sim s^0$ because of the same material that is used in small scale models. Hence Equation 3.1 can be modified as;

$$s^3 s^0 \frac{dT}{dt} \sim s^{5/2} \tag{3.4}$$

The temperature is independent from scale rules in the object, so the time scale can be invented as;

$$t \sim s^{1/2} \tag{3.5}$$

The structural scaling rule can be derived from the relevant equations, and the stress in one-dimensional form of structural member is used providing that there is no loss of generalisation;

$$\varepsilon = \frac{\partial v}{\partial x} \tag{3.6}$$

$v$ is a deformation vector in x direction and if it is scaled like $v \sim s$, the scaled of strain will be $\varepsilon \sim s^0$ which means the strain value between prototype and model is a constant.

Stress may be related to force or strain;

$$\sigma = \varepsilon E, \ \sigma = \frac{\partial F}{\partial x \partial y} \tag{3.7}$$

Since the same material is used in prototype and model, elastic modulus, stress and force are scaled by;

$$\sigma \sim s^0 \text{ and } F \sim s^2 \tag{3.8}$$

If a beam-column model can be modelled as shown in Figure 3.1, the bending resistance and external moment may be written as;

$$-EI\frac{d^2y}{dx^2} = Py + M_1 + (M_2 - M_1)\frac{x}{L} \tag{3.9}$$

y is the transverse deflection, E is the elastic modulus, and P is the axial force which occurred from the elevated temperature of the beam. M is the moment that applied and L is the length of the beam. The deflection shape, which is shown in Figure 3.1, should be similar to that of prototype providing that $\frac{dy}{dx} \sim s^0$. If the model is geometrically scaled (x~ $s$), the scaling factor for transverse deflection will be y~ $s$.

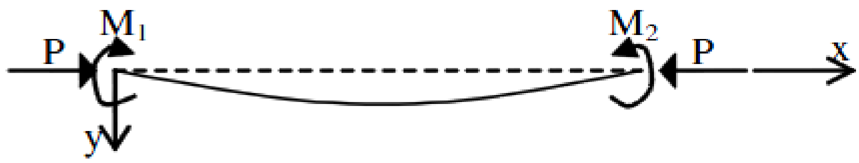


Figure 3.1: Beam-column model (Wang, 2006, p. 47)

If the model is geometrically scaled, A~ $s^2$, V~ $s^3$ and $I \sim s^4$ can be defined. When the same material is used for both prototype and model, the scaling for mass is m~ $s^3$. When these relations are put into Equation 3.9;

$$-s^{0}s^{4}\frac{s}{s^{2}} \sim \mathrm{P}s \sim \mathrm{M}_1 \sim (\mathrm{M}_2 - \mathrm{M}_1)\frac{s}{s} \qquad (3.10)$$

As can be pointed out from Equation 3.10 that, the scale factor for force and moment are; $\mathrm{P} \sim s^{2}$ and $\mathrm{M} \sim s^{3}$ (3.11)

In order to calculate the axial force (P), beam shortening effect due to vertical deflection and resistance to thermal expansion effect due to elevated temperature should be determined. (Yin & Wang, 2005)

$$P = K\Delta L = K\left(\int_{0}^{L}\left[1+\left(\frac{dy}{dx}\right)^{2}\right]^{1/2} dx - L - \alpha(T - T_{\infty})L\right) \qquad (3.12)$$

K is the stiffness of the structural members and also the scale factor for $\Delta L$ is $\Delta L \sim s^{1}$. That's why the end axial stiffness should be scaled as;

$$K \sim s \qquad (3.13)$$

By using Equation 3.13, the boundary constraint on a small scaled model should be designed and the axial forces and deformation need to be scaled properly.

When the same material is used for prototype and model, all those scaling rules can be shown below in Table 3.1

| Quantities | Scale Factor |
|---|---|
| **Length, L** | $s$ |
| **Mass, m** | $s^{3}$ |
| **Density, $\rho$** | $s^{0}$ |
| **Heat generation rate, $\dot{Q}$** | $s^{5/2}$ |
| **Heat loss rate, $\dot{q}$** | $s^{5/2}$ |
| **Temperature, θ** | $s^{0}$ |
| **Time, t** | $s^{1/2}$ |
| **Strain, $\varepsilon$** | $s^{0}$ |
| **Stress, $\sigma$** | $s^{0}$ |
| **Elastic modulus, E** | $s^{0}$ |
| **Force, F or P** | $s^{2}$ |
| **Deformation, $v$** | $s$ |
| **Area, A** | $s^{2}$ |
| **Volume, V** | $s^{3}$ |
| **Moment of inertia, $I$** | $s^{4}$ |
| **Moment, $M$** | $s^{3}$ |
| **Axial stiffness, $K$** | $s$ |

Table 3.1: Summary of scale factors for structural scaling

## 3.2 Theoretical Development of Insulation Scaling

After theoretical development of structural scaling, insulation for fire protection must be scaled due to the heat transfer through solids in compartment fires. Under these conditions, the equation can be show as;

$$m_s c_s \frac{dT_s}{dt} + m_i c_i \frac{dT_i}{dt} \sim \frac{\mathrm{k_i}}{\delta_\mathrm{i}} A_s (T_f - T_s) \tag{3.14}$$

The structural materials (e.g. steel) and the insulation store the heat. The thermal conductivity of steel is higher than that in the insulation hence; it is considered that the temperature may be considered as uniform in steel. On the other hand, there can be a simple assumption that the temperature of insulation surface is equal to the hot gas temperature since thermal resistances of radiation and convection are small at the solid boundaries.

In order to calculate the thickness of insulation in a small scale model, Equation 3.14 must be scaled at different scales. There are different scaling approaches which can be derived depending on the heat capacity of insulation. (Wang, 2006)

**Consideration of the heat capacity of insulation**

If the heat capacity of insulation is that important, the insulation properties can be obtained from Equation 3.14 for scaled model by using dimensionless ratios. The equation is made as dimensionless providing that the temperature and time are in terms of the ratios $\hat{T} = \frac{T}{T_\infty}$ and $\hat{t} = \frac{t}{t_r}$. After some arranging Equation 3.14 becomes:

$$\frac{k_i}{\delta_i} \sim \left(\frac{\mathrm{m_s c_s}}{\mathrm{t}_r A_s}\right) \frac{d\hat{T}_s}{d\hat{t}} \left(\frac{1}{\hat{T}_f - \hat{T}_s}\right) \frac{T_\infty}{T_\infty} + \left(\frac{m_i c_i}{\mathrm{t}_r A_s}\right) \frac{d\hat{T}_i}{d\hat{t}} \left(\frac{1}{\hat{T}_f - \hat{T}_s}\right) \frac{T_\infty}{T_\infty} \sim \frac{\mathrm{m_s c_s}}{\mathrm{t}_r A_s} + \frac{m_i c_i}{\mathrm{t}_r A_s} \tag{3.15}$$

Where, $m_i$ which is the mass of insulation can be written as:

$$m_i \approx DL\delta_i \rho_i \tag{3.16}$$

When Equation 3.16 is put into the Equation 3.15;

$$\frac{k_i}{\delta_i} \sim \frac{m_s c_s}{s^{5/2}} + \frac{DL\delta_i \rho_i c_i}{s^{5/2}} \tag{3.17}$$

Where D is sectional perimeter of the insulated steel member, L is the length of steel member. $(\frac{m_s c_s}{s^{5/2}})$ is related to steel and $(\frac{DL\delta_i \rho_i c_i}{s^{5/2}})$ is related to the insulation.

Preserving the insulation term in Equation 3.17,

$$\frac{k_i}{\delta_i} \sim \frac{DL\delta_i \rho_i c_i}{s^{5/2}} \tag{3.18}$$

If $\delta_i$ is solved, the equation 3.19 can be occurred.

$$\delta_i^{\ 2} \sim s^{1/2} \frac{k_i}{\rho_i} \sim \mathrm{s}^{1/2} \tag{3.19}$$

Since thermal conductivity depends on its density for many insulation materials $(k_i \sim \rho_i)$ and L ~ D ~ $s^1$, $c_i \sim s^0$. Hence, the insulation thickness for scaled model can be estimated:

$$\delta_i \sim \mathrm{s}^{1/4} \tag{3.20}$$

As it is mentioned in the previous sub-title that $m_s = s^3$ for a geometrically scaled structure. The rules for scaling of fire protection material properties can be determined by substituting Equation 3.20 into Equation 3.17 which is the steel term;

$$k_i \sim \rho_i \sim \mathrm{s}^{3/4} \tag{3.21}$$

It can be understood from Equation 3.21 that the scaling for insulation is not geometrically. Adjustment must be made to the thickness and the thermal properties of the insulation material. After then, Equation 3.22 can be obtained.

According to the Equation 3.21, density of the insulation can be changed by temperature and time. Because of this reason, the changing in the insulation property is unpredictable and impracticable. For example, Equation 3.21 shows that density is a proportion of the scale factor. That’s why it needs to be used lighter insulating materials for small scale models. In other words, lighter insulating material for scaled models means light-weight materials which may not exist in the design procedure. In order to solve this problem, the same insulation material as used in the prototype can be used in the model, so the Equation 3.21 can be changed to $k_i \sim \rho_i \sim \mathrm{s}^0$. After this changing, the Equation 3.17 becomes;

$$\frac{1}{\delta_i} \sim \frac{m_s c_s}{s^{5/2}}, \frac{1}{\delta_i} \sim \frac{\delta_i}{s^{1/2}} \tag{3.22}$$

Using the insulation term, the scale modelling of insulation thickness must be $\delta_i \sim \mathrm{s}^{1/4}$. According to this scaling, the mass of steel must be modelled to $m_s \sim s^{9/4}$

while $m_s \sim s^3$. Therefore, it needs to increase the mass of steel. The differences between the masses are,

$$\Delta m = (s^{9/4} - s^3)m_p \tag{3.23}$$

Increasing the mass can be achieved by adding more steel, $\Delta m$, to the steel elements under the insulation. (Wang, 2006)

**Ignore the heat capacity of insulation**

As it is explained in Equation 3.21, insulation materials are usually light weight, so the mass of the insulation and specific heat of the steel $(m_i c_i)$ are smaller than the mass of the steel $(m_s c_s)$, and specific heat of the steel. Because of this reason, the heat capacity of insulation may be ignored for structures which have light weight and really thin insulation. After this assumption, Equation 3.14 can be written as;

$$m_s c_s \frac{dT_s}{dt} \sim \frac{\mathrm{k_i}}{\delta_\mathrm{i}} A_s (T_f - T_s) \tag{3.24}$$

The same procedure, the temperature and time are written in terms of ratios $\hat{T} = \dfrac{T}{T_\infty}$ and $\hat{t} = \dfrac{t}{t_r}$ Equation 3.24 becomes,

$$\frac{k_i}{\delta_i} \sim \left(\frac{\mathrm{m_s c_s}}{\mathrm{t}_r A_s}\right) \frac{d\hat{T}_s}{d\hat{t}} \left(\frac{1}{\hat{T}_f - \hat{T}_s}\right) \frac{T_\infty}{T_\infty} \tag{3.25}$$

$A_s \sim s^2$ , $m_s \sim s^3$ and $\mathrm{c_s}$ is not very significantly for typical insulation materials, so that the insulation on scaled model might be written;

$$\frac{k_i}{\delta_i} \sim \left(\frac{\mathrm{m_s c_s}}{\mathrm{t}_r A_s}\right) \sim \frac{s^3 s^0}{s^{1/2} s^2} \sim s^{1/2} \tag{3.26}$$

When the same material for insulation is used in both prototype and model for a scale ($k_i \sim \mathrm{s}^0$), the thickness of insulation must be scaled;

$$\delta_i \sim s^{-1/2} \tag{3.27}$$

A summary of scaling rules based on all Equations, which are shown above, can be shown in Table 3.2. The fire compartment and the structure are both geometrically scaled, and the time is scaled according to $t \sim \mathrm{s}^{1/2}$ (Equation 3.5). (Wang, 2006)

| Design parameters | Scaling rules |
|---|---|
| **Scaling rules for fuel design wood cribs** | |
| **Thickness of wood sticks, $b_c$** | $s^{1/3}$ |
| **Spacing between wood sticks, $s_c$** | $s^{1/3}$ |
| **Length of wood sticks, $L_c$** | $s^{7/6}$ |
| **Number of layers, $N_c$** | $s^{1/3}$ |
| **Number of wood stick per layer, $n_c$** | $s^{5/6}$ |
| **Scaling rules for compartment design** | |
| **Wall material, $k_w$ and $\rho_w$** | $s^{3/2}$ |
| **Thickness of wall, $\delta_w$** | $s^{1/4}\left(\frac{k_w}{\rho_w c_w}\right)^{1/2}$ |
| **Scaling rules for insulation on steel structures** | |
| **Properties of insulation, $k_i$ and $\rho_i$** | $s^0$ |
| **Thickness of insulation, $\delta_i$** | $s^{-1/2}$ |
| **Scaling rules for structures** | |
| **Structural loadings, P and M** | $P \sim s^2$ , $M \sim s^3$ |
| **Boundary constrain, K** | s |

Table 3.2: Scaling rules for fire, insulation and structures (Wang, 2006, p. 93)

After applying the scaling rules, the section sizes and section properties of small-scaled are found. The drawings of the frame of the full-scaled and small-scaled structure are shown in Appendix B. Plan of the structure for both small-scaled and real structures are shown in Appendix B.

## 3.3 Composite Beam Design and Modelling in Fire

The analysis and design of composite beam with steel column and without concrete encasement is divided into two steps;

- Thermal analysis, in other words to estimate the temperature distribution in the cross section,
- Mechanical analysis, for calculation of the resistances of the member under fire.

*Thermal analysis*; EC4 Part 1.2 (BSI 2005b) is about the design of composite steel and concrete structures-general rule and structural fire design which applies the same rules with the EC3 Part 1.2 to calculate the temperatures of unprotected or protected sections.

*Mechanical analysis*; In EC4 Part 1.2 (BSI 2005b) two methods are given to estimate the sagging bending moment resistance of beams without concrete encasement. One of them is the Critical Temperature Method and the other one is Bending Moment

Resistance Method. However, in this dissertation The Critical Temperature Method will be considered.

The Critical Temperature Method

If the simply supported composite beams including hot-rolled down stand steel sections up to 500 mm depth and concrete slabs whose thickness is not less than 120 mm, this method can be used to calculate the temperature and also it is assumed that the temperature distribution on the steel sections is uniform.

The critical temperature is a function of the load level for fire design that is calculated as;

$$\eta_{fi,t} = = \frac{M_{fi,Sd}}{M_{pl,Rd}} \tag{3.28}$$

Where $M_{fi,Sd}$ is the action of loads in fire and $M_{pl,Rd}$ is the resistance bending moment of the section, $M_{fi,Sd}$ is calculated as,

$$M_{fi,Sd} = \frac{q_{fi}\ L^2}{8} \tag{3.29}$$

$$q_{fi} = \sum \gamma_{GA} G_k + \psi_{1,1}\ Q_{k,1} + \sum \psi_{2,i}\ Q_{k,i} + \sum A_d \tag{3.30}$$

Where, $q_{fi}$ is the design load in fire and $\gamma_{GA} = 0.5$ $\psi_{1,1} = 1$ .

The critical temperature of the steel section is determined from the load level and from the strength of the steel at elevated temperature.

$$f_{a\max,\theta_{cr}} = 0.9\eta_{fi,t}\, f_{ay,20^o C} \tag{3.31}$$

The strength reduction coefficient at time t is determined from Equation 3.32 can be shown below.

$$k_{\max,\theta} = \frac{f_{a\max,\theta_{cr}}}{f_{ay,20^o C}} \tag{3.32}$$

Finally critical temperature ($\theta_{crit}$) can be found by using the EC4, Part 1.2, Table 3.2, usually it needs to interpolate the values to work out the critical temperature.

### 3.3.1 Design of Full-Scaled Composite Beam in Fire (Primary Beam)

The calculations for full-scaled model and reduced scale model have been done properly. First of all the loads for prototype in terms of permanent and variable have been determined and according to these loads, design bending moment ($M_{Sd}$) has been calculated. After then, Universal Beam (UB) section has been selected due to the design bending moment. Resistance bending moment ($M_{pl,Rd}$) must be more than design bending moment, so this check has been approved. The second step, which was defined above, is to estimate the critical temperature ($\theta_{crit}$) for the composite beam. At the same time the fire resistance time (required time) according to the critical temperature has been estimated from the equation for heating of unprotected steel cross-sections either computationally or using the Fire Excel sheets (2010). This step was done by using the Excel Spread Sheets and also checked by hand calculation which is shown in Appendix A.

The calculations and quantities to find the critical temperature in the beam can be shown in Table 3.4.

As can be seen from Table 3.3 that the fire resistance time is 15.6 minutes < 90 minutes so it is necessary to reduce the heating of the steel part by using fire protection material. Plasterboard is considered as a protection material for full-scaled composite beam. The thickness, density, specific heat and thermal conductivity of plasterboard can be seen in Table 3.5. As fire compartment, it is considered externally fully glazed over 3.0 m from floor to ceiling height for both primary and secondary beams. The properties of fire compartment can be shown below.

| **Opening and Enclosure** | |
|---|---|
| **Floor Area, $A_f$** | 36.0 $m^2$ |
| **Total vertical opening, $A_v$** | 18.0 $m^2$ |
| **Average of windows height on all walls, $h_{eq}$** | 3.0 m |
| **Total area of enclosure, $A_t$** | 168.0 $m^2$ |
| **Density of wall material, $\rho_w$** | 1600 $kg/m^3$ |
| **Specific heat, $c_w$** | 840 J/kg$^o$K |

Table 3.3: The properties of fire compartment

| Design Specification | |
|---|---|
| **Characteristic floor loading** | $G_k = 4$ kN/m$^2$   $Q_k = 5$ kN/m$^2$ |
| **Floor sizes** | Span B = 6 m   Span L = 6 m |
| **Material properties** | Steel grade, $f_y = 275$ N/mm$^2$<br>Concrete grade, $f_{ck} = 30$ N/mm$^2$ |
| **Selected section** | UB 305×165×54 |
| **Section characteristics** | Thickness of concrete slab, $h_c = 130$ mm<br>Effective width of concrete slab, $b_{eff} = 1600$ mm<br>Neutral axis, $x_c = 69.56$ mm |
| **Ultimate limit state design at ambient temperature** | Partial factors, $\gamma_G = 1.35$ and $\gamma_{Q,1} = 1.5$<br>Design loads, $G_d = 32.4$ kN/m and $Q_d = 45$ kN/m |
| **Design bending moment** | $M_{Sd} = 348.3\, kNm$ |
| **Resistance bending moment** | $M_{pl,Rd} = 473.8\, kNm\ [> M_{Sd}]\, OK$ |
| **Action and combination factors** | $\gamma_{GA} = 0.5$ and $\psi_{1,1} = 1.0$ |
| **Design load in fire** | $q_{fi} = 42$ kN/m |
| **Action of loads in fire** | $M_{fl,Sd} = 189\, kNm$ |
| **Load level for fire design** | $\eta_{fi,t} = 0.4 < [1]$ OK |
| **Strength of the steel at elevated temperature** | $f_{a\max,\theta_{cr}} = 99$ N/mm$^2$ |
| **Strength reduction coefficient at time t** | $k_{max,\theta} = 0.36$ |
| **Critical temperature** | $\theta_{crit} = 646.2\ ^oC$ |
| **Fire resistance time for unprotected steel** | t = 15.6 minutes |
| **Protected Steel temperature for 90 minutes** | $\theta_a = 542.8\ ^oC < \theta_{crit}$   $(OK)$ |

Table 3.4: Design of full-scaled composite beam in fire (Primary beam)

| Properties of Protection Material | |
|---|---|
| **Material** | Plasterboard |
| **Thickness, $d_p$** | 20 mm |
| **Density, $\rho_p$** | 950 kg/m$^3$ |
| **Specific Heat, $c_p$** | 840 J/kg$^o$K |
| **Thermal Conductivity, $\lambda_p$** | 0.160 W/m$^o$K |

Table 3.5: Properties of protection material (plasterboard)

With the aid of fire excel sheet, the steel temperature will be estimated 542.8$^o$C at 90 minute if the standard fire is considered, hence it is less than the critical temperature ($\theta_{crit} = 646.2\ ^oC$). That means the thickness of fire protection is suitable for composite beam.

### 3.3.2 Design of Full-Scaled Composite Beam in Fire (Secondary Beam)

Design of secondary beam in fire has been done by using Excel spreadsheet. The section was chosen as UB 305×102×28 depending on the design bending moment. After chosen the section, critical temperature method was applied to estimate the critical temperature ($\theta_{crit}$) in the beam. The fire resistance time (required time) according to the critical temperature has been estimated from the equation for heating of unprotected steel cross-sections either computationally or using the Fire Excel sheets (2010). After then, fire compartment was defined in terms of floor area, average windows height on all walls and total area of vertical opening and enclosure. The fire resistance time is considered 90 minutes for this structure, so the time for unprotected steel sections was less than 90 minutes. In other words, fire protection was needed for composite beam to protect against fire for 90 minutes. As fire protection material, plasterboard was considered. Depending on the thickness of insulation, the protected steel temperature was checked against the critical temperature. In this design of beam the standard fire is considered. All calculations to design these secondary beams can be shown in Table 3.6. The detailed drawings for full-scaled composite beam are shown in Appendix B. The hand calculations for secondary beam are shown in Appendix A.

| Design Specification | |
|---|---|
| **Characteristic floor loading** | $G_k = 4$ kN/m$^2$ $Q_k = 5$ kN/m$^2$ |
| **Floor sizes** | Span B = 3 m Span L = 6 m |
| **Material properties** | Steel grade, $f_y = 275$ N/mm$^2$<br>Concrete grade, $f_{ck} = 30$ N/mm$^2$ |
| **Selected section** | UB 305×102×28 |
| **Section characteristics** | Thickness of concrete slab, $h_c = 130$ mm<br>Effective width of concrete slab, $b_{eff} = 850$ mm<br>Neutral axis, $x_c = 68.3$ mm |
| **Ultimate limit state design at ambient temperature** | Partial factors, $\gamma_G = 1.35$ and $\gamma_{Q,1} = 1.5$<br>Design loads, $G_d = 16.2$ kN/m & $Q_d = 22.5$ kN/m |
| **Design bending moment** | $M_{Sd} = 174.2\ kNm$ |
| **Resistance bending moment** | $M_{pl,Rd} = 247.0\ kNm\ [> M_{Sd}]\ OK$ |
| **Action and combination factors** | $\gamma_{GA} = 0.5$ and $\psi_{1,1} = 1.0$ |
| **Design load in fire** | $q_{fi} = 21$ kN/m |
| **Action of loads in fire** | $M_{fl,Sd} = 94.5\ kNm$ |
| **Load level for fire design** | $\eta_{fi,t} = 0.4 < [1]$ OK |

| | |
|---|---|
| **Strength of the steel at elevated temperature** | $f_{a\max,\theta_{cr}}$ = 94.7 N/mm$^2$ |
| **Strength reduction coefficient at time t** | $k_{max,\theta}$ = 0.344 |
| **Critical temperature** | $\theta_{crit}$ = 652.4 $^o$C |
| **Fire resistance time for unprotected steel** | t = 12.38 minutes |
| **Protected Steel temperature for 90 minutes** | $\theta_a$ = 592.6 $^o$C < $\theta_{crit}$ (*OK*) |
| **Properties of Protection Material** | |
| **Material** | Plasterboard |
| **Thickness, $d_p$** | 25 mm |
| **Density, $\rho_p$** | 950 kg/m$^3$ |
| **Specific Heat, $c_p$** | 840 J/kg$^o$K |
| **Thermal Conductivity, $\lambda_p$** | 0.160 W/m$^o$K |

Table 3.6: Design of full-scaled composite beam in fire (Secondary beam)

### 3.3.3 Design of Small-Scaled Composite Beams in Fire

Design of 1/5-scale ( $s = 1/5$) composite beams follows the same procedure. However, first of all, prototype composite beams (UB 305×165×54 and UB 305×102×28) are modelled as 1/5-scale which is shown Table 3.7, and then resistance bending moment needs to be calculated according to the section sizes of model. After calculated the resistance bending moment, it must be equal or bigger than design bending moment. Resistance bending moment is equal to design bending moment, the primary and variable loads can be estimated from design bending moment. However, the loads for prototype are lower than the loads for model. Hence, it should be put more weights or loads on 1/5-scale model such as sand to make deflection under fire conditions. After calculating the primary and variable loads, critical temperature can be estimated and also the resistance time can be modelled according to the time modelling rules. It is highly possible that the resistance time for unprotected steel will be small value. Therefore, it needs to be protected by protection material such as plasterboard, but the thickness of protection must be modelled according to the rules of insulation scaling.

If the heat capacity of insulation materials is neglected and the same material is used in both prototype and model, the thickness of protection material might be estimated. It can be shown in Table 3.9. Section properties of 1/5-scaled model can be shown in Table 3.7. The detailed drawings for full-scaled composite beam are shown in Appendix B. The hand calculations for secondary beam are shown in Appendix A.

| Section Properties | Primary | Secondary |
|---|---|---|
| **Depth of Section "h" (mm)** | 62.08 | 61.74 |
| **Width of Section "b" (mm)** | 33.38 | 20.36 |
| **Thickness of web "s" (mm)** | 1.58 | 1.2 |
| **Thickness of Flange "t" (mm)** | 2.74 | 1.76 |
| **Root Radius "r" (mm)** | 1.78 | 1.52 |
| **Depth between fillets "d" (mm)** | 53.04 | 55.18 |
| **Ratios for Local Buckling of Flange "b/2t"** | 6.091 | 5.78 |
| **Ratios for Local Buckling of Web "d/s"** | 33.570 | 45.98 |
| **Second Moment of Area of Axis x-x "$I_x$" ($cm^4$)** | 18.72 | 8.59 |
| **Second Moment of Area of Axis y-y "$I_y$" ($cm^4$)** | 1.7008 | 0.25 |
| **Elastic Modulus of Axis x-x "$Z_x$" ($cm^3$)** | 6.032 | 2.784 |
| **Elastic Modulus of Axis y-y "$Z_y$" ($cm^3$)** | 1.016 | 0.244 |
| **Plastic Modulus of Axis x-x "$S_x$" ($cm^3$)** | 6.768 | 3.224 |
| **Plastic Modulus of y-y "$S_y$" ($cm^3$)** | 1.568 | 0.39 |
| **Area of Section "A" ($cm^2$)** | 2.752 | 1.44 |

Table 3.7: Section properties of 1/5 scaled-model

The results of calculations of 1/5-scaled model can be shown in Table 3.8.

| Design Specification | Primary Beam | Secondary Beam |
|---|---|---|
| **Characteristic floor loading ($kN/m^2$)** | $G_k$ = 7.44 $Q_k$ = 5.00 | $G_k$ = 7.44 $Q_k$ = 5.00 |
| **Floor sizes (m)** | Span B = 1.2<br>Span L = 1.2 | Span B = 0.6<br>Span L = 1.2 |
| **Material properties ($N/mm^2$)** | Steel grade, $f_y$ = 275<br>Concrete grade, $f_{ck}$ = 30 | $f_y$ = 275<br>$f_{ck}$ = 30 |
| **Selected section** | 1/5-scale model of<br>UB 305×165×54 | 1/5-scale model of<br>UB 305×102×28 |
| **Section characteristics (mm)** | Thickness of concrete slab, $h_c$ = 26<br>Effective width of concrete slab, $b_{eff}$ = 320<br>Neutral axis,<br>$x_c$ = 13.9118 | $h_c$ = 26<br>$b_{eff}$ = 170<br>$x_c$ = 13.7 |
| **Ultimate limit state design at ambient temperature (kN/m)** | Partial factors,<br>$\gamma_G$ = 1.35 and $\gamma_{Q,1}$ = 1.5<br>Design loads,<br>$G_d$ = 12.0528<br>$Q_d$ = 9.00 | $\gamma_G$ = 1.35 $\gamma_{Q,1}$ = 1.5<br>$G_d$ = 6.0264<br>$Q_d$ = 4.5 |
| **Design bending moment (kNm)** | $M_{Sd} = 3.7895$ | $M_{Sd} = 1.8948$ |
| **Resistance bending moment (kNm)** | $M_{pl,Rd} = 3.7904$<br>$M_{pl,Rd} > M_{Sd}$ (OK) | $M_{pl,Rd} = 1.9807$<br>$M_{pl,Rd} > M_{Sd}$ (OK) |

| | | |
|---|---|---|
| **Action and combination factors** | $\gamma_{GA}$ = 0.5 and $\psi_{1,1}$ = 1.0 | $\gamma_{GA}$ = 0.5 and $\psi_{1,1}$ = 1.0 |
| **Design load in fire (kN/m)** | $q_{fi}$ = 10.464 | $q_{fi}$ = 5.232 |
| **Action of loads in fire (kNm)** | $M_{fl,Sd} = 1.8835$ | $M_{fl,Sd} = 0.9418$ |
| **Load level for fire design** | $\eta_{fi,t}$ = 0.5 < [1] (OK) | $\eta_{fi,t}$ = 0.476 < [1] (OK) |
| **Strength of the steel at elevated temperature ($N/mm^2$)** | $f_{a\max,\theta_{cr}}$ = 123.75 | $f_{a\max,\theta_{cr}}$ = 117.68 |
| **Strength reduction coefficient at time t** | $k_{max,\theta}$ = 0.45 | $k_{max,\theta}$ = 0.42 |
| **Critical temperature** | $\theta_{crit}$ = 608.3 $^{o}$C | $\theta_{crit}$ = 620.83 $^{o}$C |
| **Fire resistance time for unprotected steel** | t = 7 minutes ($t \sim s^{1/2}$) | t = 5.54 minutes ($t \sim s^{1/2}$) |
| **Thickness of fire protection material** | $d_p$ = 45 mm ($d_p \sim s^{-1/2}$) | $d_p$ = 55.90 mm ≈ 56 mm ($d_p \sim s^{-1/2}$) |

Table 3.8: Design of small-scaled composite beams in fire

| **Properties of Protection Material for Composite Beams** | |
|---|---|
| **Material** | Plasterboard |
| **Thickness, $d_p$** | 45 mm and 56 mm |
| **Density, $\rho_p$** | 950 $kg/m^3$ |
| **Specific Heat, $c_p$** | 840 $J/kg^{o}K$ |
| **Thermal Conductivity, $\lambda_p$** | 0.160 $W/m^{o}K$ |

Table 3.9: Properties of protection material (plasterboard)

# CHAPTER – 4

## 4.1 Composite Slab Design and Modelling in Fire (Unprotected)

Composite slabs are usually designed as unpropped construction when cast put onto ribbed steel decking. This system has advantages in terms of speed and simple construction. It must ensure all three criteria which are integrity criterion (“E”), insulation criterion (“I”) and load-bearing criterion (“R”). One assumption is that the steel decking is not insulated but is directly exposed to fire over its length in other words it is heated directly. Moreover, there is no protection material between the structural concrete slab and surface screeds.

As considering the insulation criterion, the thickness at full depth sections (“ribs) and at the thinner sections (“trough”) of composite slab has an effect on the insulation of composite slab. The cross-section of composite slab is subjected to a two dimensional variation of temperature of the type that can be determined by a constant temperature (isotherms). The limiting isotherm is used to find the parts of concrete section which are neglected and considered in calculating the hogging resistance and also is used to determine the “effective thickness” factor to simplify the insulation criterion.

The aim of the insulation criterion is to make sure that the average temperature at the top surface does not exceed 140 $^{o}$C and that the maximum temperature does not exceed 180 $^{o}$C at the fire resistance period which is specified. (Burgess 2010a)

$$t_i = a_0 + a_1 h_1 + a_2 \Phi + a_3 \frac{A}{L_r} + a_4 \frac{1}{l_3} + a_5 \frac{A}{L_r}\frac{1}{l_3} \quad \text{EC4 Part 1.2 Annex D (D.1)} \qquad (4.1)$$

Where, $A/L_r$ is the section factor for the rib outstands,

$h_1$ is the depth of the thinner portion of the slab,

$l_3$ is the width of the thinnest section, the “trough” of the profile,

and $\Phi = \left( \sqrt{{h_2}^2 + \left( l_3 + \frac{l_1 - l_2}{2} \right)^2} - \sqrt{{h_2}^2 + \left( \frac{l_1 - l_2}{2} \right)^2} \right) / l_3$ is a “view factor” which defines the reduced surface area exposed to radiation by non-flat surfaces. All parameters can be seen in Figure 4.1 below. (Burgess 2010a)

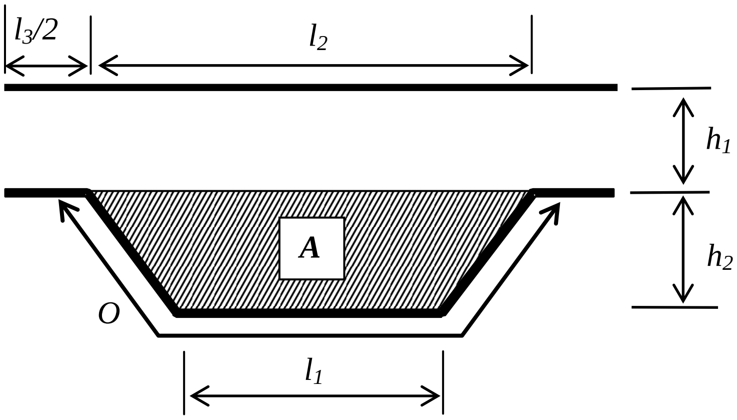


Figure 4.1: Relevant dimensions of a ribbed slab for insulation and resistance (Burgess 2010a)

The coefficients in Equation 4.1 are taken from EC4 Part 1.2 Annex D (Table D.1) which is for normal weight and light weight concrete.

When criterion "R" is considered, both strength and flexural stiffness of slab decrease due to the high temperature. Rules which are given in EC4 Part 1.2, estimation of load bearing capacity are based on plastic global analysis.

**Sagging moment resistance**

The steel decking temperatures vary for different parts in terms of bottom flange, web, and top flange. The equation for these with the insulation criterion can be shown below.

$$\theta = b_0 + b_1 \frac{1}{l_3} + b_2 \frac{A}{L_r} + b_3 \Phi + b_4 \Phi^2 \qquad (4.2)$$

The coefficients for normal-weight and light-weight concrete in Equation 4.2 are found in EC4 Part 1.2 Annex D (D.2) Table D.2.

The temperature of the reinforcement depends on its place outside of the heated surface. These distances are $u_1, u_2$ *and* $u_3$ which are shown in Figure 4.2, and also the function of the mean position ("z") of these distances means the reinforcement temperature as;

$$\frac{1}{z} = \frac{1}{\sqrt{u_1}} + \frac{1}{\sqrt{u_2}} + \frac{1}{\sqrt{u_3}} \qquad (4.3)$$

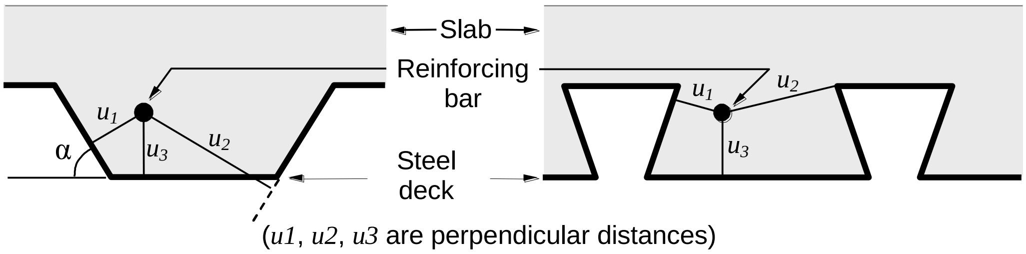


Figure 4.2: Geometrical position of the rebar (Burgess 2010a, p. 8)

There are some limitations on the edge distances of the reinforcement which are that $u_1 \geq$ 50mm, $u_2 \geq$ 50mm, and $u_3 \geq$ 35mm. Equation (3.36) shows the reinforcement temperature at different times when standard fire is considered;

$$\theta_s = c_0 + c_1 \frac{u_3}{h_2} + c_2 z + c_3 \frac{A}{L_r} + c_4 \alpha + c_5 \frac{1}{l_3} \tag{4.4}$$

The variables which are included in this equation are found in EC4 Part 1.2 Annex D (D.2) Table D.3.

**Hogging moment resistance**

**Simplified "effective thickness" method**

Effective thickness method ( $h_{eff}$ ) is a more conservative method only applicable in restricted circumstances. Besides, this method is also suitable for flat slabs. An effective slab thickness is calculated by;

$$h_{eff} = h_1 + 0.5 h_2 \left( \frac{l_1 + l_2}{l_1 + l_3} \right) \text{ for } h_2 / h_1 \leq 1.5 \text{ and } h_1 > 40 \text{ mm} \tag{4.5}$$

$$h_{eff} = h_1 \left[ 1 + 0.75 \left( \frac{l_1 + l_2}{l_1 + l_3} \right) \right] \text{ for } h_2 / h_1 > 1.5 \text{ and } h_1 > 40 \text{ mm} \tag{4.6}$$

All variables, which have seen in Equation 4.5 and 4.6, can be shown in Figure 4.3.

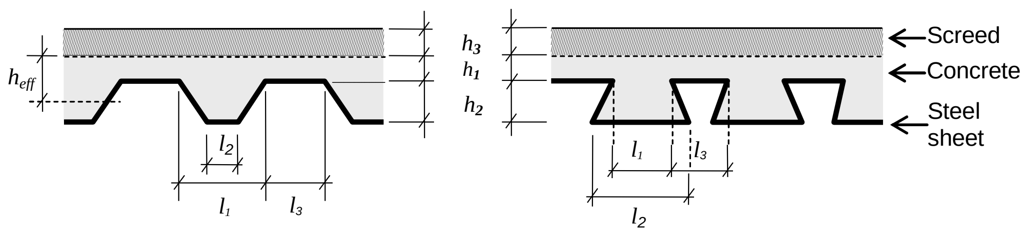


Figure 4.3: Slab dimensions for estimation of effective thickness
(Burgess 2010a, p. 11)

When $l_3 > 2l_1$ the effective thickness is taken as the continuous thickness $h_1$. As it mentioned before, this also applies to flat slabs.

**General method**

Using this method to calculate the hogging moment resistance is to use the concrete at normal strength in compression, on the other hand hot face of concrete which lies beyond the isotherm is neglected at the required fire resistance time. The concrete temperature is limited in the isotherm four points from I to IV which can be shown in Figure 4.4.

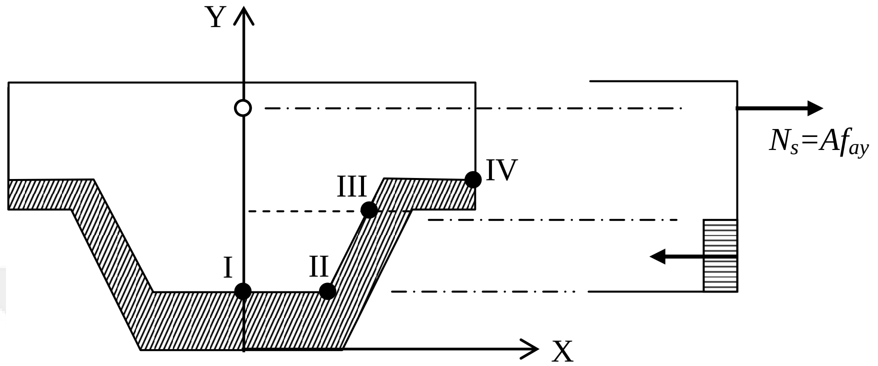


Figure 4.4: Location of the isotherm for limiting concrete temperature in hogging (Burgess 2010a, p. 9)

Equation 4.7 shows the value of limiting temperature can be shown below.

$$\theta_{lim} = d_0 + d_1 N_s + d_2 \frac{A}{L_r} + d_3 \Phi + d_4 \frac{1}{l_3} \tag{4.7}$$

The coefficients for normal and light weight concrete are taken from table in EC4 Part 1.2 Annex D (D.3) Table D.4.

The positions of four points, which limit the temperature isotherm, are calculated as;

Point I: $$\begin{cases} X_I = 0 \\ Y_I = \dfrac{1}{\left(\dfrac{1}{z} - \dfrac{4}{\sqrt{l_1 + l_3}}\right)^2} \end{cases}$$

Point II: $$\begin{cases} X_{II} = \dfrac{1}{2} l_2 + \dfrac{Y_I}{sin\ \alpha}(cos\,\alpha - 1) \\ Y_{II} = \dfrac{1}{\left(\dfrac{1}{z} - \dfrac{4}{\sqrt{l_1 + l_3}}\right)^2} \end{cases}$$

Point III: $$\begin{cases} X_{III} = \dfrac{1}{2} l_1 - \dfrac{b}{\sin \alpha} \\ Y_{III} = h_2 \end{cases}$$

Point IV: $\begin{cases} X_{IV} = \dfrac{1}{2} l_1 \\ Y_{IV} = h_2 + b \end{cases}$ Where,

$$b = \frac{1}{2} l_1 \sin \alpha \left(1 - \frac{\sqrt{a^2 - 4ac}}{a}\right) \text{ in "}b\text{", } a = \left(\frac{1}{z} - \frac{1}{\sqrt{h_2}}\right) \text{ and } \begin{cases} c = -8(1 + \sqrt{1+a}\,) \text{ if } a \geq 8 \\ c = +8(1 + \sqrt{1+a}\,) \text{ if } a < 8 \end{cases}$$

(Burgess 2010a)

## 4.2 Design of Full-Scaled Composite Slab in Fire

First of all the loads for full scaled composite slab have been determined in terms of steel sheet load, concrete and finishes as the permanent loads and variable loads. Suitable steel decking has been chosen from Corus whose properties can be shown below.

| Name | Profile | Deck Depth, $h_2$ (mm) | Trough Spacing, $l_1$ (mm) | Trough Width, $l_2$ (mm) | Crest Width, $l_3$ (mm) |
|---|---|---|---|---|---|
| **Corus Pmf Comflor 51** | Re-entrant | 51 | 112.5 | 137.5 | 40 |

Table 4.1: Steel decking properties (Corus 2007)

Effective thickness of the composite slab has been found based on steel decking properties using effective thickness method. After calculation the effective thickness, design loads at ambient temperature has been calculated to estimate the design moments in terms of sagging moment at span ($M_{sag}$) and hogging moment at mid support ($M_{hog}$). However, applied sagging and hogging moment depend on reduction factor which is related to the load combination factor ($\psi_{1,1}$). On the other hand, there is a limitation for steel sheet profile which needs to be checked according to EC4, Part 1.2, Annex D, Section D.5.

Scope of application

EC4, Part 1.2, Annex D, Section D.5

| Field of application | | Actual values | | | |
|---|---|---|---|---|---|
| Re-entrant steel sheet profiles | Trapezoidal steel sheet profiles | | | | |
| 70 mm ≤ $l_1$ ≤ 135 mm | 80 mm ≤ $l_1$ ≤ 155 mm | $l_1$ = | 112.5 | mm | [ OK ] |
| 110 mm ≤ $l_2$ ≤ 150 mm | 32 mm ≤ $l_2$ ≤ 132 mm | $l_2$ = | 137.5 | mm | [ OK ] |
| 38.5 mm ≤ $l_3$ ≤ 97.5 mm | 40 mm ≤ $l_3$ ≤ 115 mm | $l_3$ = | 40 | mm | [ OK ] |
| 50 mm ≤ $h_1$ ≤ 130 mm | 50 mm ≤ $h_1$ ≤ 125 mm | $h_1$ = | 79 | mm | [ OK ] |
| 30 mm ≤ $h_2$ ≤ 60 mm | 50 mm ≤ $h_2$ ≤ 100 mm | $h_2$ = | 51 | mm | [ OK ] |

[ The slab is WITHIN the scope of application ]

Figure 4.5: Scope of application (Fire 11 Excel Spreadsheet)

All calculations, which have been done by fire excel spreadsheet and hand-calculation, can be shown in Table 4.2.

| **Design Specification** | |
|---|---|
| **Characteristic floor loading** | <u>Permanent Loads:</u><br>Steel sheet, $G_{p,k}$ = 0.20 kN/m$^2$<br>Concrete, $G_{c,k}$ = 2.80 kN/m$^2$<br>Finishes, $G_{f,k}$ = 1.00 kN/m$^2$<br><u>Variable Loads:</u><br>Live load, $Q_{k,1}$ = 5.00 kN/m$^2$ |
| **Material properties** | <u>Steel Sheet:</u><br>Yield stress: $f_{p,y}$ = 255 N/mm$^2$<br>Geometry of cross section, $h_1$ = 79 mm<br>Thickness, $t_p$ = 0.7 mm<br>Cross-sectional area, $A_p$ = 1296.8 mm$^2$/m<br><u>Concrete:</u><br>Type, light-weight $f_{c,k}$ = 30 N/mm$^2$<br>Height, $h_c$ = 130 mm<br>Cross-sectional area, $A_c$ = 120803.3 mm$^2$/m |
| **Effective thickness of slab** | $h_{eff}$ = 120.8 mm |
| **Ultimate limit state design at ambient temperature** | Partial factors, $\gamma_G$ = 1.35 and $\gamma_{Q,1}$ = 1.5<br>Design loads, $G_d$ = 5.4 kN/m$^2$ and $Q_d$ = 7.5 kN/m$^2$<br><u>Design moment:</u><br>Sagging moment at span, $M_{sag}$ =32.51 kNm/m<br>Hogg. moment at mid-support, $M_{hog}$ =58.05 kNm/m |
| **Design at fire situation** | Combination factor, $\psi_{1,1}$ = 0.5<br>Reduction factor, $\eta_{fi}$ = 0.504<br>Applied sagging moment, $M_{fi,Sd,sag}$ = 16.4 kNm/m<br>Applied hogging moment, $M_{fi,Sd,hog}$ = 29.3 kNm/m |

Table 4.2: Design of full-scaled composite slab in fire

After all design calculations, this stage is to work out the fire resistance according to the thermal insulation criterion. Fire resistance time is considered as 90 minutes for this building. Sagging moment resistance and hogging moment resistance has been calculated according to the design rules which were described above. In other words, the temperature of rebar and the parts of steel decking such as lower flange, web and upper flange, and also compressive resistance of concrete and plastic moment resistance of slab have been calculated. All results for sagging moment can be shown in Table 4.3 below to estimate the sagging moment resistance. Hence, sagging moment resistance of slab should be compared with the design sagging moment.

| Sagging Moment Resistance of Slab | |
|---|---|
| **Considered standard fire resistance time** | R = 90 min. |
| **Fire resistance time of slab** | $t_i$ = 128.2 min. |
| **Sagging moment resistance** | $M_{fi,Rd,sag}$ = 43.3 kNm/m<br>$M_{fi,Rd,sag} > M_{fi,Sd,sag}$ = 16.380 kNm<br>**The composite slab is SATISFACTORY against sagging moment** |
| **Compressive resistance of concrete** | $F_c$ = 85.4 kN |
| **Plastic moment resistance of concrete** | $M_c$ = 0.937 kNm |
| **Plastic moment resistance of slab [EC4, Part 1.2, Section 4.3.1]** | $M_{fi,Rd}$ = 6.597 kNm |

Table 4.3: Calculations for sagging moment

As can be seen from Table 4.3 and also shown in Appendix, sagging moment resistance of slab is more than sagging design moment, so the composite slab is adequate.

The coefficients (e.g. $b_0, b_1, b_2$) for the determination of temperature of the steel decking parts are obtained from EC4, Part 1.2, Annex D, Section D.2. In terms of coefficients of rebar; the location and diameter of rebar, which were calculated, are shown in Table 4.4.

| Properties of rebar in the rip | |
|---|---|
| **Yield strength,** $f_{s,y}$ | 500 N/mm$^2$ |
| **Rebar diameter,** $\Phi$ | 20 mm |
| **Distance,** $u_3$ | 50 mm |
| **Distance,** $u_1$ | 56.3 mm |
| **Distance,** $u_2$ | 56.3 mm |
| **Angle of web,** $\alpha$ | 103.8$^o$ |
| **Rebar position in the rib,** $z$ | **2.45 mm$^{-0.5}$** |
| **Temperature,** $\theta_\delta$ | **552.5 $^o$C** |

Table 4.4: Properties for the determination of temperature of rebar in the rib

The coefficients (e.g. $c_0, c_1, c_2$) for the determination of temperature of the rebar in the rib are obtained from EC4, Part 1.2, Annex D, Table D.3. Besides, the values of reduction factors ($k_{y,a}$) and carrying capacities ($Z$) were taken from EC3, Part 1.2, Table E.1 for steel sheet and EC4, Part 1.2, Table 3.4 for rebar.

The calculation for hogging moment resistance follows the same procedure however, the differences is to use the tension bar and its properties that is shown in Table 4.5.

| Hogging Moment Resistance of Slab | |
|---|---|
| **Considered standard fire resistance time, R** | 90 minutes |
| **Yield strength of tension bar,** $f_{s,y}$ | 500 N/mm$^2$ |
| **Rebar diameter,** $\Phi$ | 20 mm |
| **Tension bar cover,** $c$ | 30 mm |
| **Angle of web,** $\alpha$ | 103.8$^o$ |
| **Normal force in hogging rebar,** $N_s$ | 245.4 kN |
| **Hogging moment resistance of slab,** $M_{fi,Rd,hog}$ | $M_{fi,Rd,hog}$ = 77.3 kNm/m<br>$M_{fi,Rd,hog} > M_{fi,Sd,hog}$ = 29.250 kNm<br>**The composite slab is SATISFACTORY against hogging moment** |

Table 4.5: Calculations for hogging moment

The coefficients (e.g. $c_0, c_1, c_2$) for the determination of temperature of the tension rebar are obtained from EC4, Part 1.2, Annex D, Table D.3. As mentioned in general method to calculate the hogging moment resistance, the coefficients to determine the limiting temperature (e.g. $d_0, d_1, d_2$) are taken from EC4, Part 1.2, Annex D, Section D.4. Location of the limiting temperature isotherm and limiting temperature ($\theta_{lim}$) and also rebar position in the rib (z) is shown Table 4.6 below.

| **a (mm)** | **c (mm)** | **b (mm)** | **Point** | **$X_i$ (mm)** | **$Y_i$ (mm)** | **$\theta_{lim}$ [$^o$C]** | **z [mm$^{-0.5}$]** |
|---|---|---|---|---|---|---|---|
| 14.056 | - 39.042 | 15.319 | I<br>II<br>III<br>IV | 0<br>27.0<br>40.5<br>66.3 | 32.7<br>32.7<br>51<br>66.3 | **727.6** | **2.005** |

Table 4.6: Location of limiting temperature isotherm

## 4.3 Design of Small-Scaled Composite Slab in Fire

The response of compressive load is more important for any model concrete because the main property of concrete as a structural material is to carry the compression loads. The behaviour of prototype concrete under compression can be seen in a model concrete. Model concrete mixes must be designed properly and carefully to represent not only the tensile strength, time dependent behaviour but also the strength and the strain-stress relation under compression. In terms of materials included in model concrete mix, the cement is the same material in both prototype and model but aggregates are different. For the model aggregates, ordinary well-graded concrete sand and sometimes fine crushed stone or pea gravel for larger-scale models are used with scaling of the particles. 'The finer particles in the model mix are limited to less than 10 % passing the U.S. No. 100 sieve (0.149 mm mesh)' (Harris & Sabnis, 1999, p. 155). The amount of aggregate which is used in concrete mix is significantly effect on the mechanical properties of model concrete.

A study about the influence of particle size distribution, shape and texture of sand in micro concrete confirmed the earlier findings (Wijayasri, 1983). The tensile strength ratio of a mix which has single size aggregate is higher than that of a well-graded mix, because the reduction in bond between the cement paste and aggregate has an effect on the tensile strength. For a given cube strength ( $f_{cu}$ ) might be modelled by simulating either the secant modulus ($E_c$) or the ultimate strain ($\varepsilon_u$) or the strain at peak stress ($\varepsilon_o$). However, the ultimate strain cannot be evaluated accurately. (Harris & Sabnis, 1999)

The modelling of composite slab, the micro concrete can be used for concrete part. For the reinforcement part, to select and model the correct reinforcement for a concrete scaled model is the single and the most important step in the all process of modelling. The process can be shown in a scheme below.

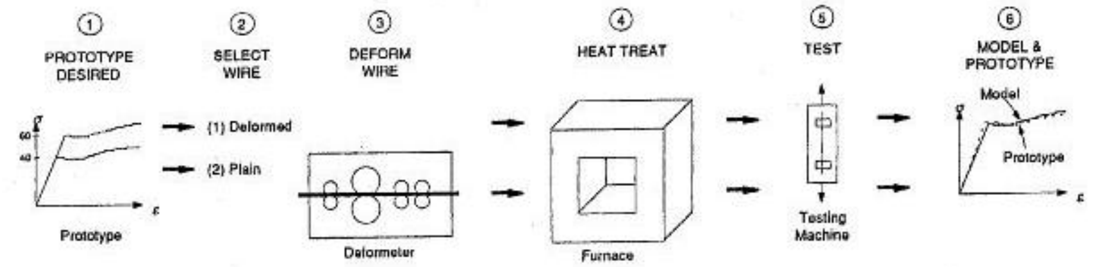


Figure 4.6: Steps needed for producing scaled model reinforcement

(Harris & Sabnis, 1999, p. 231)

The first step is to determine the required prototype stress-strain curve. If the model wire is plain, it needs to be deformed and then tested to represent the required stress-strain properties. If the model wire is one of deformed bars, it may not require annealing in order to satisfy the requirements of stress-strain properties. Although deformed bars are used, some annealing will always be required and a compromise must sometimes be made on the spacing and height of the available surface deformations. (Harris & Sabnis, 1999)

For this modelling of composite slab, Black annealed wire can be considered as model reinforcement. Micro concrete models may be reinforced with black annealed wire which can be found in the form of rolls. The wire is cold-drawn and annealed in the special factory. Before used in models, it must be straightened by pulling. Hence this process strains the wire sufficiently to destroy the yield point. The type of wires can be found in Figure 4.7. Each curve has different characteristic property when they used in the micro concrete models.

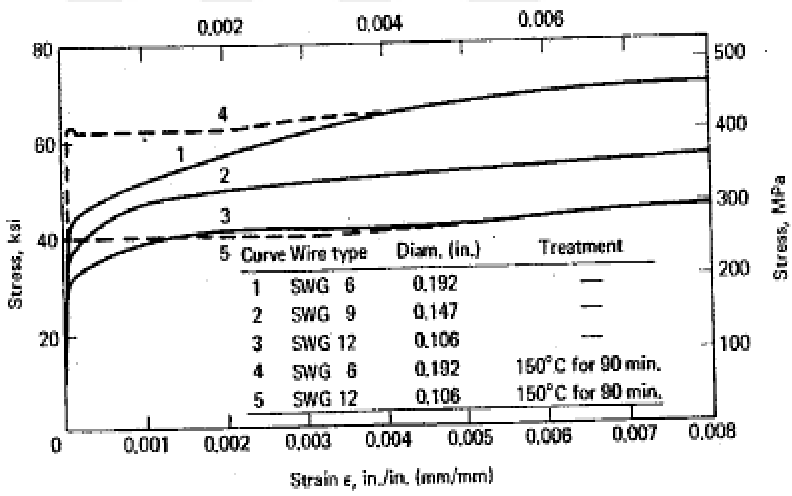


Figure 4.7: Stress-strain curves of wires (Harris & Sabnis, 1999, p. 233)

Curves 4 and 5 are more suitable for the stress-strain curves of prototype reinforcing steel, because the shape and the behaviour of curves are quite close to the reinforcing steel behaviour in prototype. Moreover, the wires, which have small-diameter, have too high strength. Because of this reason, when they are used in the concrete model, they will be useful in model studies. It must be noted that when the wires annealed, the yield strength can be reduced to the desired value.

If the composite slab is modelled 1/5-scale, the overall floor zone will be 150 mm including raised floor, slab, beam and services such as ceiling & lighting. The drawing can be shown in Appendix B.

## 4.4 Design of Wood Cribs

The fire power in a scaled model should be according to the Equation 3.2 which is $\dot{Q} \sim s^{5/2}$. A typical office fuel load is between 20 kg/m$^2$ and 60 kg/m$^2$ (Wang et al., 2007). In the design of wood cribs, 40 kg/m$^2$ is assumed as the fuel load for a typical floor. Using the typical floor area of 36 m$^2$, the approximate burning rate is calculated by,

$$\dot{m} \approx \frac{m}{t} = \frac{40\ kg/m^2 \times 36\ m^2}{120\ \text{min} \times 60\ s/\text{min}} = 0.20\ \text{kg/s}$$

The average burning rate is scaled according to the $\dot{m} \sim s^{5/2}$. Hence, the burning rate of the fuel in the 1/5-scale model is approximately 3.58 g/s and the burning time according to the time scale ($t \sim s^{1/2}$) is approximately 53.7 minutes. Wood cribs can be made of pine whose density is 530 kg/m$^3$. They are used as the fuel in the model. The total mass of fuel is calculated as,

3.58 g/s × 53.7 min×60 s/min = 11.53 kg

(11.53 kg×9.81 N/kg = 113.11 N = 0.11kN)

The weight of one wood crib is 0.11 kN. If this load converts to the uniform distributed load, it will be 0.08 kN/m$^2$. When three wood cribs are used for a small-scaled slab the increase of the total load will be 0.24 kN/m$^2$. Therefore, the total variable loads have been increased from 4 kN/m$^2$ to 7.44 kN/m$^2$ in the design of composite beam. The weight of wood cribs is added to 4 kN/m$^2$.

Wood sticks were designed as square cross-sections. The design parameters of wood cribs can be shown in Table 4.7. They were scaled according to the scaling rules which were shown in Table 3.2.

| Fire scenario | | | | |
|---|---|---|---|---|
| **Scale** | $N_c$ | $n_c$ | $b_c$ (mm) | $L_c$ ( mm) |
| **1** | 5 | 24 | 19.1 | 800 |
| **1/5** | 3 | 6 | 11 | 122 |

Table 4.7: Design parameters of cribs

The properties of wood cribs can be drawn in Figure 4.8.

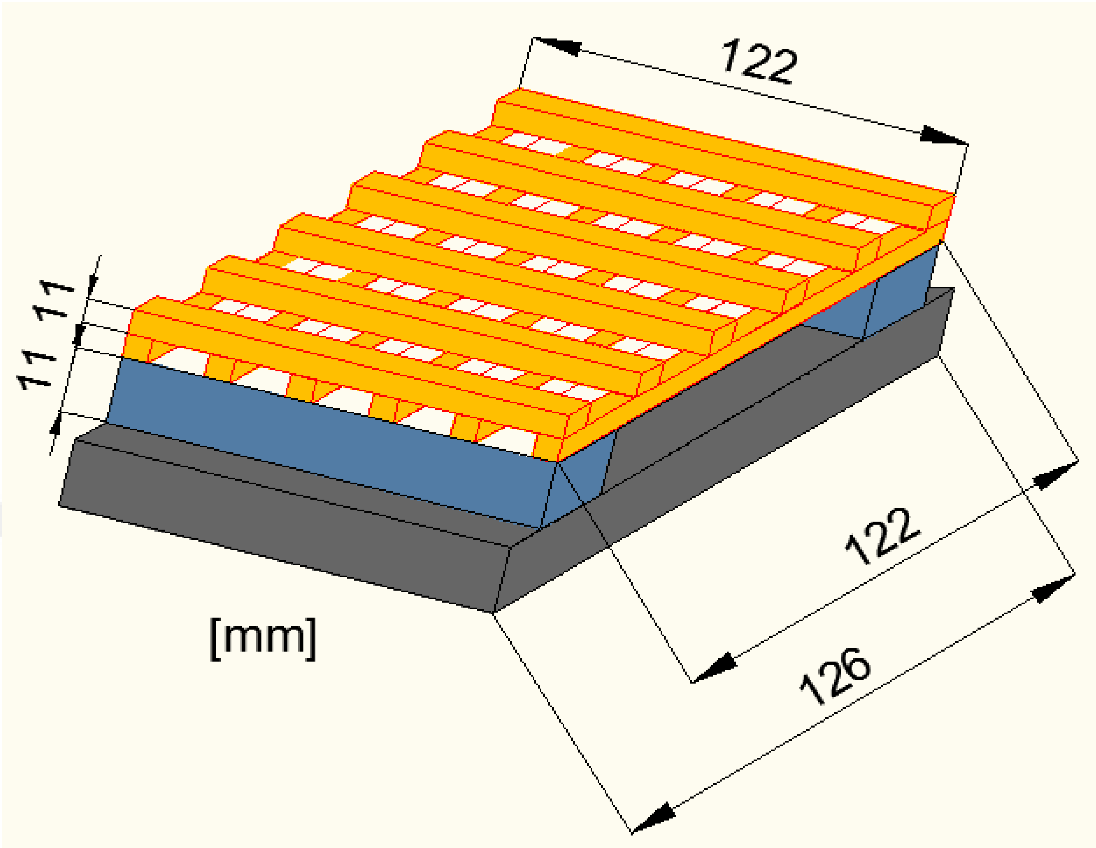


Figure 4.8: Configuration of wood cribs

# CHAPTER – 5

## 5.1 Steel Column Design and Modelling in Fire

The first important issue, which needs to be considered, is buckling resistance of the column section depending on the total design axial load. Moreover this axial load changes with the column position in terms of edge, corner, internal. After checking all these things, column is expected to be stable with fire protection under fire conditions. The equations, which are shown below, are taken from EC3 Part 1-2 (BSI, 2005c) and EC3 Part 1-1.

### Lateral-Torsional Buckling

When the compression flange is not continuously restrained, the design resistance moment against lateral-torsional buckling for Class 1 or 2 sections is calculated by equation which comes from Eurocode 3 Part 1-1.

$$M_{b,fi,t,Rd} = \chi_{LT,fi} W_{pl,y} k_{y,\theta,com} \frac{f_y}{\gamma_{M,fi}} \tag{4.1}$$

Where, $\chi_{LT,fi}$ : Lateral-torsional buckling reduction factor in fire design situation

$k_{y,\theta,com}$ : Yield strength reduction factor at the maximum compression flange temperature at time t

The lateral torsional buckling reduction factor $\chi_{LT,fi}$ is determined at normal temperature from EC3, Part 1.1, Section 6.3.1.2. Otherwise, the normalised slenderness used is adapted to the high-temperature steel properties;

$$\bar{\lambda}_{LT,\theta,com} = \bar{\lambda}_{LT} \sqrt{\frac{k_{y,\theta,com}}{k_{E,\theta,com}}} \tag{4.2}$$

Where, $k_{E,\theta,com}$ : Elastic modulus reduction factor at the maximum compression flange temperature at time t

The imperfection factor "α" for fire situation is determined as,

$$\alpha = 0.65 \sqrt{\frac{235}{f_y}} \tag{4.3}$$

The design buckling resistance of columns for Class 1, 2 and 3 is calculated as,

$$N_{b,fi,t,Rd} = \chi_{fi} A\, k_{y,\theta,max} \frac{f_y}{\gamma_{M,fi}} \tag{4.4}$$

It can be understood from Equation 4.4 that there is a reduction in strength and an increase in normalised slenderness at high temperatures.

The normalised slenderness of the column for the maximum temperature is,

$$\bar{\lambda}_{\theta,max} = \bar{\lambda} \sqrt{\frac{k_{y,\theta,max}}{k_{E,\theta,max}}} \tag{4.5}$$

The buckling length "$l_{fi}$", which takes different values for top storey and intermediate storeys, can be shown in Figure 5.1.

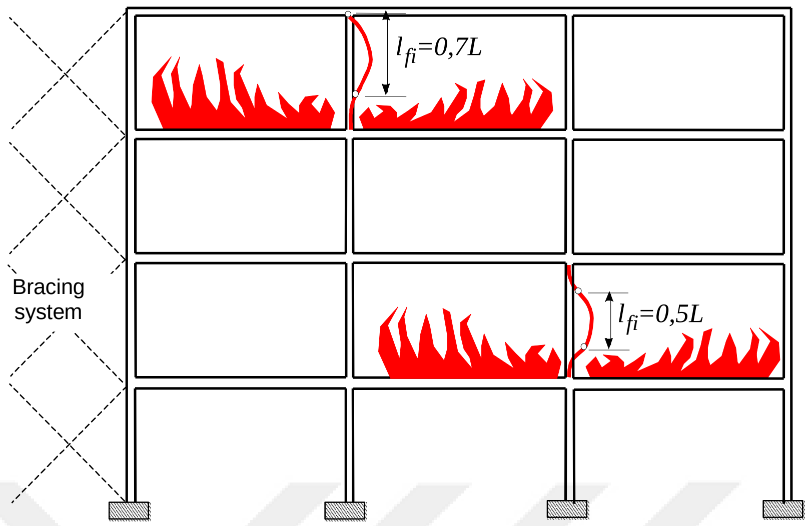


Figure 5.1: Buckling lengths of column in fire (Burgess, 2010b, p. 17)

## 5.2 Design of Full-Scaled Steel Columns in Fire

The loading conditions, floor and column height and also material properties are identical for all type of columns in terms of internal, edge and corner. They are shown in Table 5.1.

| General specification of columns | |
|---|---|
| **Characteristic floor loading** | $G_k$ = 4 kN/m$^2$ $Q_k$ = 5 kN/m$^2$ |
| **Floor and column sizes** | Span B = 6 m Span L = 6 m<br>Column height = 4 m |
| **Material properties** | Steel grade, $f_y$ = 275 N/mm$^2$<br>Elastic Modulus, E = 210000 N/mm$^2$ |

Table 5.1: General specification of columns

In terms of insulation, all columns are protected by box protection. Their properties are shown in Table 5.2.

| Properties of Protection Material | Internal | Edge | Corner |
|---|---|---|---|
| **Material** | Box protection | Box protection | Box protection |
| **Thickness, $d_p$** | 10 mm | 10 mm | 10 mm |
| **Density, $\rho_p$** | 2100 kg/m$^3$ | 2100 kg/m$^3$ | 2100 kg/m$^3$ |
| **Specific Heat, $c_p$** | 900 J/kg$^o$K | 900 J/kg$^o$K | 900 J/kg$^o$K |
| **Thermal Conductivity, $\lambda_p$** | 1.50 W/m$^o$K | 1.50 W/m$^o$K | 1.50 W/m$^o$K |

Table 5.2: Insulation properties of full-scaled columns

### 5.2.1 Design of Internal Columns

Internal columns carry the maximum load compared with corner and edge columns. The design of column in fire applies the similar procedure with beam design however they should be checked against the ultimate limit state design at ambient temperature whether they will satisfy the lateral torsional buckling. The summary of design in terms of loading conditions, material properties of steel and concrete, design axial compression and buckling resistance can be shown in Table 5.3.

| Design Specification | |
|---|---|
| **Selected section** | UC 254×254×132 |
| **Floor area** | 36 $m^2$ |
| **Section classification** | Web, d/s = 15.6 (Section is Class 1)<br>Flange, b/2t = 6.31 (Section is Class 1)<br>Therefore, the section is Class 1.<br>(EC3, Table 5.2) |
| **Ultimate limit state design at ambient temperature** | Partial factors, $\gamma_G$ = 1.35 and $\gamma_{Q,1}$ = 1.5<br>Design loads, $G_d$ = 194.4 kN/m<br>$Q_d$ = 270 kN/m<br>One floor total load = 464.4 kN<br>Number of floors = 5<br>Design load from upper 4 floors = 1857.6 kN<br>Extra factored dead load (cladding etc.) = 45 kN<br>**Total design axial compression load, $N_{sd}$ = 2367 kN** |
| **Design at normal temperature** | Buckling resistance, $N_{b,Rd}$ = 2715.24 kN<br>**$N_{b,Rd} > N_{sd}$ (OK)** |

Table 5.3: Design of full-scaled steel internal columns in fire

After checking the buckling resistance of section, the column can be designed at fire situation. Design loading in fire is figured out to compare with buckling resistance at time t with uniform temperature. As fire compartment, it is considered externally fully glazed over 3.0 m from floor to ceiling height. It can be shown in Figure 5.2. The properties of fire compartment can be shown in Table 5.4.

| Opening and Enclosure | |
|---|---|
| **Floor Area, $A_f$** | 36.0 $m^2$ |
| **Total vertical opening, $A_v$** | 18.0 $m^2$ |
| **Average of windows height on all walls, $h_{eq}$** | 3.0 m |
| **Total area of enclosure, $A_t$** | 168.0 $m^2$ |
| **Density of wall material, $\rho_w$** | 1600 $kg/m^3$ |
| **Specific heat, $c_w$** | 840 $J/kg^oK$ |

Table 5.4: Fire compartment properties

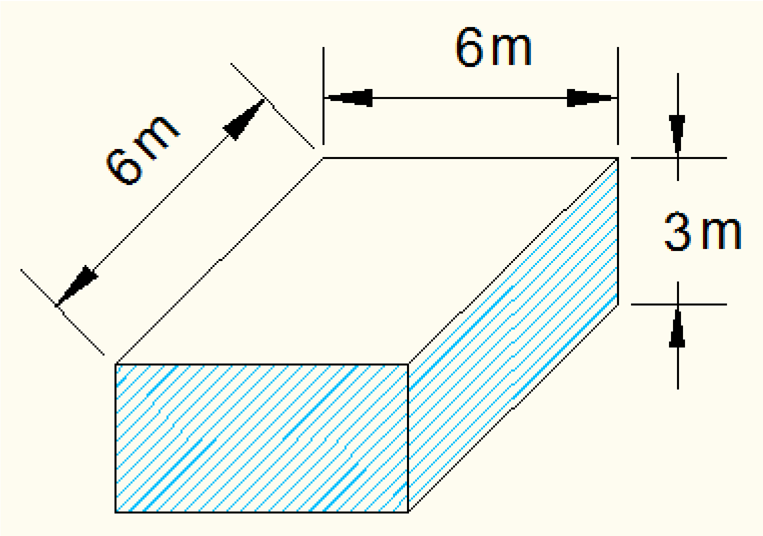


Figure 5.2: Fire compartment

Internal columns are protected by box protection whose properties can be seen below.

After box protection for 90 minutes, the steel temperature is 1001.9 °C while maximum temperature is 1049.0 °C when the standard fire is considered for internal columns.

Lastly, buckling resistance ( $N_{bi,fi,t,Rd}$ ) at time t with uniform $\theta_a$ is 2322.6 kN while design loading in fire ( $N_{fi,sd}$ ) is 1192.74 kN. $N_{bi,fi,t,Rd} > N_{fi,sd}$ , so this internal column can resist 90 minutes to fire.

### 5.2.2 Design of Edge Columns

The method of design of edge columns is the same as the design of internal columns. The same procedure which has been shown in the design of internal columns applied to design of edge columns under fire conditions. With the aid of fire excel spread sheets, the section will be UC 203×203×86. The summary of design can be shown in Table 5.5.

| Design Specification | |
|---|---|
| **Selected section** | UC 203×203×86 |
| **Floor area** | 18 $m^2$ |
| **Section classification** | Web, d/s = 12.7 (Section is Class 1)<br>Flange, b/2t = 5.1 (Section is Class 1)<br>Therefore, the section is Class 1.<br>(EC3, Table 5.2) |
| **Ultimate limit state design at ambient temperature** | Partial factors, $\gamma_G$ = 1.35 and $\gamma_{Q,1}$ = 1.5<br>Design loads, $G_d$ = 97.2 kN/m<br>$Q_d$ = 135 kN/m<br>One floor total load = 232.2 kN<br>Number of floors = 5<br>Design load from upper 4 floors = 928.8 kN<br>Extra factored dead load (cladding etc.) = 45 kN<br>**Total design axial compression load, $N_{sd}$ = 1206 kN** |
| **Design at normal temperature** | Buckling resistance, $N_{b,Rd}$ = 1881.53 kN<br>**$N_{b,Rd} > N_{sd}$ (OK)** |

Table 5.5: Design of full-scaled steel edge columns in fire

The properties of fire compartment are identical which was shown in the design of internal columns.

Edge columns are protected by box protection whose properties were shown in Table 5.4. The thickness of insulation ($d_p$) is 10 mm for edge columns. After box protection for 90 minutes, the steel temperature is 1002.0 $^oC$ while maximum temperature is 1049.0 $^oC$ when the standard fire is considered for edge columns.

Buckling resistance ( $N_{bi,fi,t,Rd}$ ) at time t with uniform $\theta_a$ is 1315.7 kN while design loading in fire ( $N_{fi,sd}$ ) is 607.674 kN. $N_{bi,fi,t,Rd} > N_{fi,sd}$ , so the edge columns can resist 90 minutes to fire.

### 5.2.3 Design of Corner Columns

Because of the position of corner columns, floor area and axial compression load for these columns changes and the section will be UC 203×203×52. The loads in terms of permanent, variable and the material properties, which have been used to design of corner columns, are the same as the design of edge and internal columns. The load conditions, material properties of steel, concrete and buckling resistance can be shown in Table 5.6.

| **Design Specification** | |
|---|---|
| **Selected section** | UC 203×203×52 |
| **Floor area** | 9 $m^2$ |
| **Section classification** | Web, d/s = 20.4 (Section is Class 1)<br>Flange, b/2t = 8.17 (Section is Class 1)<br>Therefore, the section is Class 1.<br>(EC3, Table 5.2) |
| **Ultimate limit state design at ambient temperature** | Partial factors, $\gamma_G$ = 1.35 and $\gamma_{Q,1}$ = 1.5<br>Design loads, $G_d$ = 48.6 kN/m<br>$Q_d$ = 67.5 kN/m<br>One floor total load = 116.1 kN<br>Number of floors = 5<br>Design load from upper 4 floors = 464.4 kN<br>Extra factored dead load (cladding etc.) = 45 kN<br>**Total design axial compression load, $N_{sd}$ = 625.5 kN** |
| **Design at normal temperature** | Buckling resistance, $N_{b,Rd}$ = 1105.17 kN<br>**$N_{b,Rd} > N_{sd}$ (OK)** |

Table 5.6: Design of full-scaled steel corner columns in fire

Corner columns are protected by box protection whose properties are identical with the edge and internal columns. The thickness of protection ($d_p$) is 10 mm for corner columns. After box protection for 90 minutes, the steel temperature is 1003.5 $^oC$ while maximum temperature is 1049.0 $^oC$ when the standard fire is considered for corner column.

Buckling resistance ( $N_{bi,fi,t,Rd}$ ) at time t with uniform $\theta_a$ is 616.2 kN while design loading in fire ( $N_{fi,sd}$ ) is 315.174 kN. $N_{bi,fi,t,Rd} > N_{fi,sd}$ , so the corner columns can resist 90 minutes to fire.

## 5.3 Design of Small-Scaled Steel Columns in Fire

All type of columns in terms of internal, edge and corner were modelled 1/5-scale. However, axial compression load was calculated depending on the characteristic floor loading of composite floor model. The section properties of 1/5-scaled columns model can be shown in Table 5.7.

| Section (1/5-scaled internal column model) | Internal | Edge | Corner |
|---|---|---|---|
| **Depth of Section "h" (mm)** | 55.26 | 44.44 | 41.24 |
| **Width of Section "b" (mm)** | 52.26 | 41.02 | 40.86 |
| **Thickness of web "s" (mm)** | 3.06 | 2.54 | 1.58 |
| **Thickness of Flange "t" (mm)** | 5.06 | 4.1 | 2.5 |
| **Root Radius "r" (mm)** | 2.54 | 2.04 | 2.04 |
| **Depth between fillets "d" (mm)** | 40.06 | 32.16 | 32.16 |
| **Ratios for Local Buckling of Flange "b/2t"** | 5.16 | 5.002 | 8.172 |
| **Ratios for Local Buckling of Web "d/s"** | 13.1 | 12.661 | 20.354 |
| **Second Moment of Area of Axis x-x "Ix" ( $cm^4$)** | 36.048 | 15.12 | 8.41 |
| **Second Moment of Area of Axis y-y "Iy" ($cm^4$)** | 12.0496 | 5.003 | 2.85 |
| **Elastic Modulus of Axis x-x "Zx" ($cm^3$)** | 13.048 | 6.8 | 4.08 |
| **Elastic Modulus of Axis y-y "Zy" ($cm^3$)** | 4.608 | 2.392 | 1.392 |
| **Plastic Modulus of Axis x-x "Sx" ($cm^3$)** | 14.952 | 7.816 | 4.536 |
| **Plastic Modulus of y-y "Sy" ($cm^3$)** | 7.024 | 3.648 | 2.112 |
| **Area of Section "A" ($cm^2$)** | 6.72 | 4.4 | 2.652 |

Table 5.7: The section properties of 1/5-scaled columns

The loading conditions, floor and column sizes and also material properties are identical for all type of columns in terms of internal, edge and corner. They are shown in Table 5.8.

| General specification of columns | |
|---|---|
| **Characteristic floor loading** | $G_k = 7.44$ kN/m$^2$ $Q_k = 5$ kN/m$^2$ |
| **Floor and column sizes** | Span B = 1.2 m Span L = 1.2 m<br>Column height = 0.8 m |
| **Material properties** | Steel grade, $f_y = 275$ N/mm$^2$<br>Elastic Modulus, E = 210000 N/mm$^2$ |

Table 5.8: General specification of columns

In terms of insulation, all columns are protected by box protection. Their properties are shown in Table 5.9.

| Properties of Protection Material | Internal | Edge | Corner |
|---|---|---|---|
| **Material** | Box protection | Box protection | Box protection |
| **Thickness, $d_p$ ($d_p$~$s^{-1/2}$)** | 22.36 ≈ 25 mm | 22.36 ≈ 25mm | 22.36 ≈ 25 mm |
| **Density, $\rho_p$** | 2100 kg/m$^3$ | 2100 kg/m$^3$ | 2100 kg/m$^3$ |
| **Specific Heat, $c_p$** | 900 J/kg$^o$K | 900 J/kg$^o$K | 900 J/kg$^o$K |
| **Thermal Conductivity, $\lambda_p$** | 1.50 W/m$^o$K | 1.50 W/m$^o$K | 1.50 W/m$^o$K |

Table 5.9: Scaling of insulation for small-scaled columns

### 5.3.1 Modelling of Internal Columns

The calculations to estimate the compression load in all type of columns have been done by using MATLAB. All MATLAB codes are shown in Appendix. The summary of modelling of internal columns is shown in Table 5.10.

| Modelling of Internal Columns | |
|---|---|
| **Selected section** | 1/5-scaled of UC 254×254×132 |
| **Floor area** | 1.44 m$^2$ |
| **Section classification** | Web, d/s = 13.1 (Section is Class 1)<br>Flange, b/2t = 5.16 (Section is Class 1)<br>Therefore, the section is Class 1.<br>(EC3, Table 5.2) |
| **Ultimate limit state design at ambient temperature** | Partial factors, $\gamma_G$ = 1.35 and $\gamma_{Q,1}$ = 1.5<br>Design loads, $G_d$ = 14.46 kN/m<br>$Q_d$ = 10.8 kN/m<br>One floor total load = 25.26 kN<br>Number of floors = 5<br>Design load from upper 4 floors = 101.04 kN<br>Extra factored dead load (cladding etc.) = 4.5 kN<br>**Total design axial compression load, $N_{sd}$=130.8 kN** |
| **Design at normal temperature** | **Buckling resistance, $N_{b,Rd}$ = 135.27 kN**<br>**$N_{b,Rd} > N_{sd}$ (OK)** |
| **Buckling resistance at time t with uniform $\theta_a$ ($N_{b,fi,t,Rd}$) and design load in fire ($N_{fi,Sd}$)** | **$N_{b,fi,t,Rd}$ = 123.95 kN**<br>**$N_{b,fi,t,Rd} > N_{fi,Sd}$ = 65.92 kN (OK)** |
| **Fire resistance time** | t = 40.25 minutes ($t \sim s^{1/2}$) |

Table 5.10: Design of small-scaled internal steel column

As can be seen from Table 5.10 that total design axial compression load ($N_{sd}$) is 130.8 kN while this load for prototype was 2367 kN. This can be concluded that the load is not proportional with the scaling factor. In other words, according to the Equation 3.11 ($P \sim s^2$), total design axial compression load should have been 94.68 kN. However, the loads on the composite floor have been increased to make the deflection (e.g. $G_k$ has been increased from 4 kN/m$^2$ to 7.44 kN/m$^2$). If it has not been increased, the total design axial compression for 1/5-scaled model would be 92.88 kN which is quite close to the scaling rule's result.

Fire compartment, which was considered externally fully glazed over 3.0 m from floor to ceiling height in prototype, can be modelled and shown in Figure 5.3. The properties and the wall materials of fire compartment can be modelled according to the scaling rules for compartment design. They are shown in Table 5.11. The scaling rules for compartment design are taken from Table 3.2.

| **Opening and Enclosure** | |
|---|---|
| **Floor Area, $A_f$** | 1.44 m$^2$ |
| **Total vertical opening, $A_v$** | 0.72 m$^2$ |
| **Average of windows height on all walls, $h_{eq}$** | 0.6 m |
| **Total area of enclosure, $A_t$** | 6.72 m$^2$ |
| **Density of wall material, $\rho_w$ ($\rho_w \sim s^{3/2}$)** | 143.11 kg/m$^3$ |
| **Specific heat, $c_w$ ($c_w \sim s^{3/2}$)** | 75.13 J/kg$^o$K |

Table 5.11: Scaling of fire compartment

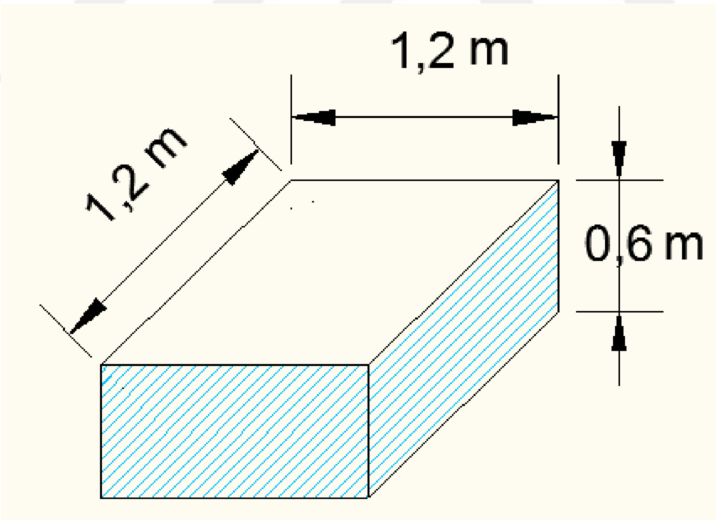


Figure 5.3: Modelling of fire compartment

### 5.3.2 Modelling of Edge Columns

The calculations to find the design axial compression load and buckling resistance have been done by MATLAB. The design loads ($G_d$ and $Q_d$) and axial compression load from 4 upper floors are half of the design loads of internal columns due to the design floor area. The results and comparisons are shown in Table 5.12.

| **Modelling of Edge Columns** | |
|---|---|
| **Selected section** | 1/5-scaled of UC 203×203×86 |
| **Floor area** | 0.72 $m^2$ |
| **Section classification** | Web, d/s = 12.66 (Section is Class 1)<br>Flange, b/2t = 5.002 (Section is Class 1)<br>Therefore, the section is Class 1.<br>(EC3, Table 5.2) |
| **Ultimate limit state design at ambient temperature** | Partial factors, $\gamma_G$ = 1.35 and $\gamma_{Q,1}$ = 1.5<br>Design loads, $G_d$ = 7.23 kN/m<br>$Q_d$ = 5.4 kN/m<br>One floor total load = 12.63 kN<br>Number of floors = 5<br>Design load from upper 4 floors = 50.52 kN<br>Extra factored dead load (cladding etc.) = 4.5 kN<br>**Total design axial compression load, $N_{sd}$=67.65 kN** |
| **Design at normal temperature** | **Buckling resistance, $N_{b,Rd}$ = 75.26 kN**<br>**$N_{b,Rd} > N_{sd}$ (OK)** |
| **Buckling resistance at time t with uniform $\theta_a$ ($N_{b,fi,t,Rd}$) and design load in fire ($N_{fi,Sd}$)** | **$N_{b,fi,t,Rd}$ = 112.56 kN**<br>**$N_{b,fi,t,Rd} > N_{fi,Sd}$ = 31.83 kN (OK)** |
| **Fire resistance time** | t = 40.24 minutes ($t \sim s^{1/2}$) |

Table 5.12: Design of small-scaled edge steel column

The comparison between small-scaled edge columns and small-scaled internal columns is that when smaller sections are modelled, the differences between the value of buckling resistance at time t with uniform $\theta_a$ ($N_{b,fi,t,Rd}$) and design load value in fire is increasing, so it can be concluded that the thickness of fire protection material can be reduced. Moreover, this comparison might be seen between buckling resistance and total design axial compression load. That's why if a column section is modelled geometrically according to the scaling rules the buckling resistance of column always will be higher than design axial compression load and the differences will be higher in small sections.

The properties of fire compartment in terms of total vertical opening, the average windows height on walls, total area of enclosure and density are considered the same as the design of internal columns. The material of walls is the light-weight concrete. The protection material, which is used in the prototype, is used in the model. The thickness of protection material can be modelled according to the scaling rules. The properties of protection material are shown below.

### 5.3.3 Modelling of Corner Columns

The same procedure applies to model the corner columns. The section properties of corner column are modelled geometrically and can be seen below. The design results are shown in Table 5.13.

| **Modelling of Corner Columns** | |
|---|---|
| **Selected section** | 1/5-scaled of UC 203×203×52 |
| **Floor area** | 0.36 $m^2$ |
| **Section classification** | Web, d/s = 20.35 (Section is Class 1)<br>Flange, b/2t = 8.17 (Section is Class 1)<br>Therefore, the section is Class 1.<br>(EC3, Table 5.2) |
| **Ultimate limit state design at ambient temperature** | Partial factors, $\gamma_G$ = 1.35 and $\gamma_{Q,1}$ = 1.5<br>Design loads, $G_d$ = 3.62 kN/m<br>$Q_d$ = 2.7 kN/m<br>One floor total load = 6.32 kN<br>Number of floors = 5<br>Design load from upper 4 floors = 25.28 kN<br>Extra factored dead load (cladding etc.) = 4.5 kN<br>**Total design axial compression load,**<br>**$N_{sd}$ = 36.1 kN** |
| **Design at normal temperature** | **Buckling resistance, $N_{b,Rd}$ = 80.8 kN**<br>**$N_{b,Rd} > N_{sd}$ (OK)** |
| **Buckling resistance at time t with uniform $\theta_a$ ($N_{b,fi,t,Rd}$) and design load in fire ($N_{fi,Sd}$)** | **$N_{b,fi,t,Rd}$ = 70.71 kN**<br>**$N_{b,fi,t,Rd} > N_{fi,Sd}$ = 15.92 kN (OK)** |
| **Fire resistance time** | t = 40.24 minutes ($t \sim s^{1/2}$) |

Table 5.13: Design of small-scaled corner steel column

# CHAPTER – 6 Conclusions and Recommendations

## 6.1 Conclusions

Design of full-scaled structures and small-scaled structures under fire conditions have been completed. The feasibility of using small-scale models to investigate the performance of steel frames in fire has been studied. Calculations to simulate composite structures in fire by using small scale models are explored. Reduced scale model testing is an economical way compared with the full scale tests. Besides, they can expose the behaviour of real structures in a fire. The scaling rules of compartment fires, insulation materials for structures are developed and presented. The calculations following the scaling rules are done by both numerical simulation and using Fire Excel Spreadsheets, and also using MATLAB. The following inferences can be made from this dissertation;

- The scaling factor ( $s = 1/5$ - scale) was applied to the all structural members, the fire compartment and the insulation. The section sizes and the insulation thickness were modelled geometrically.
- The time scale ( $t \sim s^{1/2}$ ) is essential and appropriate scaling rules that were involved in the fire modelling in terms of fire resistance time of unprotected steel and composite structures.
- The proposed scaling rules for designing compartment, insulation on steel structures and structures have been performed based on the time scale ( $t \sim s^{1/2}$ ). The comparisons of results between the different types of columns have been shown and the strategy of partial scaling was used in this dissertation which is appropriate and effective.
- When the same material is used in both prototype and model, the behaviour of the structural models can be identical with the full-scaled structures. Moreover in terms of insulation material, the thickness of the protection material in the model is more than that in the real structure in order to resist the structure to the proposed fire resistance time.
- The loads, which have been used in real structure, have been increased by putting additional sand bags and also the weight of wood cribs on model so as to make the same deflection as that in prototype.

- The tests of insulated steel structural members in scaled compartment fires show the similar temperature of steel profiles. This aid to be economical for testing that can reveal the behaviour of real steel structures.
- The testing of composite beams in scaled fires showed that the comparison of the critical temperatures of beams is quite good and the relative difference is within 6 %. It can be concluded that the failure mechanism, failure time (fire resistance time for unprotected sections) and failure temperature can represent the prototype.
- A slab model with micro concrete and black annealed wire can be considered as a small-scaled composite slab. However, fabrication of wires is a complex process. They need to be produced accurately and carefully to predict the similar behaviour with the full-scaled composite slab. Otherwise, the accuracy of the technique may be low.
- Depending on the heat capacity of insulation, the thickness of insulation is modelled as a scale factor. If the heat capacity of insulation is ignored, the scale factor of insulation thickness can be as $\delta_i \sim s^{-1/2}$ while this scale factor is $\delta_i \sim s^{1/4}$ when the heat capacity of insulation is considered.

## 6.2 Suggestion on future works

There are some issues which need to be improved on scaling the structures. They are discussed and shown below.

- As discussed in previous chapters, the structural performance depends on the temperature under fire condition. The accuracy of the structural behaviour depends on the accuracy of fire scaling. Hence, the scaling part is quite important about behaviour of the real structural system. Many researches can be performed on the conducting scaled fires.
- The modelling of connections between composite slab with steel decking and composite beam with concrete and steel should be improved. Moreover, the different type connections behave differently, so research on scale modelling of these connections could be conducted.
- Research on scale modelling of different structural types such as timber and masonry subjected to fire could be done.
- The behaviour of scale testing of full structures in fire rather than individual members design and modelling of them will be different in terms of local failure and global failure.
- Scale modelling of shear connectors and the behaviour of them in fire-induced phenomena could be conducted.
- The various designs of structural members on different floors will show different behaviour under fire conditions and also it can be resulted in the economical benefit.
- Research on scale modelling of smaller sections should be improved and compared the behaviour in fire with the bigger sections. In other words, the materials, which will be used for smaller sections when they are modelled, should be investigated and conducted.
- Scale testing and modelling of structures exposed to fire require research on theoretical, experimental and finite element validation.

# REFERENCES


Bailey, C. G. & Moore, D. B. (2000), "The structural behaviour of steel frames with composite floor slabs subject to fire: Part 1: Theory" *Structural Engineer*, vol. 78, no. 11, pp. 19–27.

Bažant, Z. P. & Zhou, Y. (2002a), "Addendum to 'Why did the World Trade Center collapse? --- Simple analysis'," *Journal of Engineering Mechanics*, vol. 128, no. 3, pp. 369–370.

Bažant, Z. P. & Zhou, Y. (2002b), "Why did the World Trade Center collapse? --- Simple analysis," *Journal of Engineering Mechanics*, vol. 128, no. 1, pp. 2–6.

BSI (2005a), BS EN 1994-1-1, *Eurocode 4: Design of Composite Steel and Concrete Structures – Part 1-1: General Rules and Rules for Buildings*, 2005: European Committee for Standardization.

BSI (2005b), BS EN 1994-1-2:2005, *Eurocode 4: Design of Composite Steel and Concrete Structures – Part 1-2: General Rules – Structural Fire Design*, 2005: European Committee for Standardization.

BSI (2005c), BS EN 1993-1-2:2005, *Eurocode 3: Design of Steel Structures – Part 1-2: General Rules – Structural Fire Design*, 2005: European Committee for Standardization.

Burgess, I. W. (2010a), Structural Analysis and Design for Fire, CIV6265, [Lecture Notes], *EC4 Fire Engineering Design of Composite Structures*, Structural Analysis and Design for Fire Module, NFATEC, University of Sheffield, Portobello Centre, B59, 4th May 2010.

Burgess, I. W. (2010b), Structural Analysis and Design for Fire, CIV6265, [Lecture Notes], *EC4 Fire Engineering Design of Steel Structures*, Structural Analysis and Design for Fire Module, NFATEC, University of Sheffield, Portobello Centre, B59, 4th May 2010.

Commission of the European Community (CEC) (1987), “Computer assisted analysis of the fire resistance of steel and composite concrete-steel structures (REFAO-CAFIR)”, Final Report, CEC Agreement 7210–SA/502.

Cooke, G. M. E., Lawson, R. M. & Newman, G. M. (1988), “Fire resistance of composite deckslabs”, *The Structural Engineer*, vol. 66, no. 16, pp. 253–261.

Corus International (2007), “ComFlor ® Decking System Composite Floor Decks”, *ComFlor Brochure*, Corus Group.

FEMA (2002), *World Trade Center Building Performance Study: Data Collection, Preliminary Observations, and Recommendations*, in *FEMA 403*, T. McAllister, Editor, Federal Emergency Management Agency: Washington D.C.

Harris, H. G. & Sabnis, G. M. (1999), *Structural Modelling and Experimental Techniques*, CRC Press LLC, Florida.

Hosser, D., Dorn, T. & El-Nesr, O. (1994) “Experimental and numerical studies of composite beams exposed to fire”, *ASCE Journal of Structural Engineering*, vol. 20, no. 10, pp. 2871–2892.

Kordina, K. (1989), “Behaviour of composite columns and girders in fire”, *Proceedings of the Second International Symposium on Fire Safety Science*, Edinburgh.

Leston-Jones, L. C., Burgess, I. W., Lennon, T. & Plank, R. J. (1997), “Elevated-temperature moment-rotation tests on steelwork connections”, *Proceedings of the Institution of Civil Engineers, Structures & Buildings* vol. 122, pp. 410–419.

Newman, G. M. & Lawson, R. M. (1991), “Fire Resistance of Composite Beams”, Technical Report, Publication 109, The Steel Construction Institute.

Pahl, P. J. (1963), Confidence Levels for Structural Models, Report No. 63-05, Department of Civil Engineering, Massachusetts Institute of Technology, Cambridge, February.

Quintiere, J. G., Marzo, M. D. & Becker, R. (2002), "A suggested cause of the fire-induced collapse of the World Trade Towers.", *Fire Safety Journal*, vol. 37, pp. 707–716.

Usmani, A. S., Chung, Y. C. & Torero, J. L. (2003), "How did the WTC towers collapse: A new theory." *Fire Safety Journal*, vol. 38, pp. 501–533.

Yin, Y. Z. & Wang, Y. C. (2005), "Analysis of catenary action in steel beams using a simplified hand calculation method, Part 1: theory and validation for uniform temperature distribution", *Journal of Constructional Steel Research*, 2005. vol. 61, pp. 183-211.

Wainman, D. E. & Kirby, B. R. (1987), *Compendium of UK Standard Fire Test Data, Unprotected Structural Steel – 1,* Ref. No. RS/RSC/S10328/1/98/B, British Steel Corporation (now Corus), Swinden Laboratories, Rotherham.

Wainman, D. E. & Kirby, B. R. (1988), *Compendium of UK Standard Fire Test Data, Unprotected Structural Steel – 2,* Ref. No. RS/RSC/S1199/8/88/B, British Steel Corporation (now Corus), Swinden Laboratories, Rotherham.

Wang, M. (2006), *Scale Modelling of Structural Behaviour*, Ph.D. thesis, University of Maryland (College Park, Md.), viewed 04 August 2010, UM Theses and Dissertations http://hdl.handle.net/1903/3841.

Wang, M., Chang, P. C., Quintiere, J. G. & Marshall, A. (2007), " Scale Modelling of the 96th Floor of World Trade Center Tower 1 ", *ASCE Journal of Performance of Constructed Facilities*, vol. 21, no. 6, pp. 414–421.

Wang, Y. C. (2002), *Steel and Composite Structures Behaviour and Design for Fire Safety*, Spon Press, London.

Wang, Y. C., Lennon, T. & Moore, D. B. (1995), “The behaviour of steel frames subject to fire”, *Journal of Constructional Steel Research*, vol. 35, pp. 291–322.

Wijayasri, S. (1983), Modelling of concrete structures, PhD thesis, North East London Polytechnic.

Xiao, Y., Choo, B. S. & Nethercot, D. A. (1994), “Composite connections in Steel and Concrete. I. Experimental Behaviour of Composite Beam-Column Connections”, *Journal Constructional Steel Research,* vol. 31, pp. 3–30.

Zhao, B. and Kruppa, J. (2004), “Structural behaviour of an open car park under real fire scenarios” *Fire and Materials*, vol. 28, no. 2-4, pp. 269-280.

# Appendix A

# Theoretical Hand Calculation

## A.1 Composite Beam Design (Full-Scaled)

The floor loading conditions, material properties and fire compartment properties are identical for both primary beams and secondary beams.

Characteristic floor loading:

Permanent; $G_k = 4$ kN/m$^2$ Span B = 6 m

Variable; $Q_k = 5$ kN/m$^2$ Span L = 6 m

Materials Properties:

Steel grade; $f_y = 275$ N/mm$^2$

Concrete grade; $f_{ck} = 30$ N/mm$^2$

Fire Compartment:

Opening and Enclosure

Floor Area, $A_f = 6 \times 6 = 36$ m$^2$

Total area of vertical opening, $A_v = 6 \times 3 = 18$ m$^2$

Average windows height on all walls, $h_{eq} = 3$ m

Total area of enclosure, $A_t = 168$ m$^2$

Opening factor, O = 0.19 [but $0.02 \leq O \leq 0.20$]

Wall material, Lightweight concrete

Density, $\rho_w = 1600$ kg/m$^3$

Specific Heat, $c_w = 840$ J/kg$^o$K ($c_w \sim s^{3/2}$)

Thermal Conductivity, $\lambda_w = 0.8$ W/m$^o$K

Fire Load Density

Type of occupancy, Average and office

Fire Protection

Type of exposure, 4-sides exposure

### 1. Primary Beam (UB 305×165×54)

| Designation | Depth of Section | Width of Section | Thickness | | Root Radius | Depth between fillets | Ratios for Local Buckling | | Second Moment of Area | | Elastic Modulus | | Plastic Modulus | | Area of Section |
|---|---|---|---|---|---|---|---|---|---|---|---|---|---|---|---|
| | | | of Web | of Flange | | | Flange | Web | Axis x-x | Axis y-y | Axis x-x | Axis y-y | Axis x-x | Axis y-y | |
| | h mm | b mm | s mm | t mm | r mm | d mm | b/2t | d/s | $I_x$ cm$^4$ | $I_y$ cm$^4$ | $Z_x$ cm$^3$ | $Z_y$ cm$^3$ | $S_x$ cm$^3$ | $S_y$ cm$^3$ | A cm$^2$ |
| UB 305x165x54 | 310.4 | 166.9 | 7.9 | 13.7 | 8.9 | 265.2 | 6.09 | 33.6 | 11700 | 1063 | 754 | 127 | 846 | 196 | 68.8 |

Figure A.1: Section properties of primary beam (from Fire Excel sheet)

Section characteristic:

Thickness of concrete slab; $h_c$ = 130 mm

Effective width of concrete slab; $b_{eff}$ = 1600 mm (L/4 + $b_o$)

$b_o \rightarrow$ width of shear connector (100 mm)

Neutral axis; $x_c = \dfrac{A_a f_{yd}}{0.85 f_{cd} b_{eff}}$ = 69.56 mm

(Neutral axis is in the concrete slab)

Ultimate Limit State Design at Ambient Temperature

Partial factor for permanent actions; $\gamma_G = 1.35$

Partial factor for variable actions; $\gamma_{Q,1} = 1.5$

Design Loads on Beams:

Permanent action, $G_d$ = 32.4 kN/m

Variable actions, $Q_d$ = 45 kN/m

Design Bending Moment, $M_{sd} = \dfrac{(45+32.4)\times 6^2}{8}$ = 348.3 kNm

Resistance Bending Moment, $M_{pl,Rd} = A\times f_{yd}\times( h/2+h_c-0.5x_c )$ = 473.8 kNm

($M_{pl,Rd} > M_{sd}$, OK )

The conditions for use of the critical temperature model are satisfied.

(h < 500 mm [=310.4], $h_c \geq$ 120 mm [= 130], simply supported beam)

Loading in fire situation is obtained from;

$$\sum \gamma_{GA} G_k + \psi_{1,1}\, Q_{k,1} + \sum \psi_{2,i}\, Q_{k,i} + \sum A_d$$

Where; $G_k$ is the permanent action,

$Q_{k,1}$ is the main variable action,

$Q_{k,i}$ are other variable actions,

$A_d$ are indirect fire actions,

For the structure analysed $\gamma_{GA}$ = 0.5 $\psi_{1,1}$ = 1.0 , so

$q_{fi} = (1\times5\times6) + (0.5\times4\times6) = 42$ kN/m

The action of loads in fire is then

$M_{fi,Sd} = (42\times6^2) / 8 = 189$ kNm

Load level for fire design

$\eta_{fi,t} = M_{fi,Sd} / M_{pl,Rd} = 189 / 473.8 = 0.4$ [< 1] OK

Critical Temperature

The critical temperature of the steel section is determined from the load level and from the strength of the steel at elevated temperature as follows:

$f_{a\ max,\theta cr} = 0.9\ \eta_{fi,t} \times f_{ay,20\ C} = 0.9 \times 0.4 \times 275 = 99\ N/mm^2$ ( MPa)

the strength reduction coefficient at time t is;

$k_{max,\theta} = 99 / 275 = 0.36$

The task is now to calculate the critical temperature (the temperature at which the yield strength decreases to the value of 99 MPa) and the time at which the critical temperature will be reached. This will then be compared with the required fire resistance period of 120 min.

By linear interpolation for $k_{max,\theta}$ from Table 3.2 of the Code the value $\boldsymbol{\theta_{crit} = 646.2\ ^oC}$ is obtained.

The required time will be estimated from the equation of unprotected steel cross-sections, either computationally or using the design sheets. Using fire excel spread sheets,

For $\Delta t = 5s$ the fire resistance time is 15.6 minutes < 90 minutes, so it is necessary to reduce the heating of the steel part by using fire protection material.

Protection Material

Material, Plasterboard

**Thickness, $d_p = 20$ mm**

Density, $\rho_p = 950\ kg/m^3$

Specific Heat, $c_p = 840\ J/kg^oK$

Thermal Conductivity, $\lambda_p = 0.16\ W/m^oK$

With the aid of fire excel sheet, the steel temperature will be estimated 542.8 $^oC$ at 90 minute if standard fire is considered, hence it is less than the critical temperature ($\theta_{crit} = 646.2\ ^oC$). That means the thickness of fire protection is suitable for composite beam.

## 2. Secondary Beam (UB 305×102×28)

| Designation | Depth of Section | Width of Section | Thickness of Web | Thickness of Flange | Root Radius | Depth between fillets | Ratios for Local Buckling: Flange | Ratios for Local Buckling: Web | Second Moment of Area: Axis x-x | Second Moment of Area: Axis y-y | Elastic Modulus: Axis x-x | Elastic Modulus: Axis y-y | Plastic Modulus: Axis x-x | Plastic Modulus: Axis y-y | Area of Section |
|---|---|---|---|---|---|---|---|---|---|---|---|---|---|---|---|
| | h mm | b mm | s mm | t mm | r mm | d mm | b/2t | d/s | $I_x$ $cm^4$ | $I_y$ $cm^4$ | $Z_x$ $cm^3$ | $Z_y$ $cm^3$ | $S_x$ $cm^3$ | $S_y$ $cm^3$ | A $cm^2$ |
| UB305x102x28 | 308.7 | 101.8 | 6 | 8.8 | 7.6 | 275.9 | 5.78 | 46 | 5366 | 155 | 348 | 30.5 | 403 | 48.5 | 35.9 |

Figure A.2: Section properties of secondary beam (from Fire Excel sheet)

<u>Section characteristic:</u>

Thickness of concrete slab; $h_c$ = 130 mm

Effective width of concrete slab; $b_{eff}$ = 850 mm (L/4 + $b_o$)

$b_o$ → width of shear connector (100 mm)

Neutral axis; $x_c = \dfrac{A_a f_{yd}}{0.85 f_{cd} b_{eff}} = 68.3$ mm

(Neutral axis is in the concrete slab)

<u>Ultimate Limit State Design at Ambient Temperature</u>

Partial factor for permanent actions; $\gamma_G = 1.35$

Partial factor for variable actions; $\gamma_{Q,1} = 1.5$

Design Loads on Beams:

Permanent action, $G_d$ = 16.2 kN/m

Variable actions, $Q_d$ = 22.5 kN/m

Design Bending Moment, $M_{sd} = \dfrac{(22.5+16.2)\times 6^2}{8} = 174.2$ kNm

Resistance Bending Moment, $M_{pl,Rd} = A\times f_{yd}\times(h/2+h_c - 0.5x_c) =$ 247 kNm

($M_{pl,Rd} > M_{sd}$, OK )

The conditions for use of the critical temperature model are satisfied.

(h < 500 mm [=310.4], $h_c \geq$ 120 mm [= 130], simply supported beam)

Loading in fire situation is obtained from;

$$\sum \gamma_{GA} G_k + \psi_{1,1}\, Q_{k,1} + \sum \psi_{2,i}\, Q_{k,i} + \sum A_d$$

Where; $G_k$ is the permanent action,

$Q_{k,1}$ is the main variable action,

$Q_{k,i}$ are other variable actions,

$A_d$ are indirect fire actions

For the structure analysed $\gamma_{GA}$ = 0.5 $\psi_{1,1}$ = 1.0 , so

$q_{fi} = (1\times5\times3) + (0.5\times4\times3) = 21$ kN/m

The action of loads in fire is then

$M_{fi,Sd} = (21\times6^2) / 8 = 94.5$ kNm

Load level for fire design

$\eta_{fi,t} = M_{fi,Sd} / M_{pl,Rd} = 94.5 / 247 = 0.38$ [ < 1] OK

Critical Temperature

The critical temperature of the steel section is determined from the load level and from the strength of the steel at elevated temperature as follows:

$f_{a\ max,\theta cr} = 0.9\ \eta_{fi,t} \times f_{ay,20\ C} = 0.9 \times 0.4 \times 275 = 94.7$ N/mm$^2$ ( MPa)

the strength reduction coefficient at time t is;

$k_{max,\theta} = 94.7 / 275 = 0.344$

The task is now to calculate the critical temperature (the temperature at which the yield strength decreases to the value of 94.7 MPa) and the time at which the critical temperature will be reached. This will then be compared with the required fire resistance period of 120 min.

By linear interpolation for $k_{max,\theta}$ from Table 3.2 of the Code the value **$\theta_{crit}$ = 652.4 $^oC$** is obtained.

The required time will be estimated from the equation of unprotected steel cross-sections, either computationally or using the design sheets. Using fire excel spread sheets,

For $\Delta t$ = 5s the fire resistance time is 12.38 minutes < 90 minutes, so it is necessary to reduce the heating of the steel part by using fire protection material.

Protection Material

Material, Plasterboard

**Thickness, $d_p$ = 25 mm**

Density, $\rho_p$ = 950 kg/m$^3$

Specific Heat, $c_p$ = 840 J/kg$^o$K

Thermal Conductivity, $\lambda_p$ = 0.16 W/m$^o$K

With the aid of fire excel sheet, the steel temperature will be estimated 592.6 $^o$C at 90 minute if standard fire is considered, hence it is less than the critical temperature ($\theta_{crit}$ = 652.4 $^o$C). That means the thickness of fire protection is suitable for composite beam.

## A.2 Composite Slab Design (Full-Scaled)

<u>Characteristic Floor Loading</u>

Permanent Loads: Steel sheet, $G_{p,k}$ = 0.20 kN/ m$^2$

Concrete, $G_{c,k}$ = 2.80 kN/ m$^2$

Finishes, $G_{f,k}$ = 1.00 kN/ m$^2$

Variable Loads: Live load, $Q_{k,1}$ = 5.00 kN/ m$^2$

<u>Material Properties</u>

Steel Sheet: Yield stress, $f_{p,y}$ = 255 N/ mm$^2$

Geometry of cross-section, $h_1$ = 79 mm

Thickness, $t_p$ = 0.7 mm

Cross-sectional area, $A_p$ = 1296.8 mm$^2$/m

| Name | Profile | Deck Depth, $h_2$ (mm) | Trough Spacing, $l_1$ (mm) | Trough Width, $l_2$ (mm) | Crest Width, $l_3$ (mm) |
|---|---|---|---|---|---|
| CORUS PMF COMFLOR 51 | Re-entrant | 51 | 112.5 | 137.5 | 40 |

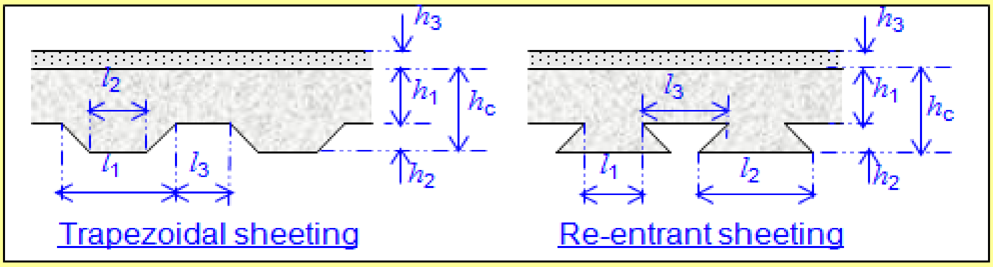


Figure A.3: Properties of steel decking (from Fire Excel Sheet)

Concrete: Type of concrete, light weight

$f_{ck}$ = 30 N/mm$^2$

Height, $h_c = h_1 + h_2$ = 130 mm

Cross-sectional area, $A_c$ = 120803.3 mm$^2$/m

Effective thickness of slab, $h_{eff} = h_1 + 0.5\, h_2\left(\frac{l_1 + l_2}{l_1 + l_3}\right)$ = 120.8 mm

**D.4 Effective thickness of a composite slab**

(1) The effective $h_{eff}$ is given by the formula:

$$h_{eff} = h_1 + 0{,}5\, h_2\left(\frac{\ell_1 + \ell_2}{\ell_1 + \ell_3}\right) \quad \text{for } h_2/h_1 \le 1{,}5 \text{ and } h_1 > 40 \text{ mm} \qquad \text{(D.15a)}$$

$$h_{eff} = h_1\left[1 + 0{,}75\left(\frac{\ell_1 + \ell_2}{\ell_1 + \ell_3}\right)\right] \quad \text{for } h_2/h_1 > 1{,}5 \text{ and } h_1 > 40 \text{ mm} \qquad \text{(D.15b)}$$

Figure A.4: Effective thickness of composite slab (Burgess, 2010a, p. 6)

Ultimate Limit State Design at Ambient Temperature

Partial factor for permanent actions, $\gamma_G = 1.35$

Partial factor for variable actions, $\gamma_{Q,1} = 1.5$

Design load at ambient temperature;

Permanent action, $G_d = 1.35 \times 4.0 = 5.4$ kN/m$^2$

Variable action, $Q_d = 1.5 \times 5.0 = 7.5$ kN/m$^2$

Total = 12.9 kN/m$^2$

Design Moment: Sagging moment at span, $M_{sag} = 0.07 \times 12.9 \times 6^2 = 32.51$ kNm/m

Hogging moment at mid support, $M_{hog} = (12.9 \times 6^2) / 8 = 58.05$ kNm/m

Design at fire situation;

Combination factor, $\psi_{1,1} = 0.5$

$Q_{k,1}/ G_{k,1} = 1.3$

Reduction factor, $\eta_{fi} = \left( \dfrac{G_k + \psi_{fi}\, Q_{k,1}}{\gamma_G\, G_k + \gamma_{Q,1}\, Q_{k,1}} \right) = 0.504$

Applied sagging moment, $M_{fi,Sd,sag} = \eta_{fi} \times M_{sag} = 16.4$ kNm/m

Applied hogging moment, $M_{fi,Sd,hog} = \eta_{fi} \times M_{hog} = 29.3$ kNm/m

Scope of application

Scope of application

EC4, Part 1.2, Annex D, Section D.5

| Field of application | | Actual values | | | |
|---|---|---|---|---|---|
| Re-entrant steel sheet profiles | Trapezoidal steel sheet profiles | | | | |
| 70 mm ≤ $l_1$ ≤ 135 mm | 80 mm ≤ $l_1$ ≤ 155 mm | $l_1$ = | 112.5 | mm | [ OK ] |
| 110 mm ≤ $l_2$ ≤ 150 mm | 32 mm ≤ $l_2$ ≤ 132 mm | $l_2$ = | 137.5 | mm | [ OK ] |
| 38.5 mm ≤ $l_3$ ≤ 97.5 mm | 40 mm ≤ $l_3$ ≤ 115 mm | $l_3$ = | 40 | mm | [ OK ] |
| 50 mm ≤ $h_1$ ≤ 130 mm | 50 mm ≤ $h_1$ ≤ 125 mm | $h_1$ = | 79 | mm | [ OK ] |
| 30 mm ≤ $h_2$ ≤ 60 mm | 50 mm ≤ $h_2$ ≤ 100 mm | $h_2$ = | 51 | mm | [ OK ] |

[ The slab is WITHIN the scope of application ]

Figure A.5: Scope of application (EC4 Part 1.2 Annex D Section D.5)

Fire Resistance according to the Thermal Insulation Criterion

Standard fire resistance, R = 90 minutes

Rib geometry factor, $A/L_r$ = 26.3 mm

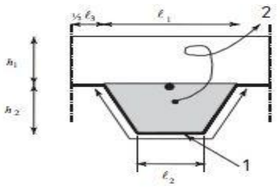


$$\frac{A}{L_r} = \frac{h_2 \cdot \left( \frac{\ell_1 + \ell_2}{2} \right)}{\ell_2 + 2\sqrt{h_2^{\,2} + \left( \frac{\ell_1 - \ell_2}{2} \right)^2}} \qquad \text{(D.2)}$$

Key
1 – Exposed surface: $L_r$
2 – Area: $A$

**Figure D.1: Definition of the rib geometry factor $A/L_r$ for ribs of composite slabs.**

Figure A.6: Rib geometry factor (EC4 Part 1.2 Annex D Section D.1)

View factor of upper flange, $\Phi = 0.136$

(2) The configuration or view factor $\Phi$ of the upper flange may be determined as follows:

$$\Phi = \left( \sqrt{h_2^2 + \left( l_3 + \frac{l_1 - l_2}{2} \right)^2} - \sqrt{h_2^2 + \left( \frac{l_1 - l_2}{2} \right)^2} \right) \bigg/ l_3 \qquad [-] \qquad (D.3)$$

Figure A.7: View factor of upper flange (EC4 Part 1.2 Annex D Section D.1)

Fire resistance, $\mathbf{t_i}$ **= 128.2 minutes** [ > specified R, fire resistance of the section is **ADEQUATE**]

**D.1 Fire resistance according to thermal insulation**

(1) The fire resistance with respect to both the average temperature rise (=140°C) and the maximum temperature rise (=180°C), criterion "I", may be determined according to the following equation:

$$t_i = a_0 + a_1 \cdot h_1 + a_2 \cdot \Phi + a_3 \cdot \frac{A}{L_r} + a_4 \cdot \frac{1}{\ell_3} + a_5 \cdot \frac{A}{L_r} \cdot \frac{1}{\ell_3} \qquad (D.1)$$

Figure A.8: Fire resistance $t_i$ (EC4 Part 1.2 Annex D Section D.1)

<u>Sagging Moment Resistance</u>

<u>Coefficients for the determination of temperature of the parts of the steel decking</u>

EC4, Part 1.2, Annex D, Section D.2

| For Lightweight concrete, R = 90 minutes | | | | | | |
|---|---|---|---|---|---|---|
| Part of steel sheet | $b_0$ [°C] | $b_1$ [°C.mm] | $b_2$ [°C.mm] | $b_3$ [°C] | $b_4$ [°C] | $\theta_a$ [°C] |
| Lower flange | 1019 | -478 | -0.91 | 32.7 | -60.8 | **986.4** |
| Web | 906 | -654 | -1.36 | 287.8 | -230.3 | **888.7** |
| Upper flange | 789 | -1847 | -0.99 | 469.5 | -313.0 | **774.8** |

Figure A.9: Temperature of the parts of steel decking (from Fire Excel sheet)

<u>Coefficients for the determination of temperature of the rebar in the rib</u>

$f_{s,y} = 500$ N/mm$^2$

Rebar diameter, $\Phi = 20$ mm

Distance $u_3 = 50$ mm

Distance $u_1 = 56.3$ mm

Distance $u_2 = 56.3$ mm

Angle of web for trapezoidal sheeting, $\alpha = \arctan [2h_2 / (l_1 - l_2)] = 103.8^o$ degree

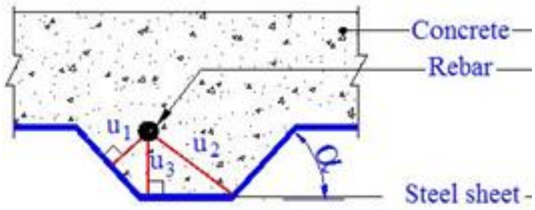


Figure A.10: Position of the rebar (from Fire Excel sheet)

EC4, Part 1.2, Annex D, Table D.3

| For Lightweight concrete, R = 90 minutes | | | | | | | |
|---|---|---|---|---|---|---|---|
| $c_0$ [°C] | $c_1$ [°C] | $c_2$ [°C.mm$^{0.5}$] | $c_3$ [°C.mm] | $c_4$ [°C / °] | $c_5$ [°C.mm] | **z [mm$^{-0.5}$]** | **$\theta_s$ [°C]** |
| 1381 | -240 | -269 | -5.46 | 2.24 | -918 | **2.45** | **552.5** |

Figure A.11: Parameters for the position of the rebar (from Fire Excel sheet)

Reduction factors ($k_{y,\theta}$) and carrying capacities (Z)

EC3, Part 1.2, Table E.1 (for steel sheet)

EC4, Part 1.2, Table 3.4 (for rebar)

| | **$\theta_a$ [°C]** | $k_{y,\theta}$ | $A_i$ [mm$^2$] | $f_{yp}$ [N/mm$^2$] | **$Z_i$ [kN]** | $z_i$ [m] | **$M_i$ [kNm]** |
|---|---|---|---|---|---|---|---|
| 1. Lower flange | 986.4 | 0.033 | 96.3 | 255 | **0.8** | 0.138 | **0.110** |
| 2. Web | 888.7 | 0.052 | 73.5 | 255 | **1.0** | 0.112 | **0.110** |
| 3. Upper flange | 774.8 | 0.085 | 28.0 | 255 | **0.6** | 0.087 | **0.053** |
| 4. Rebar | 552.5 | 0.528 | 314.2 | 500 | **83.0** | 0.088 | **7.261** |

Figure A.12: Reduction factors ($k_{y,\theta}$) and carrying-capacities (Z) from Excel sheet

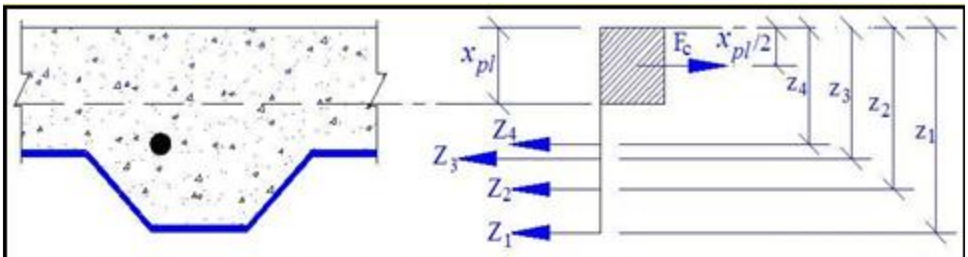


Stress distribution for sagging bending (if neutral axis is above steel sheeting)

Figure A.13: Stress distribution for sagging bending (from Fire Excel sheet)

Neutral axis, $x_{pl} = A_p f_{yp,d} / (0.85 b f_{cd}) = \sum Z_i / [0.85(l_1 + l_3) f_{cd}]$

Where $b = l_1 + l_3$

$x_{pl} = 21.955$ mm

Compressive resistance of concrete, $F_c = 0.85\ fcd \times b \times x_{pl} = 85.4$ kN

Plastic moment resistance of concrete, $M_c = F_c \times (x_{pl}/2) = 0.937$ kNm

Plastic moment resistance of slab, [EC4, Part 1.2, Section 4.3.1]

$M_{fi,Rd} = \sum A_i z_i k_{y,\theta}(f_{yp}/\gamma_{M,fi}) + 0.85b\,(f_{cd}/\gamma_{M,fi})\,x_{pl} = 6.597$ kNm

***Sagging moment resistance of slab, $M_{fi,Rd,sag}$ = 43.3 kNm/m***

[$M_{fi,Rd,sag} > M_{fi,Sd,sag} = 16.380$ kNm, section is SATISFACTORY for fire resistance]

**<u>Hogging Moment Resistance</u>**

<u>Coefficients for the determination of temperature of the tension rebar</u>

$f_{s,y} = 500$ N/mm$^2$

$u_3/h_2 = 0.75$ [EC4, Part 1.2, Annex D, Section D.3.(6)]

Rebar diameter, $\Phi = 20$ mm

Tension bar cover, c = 30 mm

Angle of web for trapezoidal sheeting, $\alpha = \arctan\,[2h_2 / (l_1 - l_2)] = 103.8^o$ degree

Normal force in hogging rebar, $N_s = (\pi \times (\Phi/2)^2) \times f_{s,y}/1000 = 245.4$ kN

EC4, Part 1.2, Annex D, Section D.3

| For Lightweight concrete, R = 90 minutes | | | | | |
|---|---|---|---|---|---|
| $c_0$ [°C] | $c_1$ [°C] | $c_2$ [°C.mm$^{0.5}$] | $c_3$ [°C.mm] | $c_4$ [°C / °] | $c_5$ [°C.mm] |
| 1381 | -240 | -269 | -5.46 | 2.24 | -918 |

Figure A.14: Coefficients for the determination of temperature of the tension rebar

<u>Coefficients for the determination of the limiting temperature</u>

EC4, Part 1.2, Annex D, Section D.4

| For Lightweight concrete, R = 90 minutes | | | | | | |
|---|---|---|---|---|---|---|
| $d_0$ [°C] | $d_1$ [°C.N] | $d_2$ [°C.mm] | $d_3$ [°C] | $d_4$ [°C.mm] | **$\theta_{lim}$ [°C]** | **z [mm$^{-0.5}$]** |
| 1159 | -2.5E-04 | -10.88 | -208.0 | -2233 | **727.6** | **2.005** |

Figure A.15: Coefficients for the determination of the limiting temperature

Location of the limiting temperature isotherm

| a [ mm ] | c [ mm ] | b [ mm ] | Point | $X_i$ [ mm ] | $Y_i$ [ mm ] |
|---|---|---|---|---|---|
| 14.056 | -39.042 | 15.319 | I | 0 | 32.7 |
| | | | II | 27.0 | 32.7 |
| | | | III | 40.5 | 51 |
| | | | IV | 76.3 | 66.3 |

Figure A.16: Location of the limiting temperature isotherm

Position of lever arm

- Equilibrium of horizontal force applied, $F_H^+ = F_H^-$

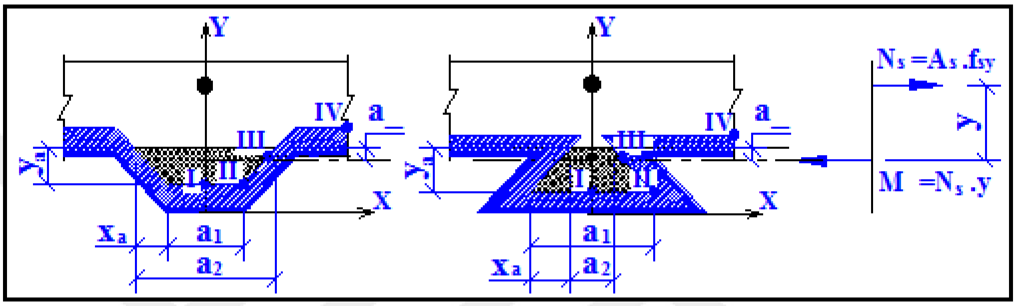


| $a_1$ [ mm ] | $a_2$ [ mm ] | $x_a$ [ mm ] | $0.85.f_{ck}.b$ [ N/mm ] | $y_a$ [ mm ] | a_ [ mm ] | y [ mm ] |
|---|---|---|---|---|---|---|
| 54.1 | 134.1 | -37.9 | 2399.3 | 102.3 | 91.3 | 48.0 |

Figure A.17: Position of lever arm

Tensile force in hogging reinforcement, $N_s = A_s f_y$ = 245436.9 N

Hogging moment resistance of slab, $M_{fi,Rd,hog} = N_s y$ = 11.789 kNm

***Hogging moment resistance of slab, $M_{fi,Rd,hog}$ = 77.3 kNm/m***

[$M_{fi,Rd,hog} > M_{fi,d}$ = 29.250 kNm, section is SATISFACTORY for fire resistance]

## A.3 Steel Column Design

### 1. Design of internal columns

Characteristic floor loading:

Permanent $G_k$ = 4.00 kN/m$^2$

Primary variable $Q_{k,1}$ = 5.00 kN/m$^2$

Span B = 6.0 m

Span L = 6.0 m

Column height = 4.0 m

Floor area, $A_{floor}$= 36.0 m$^2$

Materials Properties:

Steel grade, $f_y$ = 275 N/mm$^2$

Elastic modulus, $E_a$ = 210000 N/mm$^2$

Selected section **UC 254×254×132**

| Designation | Depth of Section | Width of Section | Thickness | | Root Radius | Depth between fillets | Ratios for Local Buckling | | Second Moment of Area | | Elastic Modulus | | Plastic Modulus | | Area of Section |
|---|---|---|---|---|---|---|---|---|---|---|---|---|---|---|---|
| | | | of Web | of Flange | | | Flange | Web | Axis x-x | Axis y-y | Axis x-x | Axis y-y | Axis x-x | Axis y-y | |
| | h mm | b mm | s mm | t mm | r mm | d mm | b/2t | d/s | $I_x$ $cm^4$ | $I_y$ $cm^4$ | $Z_x$ $cm^3$ | $Z_y$ $cm^3$ | $S_x$ $cm^3$ | $S_y$ $cm^3$ | A $cm^2$ |
| UC 254x254x132 | 276.3 | 261.3 | 15.3 | 25.3 | 12.7 | 200.3 | 5.16 | 13.1 | 22530 | 7531 | 1631 | 576 | 1869 | 878 | 168 |

Figure A.18: Section properties of internal columns (from Fire Excel sheet)

Section Classification; Coefficient $\varepsilon = (235/f_y)^{0.5} = 0.924$

| EC3, Table 5.2 | Limitation | | |
|---|---|---|---|
| | Class 1 | Class 2 | Class 3 |
| **Web** (subject to compression) | 30.51 | 35.13 | 38.83 |
| **Flange** (subject to compression) | 8.32 | 9.24 | 12.94 |

Figure A.19: Section classification (from Fire Excel sheet)

Web, d/s = 15.6 [Section is Class 1]

Flange, b/2t = 6.31 [Section is Class 1] Therefore, the section is Class 1.

Ultimate Limit State Design at Ambient Temperature

Partial factor for permanent actions; $\gamma_G = 1.35$

Partial factor for variable actions; $\gamma_{Q,1} = 1.5$

Design load for directly above:

Permanent action, $G_d = A_{floor} \times \gamma_G \times G_k = 194.4$ kN

Variable actions, $Q_d = A_{floor} \times \gamma_{Q,1} \times Q_{k,1} = 270.0$ kN

One floor total = 464.4 kN

Number of floors = 5

Design load from upper floors = 4 × 464.4 = 1857.6 kN

Extra factored dead load (Cladding, walls) = 45 kN

**Total design axial compression load, $N_{sd}$ = (464.4 × 5) + 45 = 2367 kN**

Design at normal temperature

Radius of gyration, $i = (I_y/A)^{0.5} = 0.066$ m

Out of plane (minor axis) slenderness, $\lambda = L_{column} / i = 60.6$

$\lambda_1 = \pi\, [E/f_y]^{0.5} = 86.815$

Normalised slenderness, $\lambda / \lambda_1 = 0.698$

Imperfection factor, $\alpha = 0.49$ (EC3, Part 1.1, Table 6.1 & 6.2)

$\Phi = 0.866$ (EC3, Part 1.1, Section 6.3.1.2)

Reduction factor, $\chi = 0.726$ (EC3, Part 1.1, Section 6.3.1.2) [but $\leq 1.0$]

**Buckling resistance, $N_{b,Rd} = \chi \times A \times f_y / \gamma_{M1} = 2715.24$ kN**

**[$N_{b,Rd} > N_{sd} = 2367$ kN, (OK)]**

Design at fire situation

Combination factor, $\psi_{1,1} = 0.5$

$Q_{k,1} / G_{k,1} = 1.3$

Reduction factor, $\eta_{fi} = \left( \dfrac{G_k + \psi_{fi} \, Q_{k,1}}{\gamma_G \, G_k + \gamma_{Q,1} \, Q_{k,1}} \right) = 0.504$

**Design loading in fire, $N_{fi,Sd} = \eta_{fi} \times N_{sd} = 1192.7$ kN**

Fire Compartment

Opening and Enclosure

Floor Area, $A_f = 6 \times 6 = 36$ m$^2$

Total area of vertical opening, $A_v = 6 \times 3 = 18$ m$^2$

Average windows height on all walls, $h_{eq} = 3$ m

Total area of enclosure, $A_t = 168$ m$^2$

Opening factor, O = 0.19 [but $0.02 \leq O \leq 0.20$]

Wall material, Lightweight concrete

Density, $\rho_w = 1600$ kg/m$^3$

Specific Heat, $c_w = 840$ J/kg$^o$K

Thermal Conductivity, $\lambda_w = 0.8$ W/m$^o$K

Fire Load Density

Type of occupancy, Average and office

Fire Protection

Type of exposure, 4-sides exposure

Protection Material

Material, Box protection

**Thickness, $d_p = 10$ mm**

Density, $\rho_p = 2100$ kg/m$^3$

Specific Heat, $c_p = 900$ J/kg$^o$K

Thermal Conductivity, $\lambda_p = 1.50$ W/m$^o$K

According to the Parametric Fire, the maximum steel temperatures and also standard fire curve can be shown below.

| Standard Fire | | |
|---|---|---|
| Max. temperature (°C) | Max. unprotected (°C) | Max. protected (°C) |
| 1049.0 | 1046.3 | 1030.2 |
| Time (minute) | 120.0 | 120.0 |

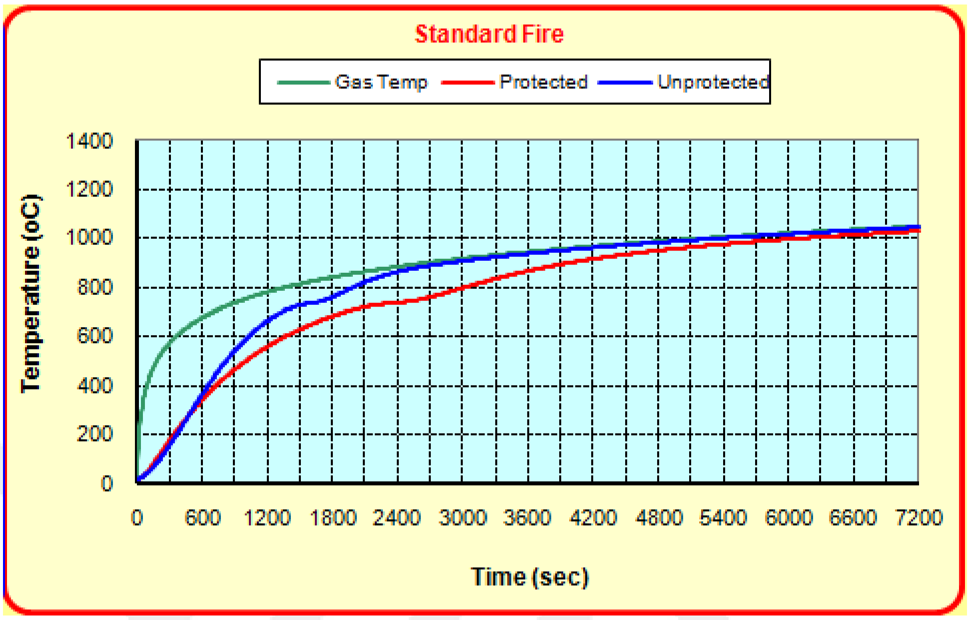


Figure A.20: The maximum steel temperatures and standard fire curve

Design resistance at maximum temperature (Parametric Fire)

From EC3, Part 1.2, Section 3.2.1, Table 3.1

| max. temperature (°C) | $k_{y,20}$ | $k_{E,20}$ |
|---|---|---|
| 446.7 | 0.897 | 0.653 |

Effective length factor = 0.7

Slenderness, $\lambda = L_{cr}/i = (0.7 \times 4) / 0.066 = 42.42$

Normalised slenderness, $\lambda / \lambda_1 = 42.42 / 86.815 = 0.489$

Normalised slenderness at $\theta_a$, $\lambda_\theta = 0.489 \times ((1/0.653)^{0.5}) = 0.573$

Imperfection factor, $\alpha = 0.601$ (EC3, Part 1.1, Table 6.1 & 6.2)

$\Phi_\theta = 0.836$ (EC3, Part 1.1, Section 6.3.1.2)

Reduction factor, $\chi_{fi} = 0.692$ (EC3, Part 1.1, Section 6.3.1.2) [but $\leq 1.0$]

Buckling resistance at time t with uniform $\theta_a$,

$\mathbf{N_{b,fi,t,Rd} = (\chi_{fi} \times A_{section} \times 100 \times k_{y,20} \times f_y) / 1000 = 2322.6\ kN}$

$\mathbf{N_{b,fi,t,Rd} > N_{fi.sd} = 1192.74\ kN}$**, OK**

## 2. Design of edge columns

The characteristic floor loads in terms of permanent and variable are the same as the loads of design of internal columns. Moreover the same process which was shown in the design of internal columns will be applied to design the edge columns.

The section will be **UC 203×203×86**

Design load for floor directly:

Permanent action, $G_d = A_{floor} \times \gamma_G \times G_k = 97.2$ kN

Variable actions, $Q_d = A_{floor} \times \gamma_{Q,1} \times Q_{k,1} = 135$ kN

One floor total = 232.2 kN

Number of floors = 5

Design load from upper floors = 4 × 232.2 = 928.8 kN

Extra factored dead load (Cladding, walls) = 45 kN

**Total design axial compression load, $N_{sd} = (232.2 \times 5) + 45 = 1206$ kN**

**Buckling resistance, $N_{b,Rd} = \chi \times A \times f_y / \gamma_{M1} = 1881.53$ kN**

**[$N_{b,Rd} > N_{sd} = 1206$ kN, (OK)]**

**Design loading in fire, $N_{fi,Sd} = \eta_{fi} \times N_{sd} = 607.7$ kN**

<u>Fire Load Density</u>

Type of occupancy, Average and office

<u>Fire Protection</u>

Type of exposure, 4-sides exposure

<u>Protection Material</u>

Material, Box protection

**Thickness, $d_p = 10$ mm**

According to the Parametric Fire, the maximum steel temperatures can be shown below.

| Parametric Fire | | |
|---|---|---|
| Max. temperature ($^oC$) | Max. unprotected ($^oC$) | Max. protected ($^oC$) |
| 648.4 | 481.8 | 526.6 |
| Time (minute) | 20.8 | 20.8 |

Figure A.21: The maximum steel temperatures

Buckling resistance at time t with uniform $\theta_a$,

**$N_{b,fi,t,Rd} = (\chi_{fi} \times A_{section} \times 100 \times k_{y,20} \times f_y) / 1000 = 1315.7$ kN**

**$N_{b,fi,t,Rd} > N_{fi.d} = 607.674$ kN, OK**

## 3. Design of corner columns

The characteristic floor loads in terms of permanent and variable are the same as the loads of design of internal columns. Moreover the same process which was shown in the design of internal columns will be applied to design the corner columns.

The section will be **UC 203×203×52**

Design load for floor directly:

Permanent action, $G_d = A_{floor} \times \gamma_G \times G_k = 48.6$ kN

Variable actions, $Q_d = A_{floor} \times \gamma_{Q,1} \times Q_{k,1} = 67.5$ kN

One floor total = 116.1 kN

Number of floors = 5

Design load from upper floors = 4 × 116.1 = 464.4 kN

Extra factored dead load (Cladding, walls) = 45 kN

**Total design axial compression load, $N_{sd} = (116.1 \times 5) + 45 = 625.5$ kN**

**Buckling resistance, $N_{b,Rd} = \chi \times A \times f_y / \gamma_{M1} = 1105.17$ kN**

**[$N_{b,Rd} > N_{sd} = 625.5$ kN, (OK)]**

**Design loading in fire, $N_{fi,Sd} = \eta_{fi} \times N_{sd} = 315.2$ kN**

Fire Load Density

Type of occupancy, Average and office

Fire Protection

Type of exposure, 4-sides exposure

Protection Material

Material, Box protection

**Thickness, $d_p = 10$ mm**

According to the Parametric Fire, the maximum steel temperatures can be shown below.

| Parametric Fire | | |
|---|---|---|
| Max. temperature (°C) | Max. unprotected (°C) | Max. protected (°C) |
| 648.4 | 562.2 | 570.0 |
| Time (minute) | 20.4 | 20.7 |

Figure A.22: The maximum steel temperatures for corner columns

Buckling resistance at time t with uniform $\theta_a$,

**$N_{b,fi,t,Rd} = (\chi_{fi} \times A_{section} \times 100 \times k_{y,20} \times f_y) / 1000 = 616.2$ kN**

**$N_{b,fi,t,Rd} > N_{fi.d} = 315.174$ kN, OK**

## A.4 Composite Beam Design (Small-Scaled)

When the chosen section for full scaled is modelled as 1/5 model, the section properties can be shown below. The same materials are used for both full-scaled and reduced-scale model.

| | |
|---|---|
| Material properties | Steel grade, $f_y = 275\ N/mm^2$<br>Concrete grade, $f_{ck} = 30\ N/mm^2$ |

Table A.1: Material properties of composite beams

Section properties of 1/5 scaled composite beam models:

| Section Properties | Primary Beam | Secondary Beam |
|---|---|---|
| **Depth of Section "h" (mm)** | 62.08 | 61.74 |
| **Width of Section "b" (mm)** | 33.38 | 20.36 |
| **Thickness of web "s" (mm)** | 1.58 | 1.2 |
| **Thickness of Flange "t" (mm)** | 2.74 | 1.76 |
| **Root Radius "r" (mm)** | 1.78 | 1.52 |
| **Depth between fillets "d" (mm)** | 53.04 | 55.18 |
| **Ratios for Local Buckling of Flange "b/2t"** | 6.091 | 5.78 |
| **Ratios for Local Buckling of Web "d/s"** | 33.570 | 45.98 |
| **Second Moment of Area of Axis x-x "$I_x$" ($cm^4$)** | 18.72 | 8.59 |
| **Second Moment of Area of Axis y-y "$I_y$" ($cm^4$)** | 1.7008 | 0.25 |
| **Elastic Modulus of Axis x-x "$Z_x$" ($cm^3$)** | 6.032 | 2.784 |
| **Elastic Modulus of Axis y-y "$Z_y$" ($cm^3$)** | 1.016 | 0.244 |
| **Plastic Modulus of Axis x-x "$S_x$" ($cm^3$)** | 6.768 | 3.224 |
| **Plastic Modulus of y-y "$S_y$" ($cm^3$)** | 1.568 | 0.39 |
| **Area of Section "A" ($cm^2$)** | 2.752 | 1.44 |

Table A.2: Section sizes of scaled composite beam models

$$M_{pl,Rd} = A \times f_{yd} \times ( h/2+h_c - 0.5x_c )$$

$M_{pl,Rd}$ can be calculated by using the equation above.

| Beam Type | hc (mm) | B-floor (mm) | L-floor (mm) | $b_{eff}$ (mm) | $x_c$ (mm) | $M_{pl,Rd}$ (kNm) | $M_{Sd}$ (kNm) |
|---|---|---|---|---|---|---|---|
| **Primary** | 26 | 1200 | 1200 | 320 | 13.9118 | **3.7904** | **3.7895** |
| **Secondary** | 26 | 600 | 1200 | 170 | 13.7 | **1.9807** | **1.8948** |

Table A.3: Resistance bending moments of composite beams

The loads for both prototype and model can be shown below.

| $q_p$ (kN/m$^2$) | $g_p$ (kN/m$^2$) | $q_m$ (kN/m$^2$) | $g_m$ (kN/m$^2$) |
|---|---|---|---|
| **5** | 4 | 5 | 7.44 |

Table A.4: Floor loading of models

$$M_{pl,Rd} = M_{sd} = \frac{(Q_d + G_d) \times L^2}{8}$$

$Q_d + G_d = (q\times1.5\times1.2) + (g\times1.35\times1.2) = 21.06$ kN/m (Primary beam)

$Q_d + G_d = (q\times1.5\times0.6) + (g\times1.35\times0.6) = 10.53$ kN/m (Secondary beam)

As can be understood from above equation, the loads for scaled model should be increased. That's why the dead load might be increased from 4 kN/m$^2$ to 7.44 kN/m$^2$. Loading in fire situation is obtained from;

$$\sum \gamma_{GA} G_k + \psi_{1,1} Q_{k,1} + \sum \psi_{2,i} Q_{k,i} + \sum A_d$$

Where; $G_k$ is the permanent action,

$Q_{k,1}$ is the main variable action,

$Q_{k,i}$ are other variable actions,

$A_d$ are indirect fire actions

For the structure analysed $\gamma_{GA} = 0.5$ $\psi_{1,1} = 1$ , so

$q_{fi} = 1\times5\times1.2 + 0.5\times7.44\times1.2 = 10.464$ kN/m (Primary beam)

$q_{fi} = 1\times5\times0.6 + 0.5\times7.44\times0.6 = 5.232$ kN/m (Secondary beam)

The actions of loads in fire are then

$M_{fi,Sd} = (10.464\times1.2^2) / 8 = 1.8835$ kNm (Primary beam)

$M_{fi,Sd} = (5.232\times1.2^2) / 8 = 0.9418$ kNm (Secondary beam)

Load level for fire design

$\eta_{fi,t} = M_{fi,Sd} / M_{pl,Rd} = 1.8835 / 3.7904 = 0.5$ [ < 1 ] OK (Primary beam)

$\eta_{fi,t} = M_{fi,Sd} / M_{pl,Rd} = 0.9418 / 1.9807 = 0.476$ [ < 1 ] OK (Secondary beam)

**Critical Temperature**

The critical temperature of the steel section is determined from the load level and from the strength of the steel at elevated temperature as follows:

$f_{a\ max,\theta cr} = 0.9\ \eta_{fi,t} \times f_{ay,20\ C} = 0.9 \times 0.5 \times 275 = 123.75$ N/mm$^2$ ( MPa)

$f_{a\ max,\theta cr} = 0.9\ \eta_{fi,t} \times f_{ay,20\ C} = 0.9 \times 0.48 \times 275 = 117.68$ N/mm$^2$ ( MPa)

the strength reduction coefficient at time t is;

$k_{max,\theta} = f_{a\ max,\theta cr} / f_{yd} = 123.75 / 275 = 0.45$

$k_{max,\theta} = f_{a\ max,\theta cr} / f_{yd} = 117.56 / 275 = 0.42$

The task is now to calculate the critical temperature (the temperature at which the yield strength decreases to the value of 123.75 MPa and the value of 117.68 MPa) and the time at which the critical temperature will be reached. This will then be compared with the required fire resistance period of 120 min.

By linear interpolation for $k_{max,\theta}$ from Table 3.2 of the Code the value $\boldsymbol{\theta_{crit,primary\ beam} = 608.3\ ^{o}C}$ and $\boldsymbol{\theta_{crit,sec.} = 608.3\ ^{o}C}$ are obtained.

The comparison between model and prototype in terms of critical temperature can be shown below table.

| Beam type | $\theta_{crit,p}$ ($^{o}$C) | $\theta_{crit,m}$ ($^{o}$C) |
|---|---|---|
| **Primary** | 646.2 | 608.3 |
| **Secondary** | 652.4 | 620.83 |

Table A.5: Critical temperatures

## A.5 Steel Column Design

All type of columns was modelled geometrically with 1/5-scale. The section properties are shown in Table A.6.

| Section (1/5-scaled internal column model) | Internal | Edge | Corner |
|---|---|---|---|
| **Depth of Section "h" (mm)** | 55.26 | 44.44 | 41.24 |
| **Width of Section "b" (mm)** | 52.26 | 41.02 | 40.86 |
| **Thickness of web "s" (mm)** | 3.06 | 2.54 | 1.58 |
| **Thickness of Flange "t" (mm)** | 5.06 | 4.1 | 2.5 |
| **Root Radius "r" (mm)** | 2.54 | 2.04 | 2.04 |
| **Depth between fillets "d" (mm)** | 40.06 | 32.16 | 32.16 |
| **Ratios for Local Buckling of Flange "b/2t"** | 5.16 | 5.002 | 8.172 |
| **Ratios for Local Buckling of Web "d/s"** | 13.1 | 12.661 | 20.354 |
| **Second Moment of Area of Axis x-x "Ix" ( $cm^4$)** | 36.048 | 15.12 | 8.41 |
| **Second Moment of Area of Axis y-y "Iy" ($cm^4$)** | 12.0496 | 5.003 | 2.85 |
| **Elastic Modulus of Axis x-x "Zx" ($cm^3$)** | 13.048 | 6.8 | 4.08 |
| **Elastic Modulus of Axis y-y "Zy" ($cm^3$)** | 4.608 | 2.392 | 1.392 |
| **Plastic Modulus of Axis x-x "Sx" ($cm^3$)** | 14.952 | 7.816 | 4.536 |
| **Plastic Modulus of y-y "Sy" ($cm^3$)** | 7.024 | 3.648 | 2.112 |
| **Area of Section "A" ($cm^2$)** | 6.72 | 4.4 | 2.652 |

Table A.6: The section properties of 1/5-scaled columns

The loading conditions, floor and column sizes and also material properties are identical for all type of columns in terms of internal, edge and corner. They are shown in Table A.7.

| **General specification of columns** | |
|---|---|
| **Characteristic floor loading** | $G_k$ = 7.44 kN/m$^2$ $Q_k$ = 5 kN/m$^2$ |
| **Floor and column sizes** | Span B = 1.2 m Span L = 1.2 m<br>Column height = 0.8 m |
| **Material properties** | Steel grade, $f_y$ = 275 N/mm$^2$<br>Elastic Modulus, E = 210000 N/mm$^2$ |

Table A.7: General specification of columns

The properties of fire compartment are identical for all type of columns.

Fire Compartment:

Opening and Enclosure

Floor Area, $A_f = 1.2 \times 1.2 = 1.44$ m$^2$

Total area of vertical opening, $A_v = 1.2 \times 0.6 = 0.72$ m$^2$

Average windows height on all walls, $h_{eq}$ = 0.6 m

Total area of enclosure, $A_t$ = 6.72 m$^2$

Opening factor, O = 0.19 [but $0.02 \leq O \leq 0.20$]

Wall material, Lightweight concrete

Density, $\rho_w$ = 143.11 kg/m$^3$ ($\rho_w \sim s^{3/2}$)

Specific Heat, $c_w$ = 75.13 J/kg$^o$K ($c_w \sim s^{3/2}$)

Thermal Conductivity, $\lambda_w$ = 0.8 W/m$^o$K

Fire Load Density

Type of occupancy, Average and office

Fire Protection

Type of exposure, 4-sides exposure

**1. Modelling of Internal Columns**

Section Classification

Web, d/s = 15.6 [Section is Class 1]

Flange, b/2t = 6.31 [Section is Class 1] Therefore, the section is Class 1.

Ultimate Limit State Design at Ambient Temperature

Partial factor for permanent actions; $\gamma_G = 1.35$

Partial factor for variable actions; $\gamma_{Q,1} = 1.5$

Floor area, $A_{floor} = 1.44\ m^2$

Design load for directly above:

Permanent action, $G_d = A_{floor} \times \gamma_G \times G_k = 14.46$ kN

Variable actions, $Q_d = A_{floor} \times \gamma_{Q,1} \times Q_{k,1} = 10.8$ kN

One floor total = 25.26 kN

Number of floors = 5

Design load from upper floors = 4 × 25.26 = 101.04 kN

Extra factored dead load (Cladding, walls) = 4,5 kN

**Total design axial compression load, $N_{sd}$ = (25.26 × 5) + 4,5 = 130.8 kN**

Design at normal temperature

Radius of gyration, $i = (I_y/A)^{0.5} = 0.0134$ m

Out of plane (minor axis) slenderness, $\lambda = L_{column} / i = 59.74$

$\lambda_1 = \pi\ [E/f_y]^{0.5} = 86.815$

Normalised slenderness, $\lambda / \lambda_1 = 0.69$

Imperfection factor, $\alpha = 0.49$ (EC3, Part 1.1, Table 6.1 & 6.2)

$\Phi = 0.8564$ (EC3, Part 1.1, Section 6.3.1.2)

Reduction factor, $\chi = 0.7320$ (EC3, Part 1.1, Section 6.3.1.2) [but $\leq 1.0$]

**Buckling resistance, $N_{b,Rd} = \chi \times A \times f_y / \gamma_{M1}$ = 135.27 kN**

**[$N_{b,Rd} > N_{sd}$ = 130.8 kN, (OK)]**

Design at fire situation

Combination factor, $\psi_{1,1} = 0.5$ $Q_{k,1} / G_{k,1} = 1.3$

Reduction factor, $\eta_{fi} = \left( \frac{G_k + \psi_{fi}\ Q_{k,1}}{\gamma_G\ G_k + \gamma_{Q,1}\ Q_{k,1}} \right) = 0.504$

**Design loading in fire, $N_{fi,Sd} = \eta_{fi} \times N_{sd}$ = 65.92 kN**

Protection Material

Material, Box protection

**Thickness, $d_p$ = 25 mm**

Density, $\rho_p = 2100\ kg/m^3$

Specific Heat, $c_p = 900\ J/kg^oK$

Thermal Conductivity, $\lambda_p = 1.50\ W/m^oK$

Design Resistance at Maximum Temperature

Effective length factor = 0.7

Slenderness, $\lambda = L_{cr}/i = (0.7 \times 4) / 0.066 = 41.82$

Normalised slenderness, $\lambda / \lambda_1$ = 42.42 / 86.815 = 0.482

Normalised slenderness at $\theta_a$, $\lambda_\theta = 0.489 \times ((1/0.653)^{0.5}) = 0.573$

Imperfection factor, $\alpha$ = 0.601 (EC3, Part 1.1, Table 6.1 & 6.2)

$\Phi_\theta$ = 0.836 (EC3, Part 1.1, Section 6.3.1.2)

Reduction factor, $\chi_{fi}$ = 0.692 (EC3, Part 1.1, Section 6.3.1.2) [but $\leq$ 1.0]

Buckling resistance at time t with uniform $\theta_a$,

$k_{y,20}$ = 0.97

**$N_{b,fi,t,Rd} = (\chi_{fi} \times A_{section} \times 100 \times k_{y,20} \times f_y) / 1000 = 123.9470$ kN**

**$N_{b,fi,t,Rd} > N_{fi.sd}$ = 65.92 kN, OK**

## 2. Modelling of Edge Columns

<u>Section Classification</u>

Web, d/s = 12.66 [Section is Class 1]

Flange, b/2t = 5.002 [Section is Class 1] Therefore, the section is Class 1.

<u>Ultimate Limit State Design at Ambient Temperature</u>

Partial factor for permanent actions; $\gamma_G$ = 1.35

Partial factor for variable actions; $\gamma_{Q,1}$ = 1.5

Floor area, $A_{floor}$ = 0.72 m$^2$

Design load for directly above:

Permanent action, $G_d = A_{floor} \times \gamma_G \times G_k$ = 7.23 kN

Variable actions, $Q_d = A_{floor} \times \gamma_{Q,1} \times Q_{k,1}$ = 5.4 kN

One floor total = 12.63 kN

Number of floors = 5

Design load from upper floors = 4 × 12.63 = 50.52 kN

Extra factored dead load (Cladding, walls) = 4,5 kN

**Total design axial compression load, $N_{sd}$ = (12.63 × 5) + 4,5 = 67.65 kN**

<u>Design at normal temperature</u>

Radius of gyration, $i = (I_y/A)^{0.5}$ = 0.0107 m

Out of plane (minor axis) slenderness, $\lambda = L_{column} / i$ = 75.02

$\lambda_1 = \pi\, [E/f_y]^{0.5}$ = 86.815

Normalised slenderness, $\lambda / \lambda_1$ = 0.8642

Imperfection factor, $\alpha$ = 0.49 (EC3, Part 1.1, Table 6.1 & 6.2)

$\Phi$ = 1.0361 (EC3, Part 1.1, Section 6.3.1.2)

Reduction factor, $\chi$ = 0.6220 (EC3, Part 1.1, Section 6.3.1.2) [but $\leq$ 1.0]

**Buckling resistance, $N_{b,Rd} = \chi \times A \times f_y / \gamma_{M1}$ = 75.26 kN**

**[$N_{b,Rd} > N_{sd}$ = 67.65 kN, (OK)]**

Design at fire situation

Combination factor, $\psi_{1,1} = 0.5$    $Q_{k,1}/ G_{k,1} = 1.3$

Reduction factor, $\eta_{fi} = \left( \dfrac{G_k + \psi_{fi}\ Q_{k,1}}{\gamma_G\ G_k + \gamma_{Q,1}\ Q_{k,1}} \right) = 0.504$

**Design loading in fire, $N_{fi,Sd} = \eta_{fi} \times N_{sd}$ = 34.1 kN**

Protection Material

Material, Box protection

**Thickness, $d_p$ = 25 mm**

Density, $\rho_p$ = 2100 kg/m$^3$

Specific Heat, $c_p$ = 900 J/kg$^o$K

Thermal Conductivity, $\lambda_p$ = 1.50 W/m$^o$K

Design Resistance at Maximum Temperature

Effective length factor = 0.7

Slenderness, $\lambda = L_{cr}/i = (0.7 \times 4) / 0.066 = 52.5169$

Normalised slenderness, $\lambda / \lambda_1 = 42.42 / 86.815 = 0.6049$

Normalised slenderness at $\theta_a$, $\lambda_\theta = 0.489 \times ((1/0.653)^{0.5}) = 0.7204$

Imperfection factor, $\alpha$ = 0.601 (EC3, Part 1.1, Table 6.1 & 6.2)

$\Phi_\theta$ = 0.98 (EC3, Part 1.1, Section 6.3.1.2)

Reduction factor, $\chi_{fi}$ = 0.612 (EC3, Part 1.1, Section 6.3.1.2) [but $\leq$ 1.0]

Buckling resistance at time t with uniform $\theta_a$,

$k_{y,20} = 0.97$

**$N_{b,fi,t,Rd} = (\chi_{fi} \times A_{section} \times 100 \times k_{y,20} \times f_y) / 1000$ = 71.8181 kN**

**$N_{b,fi,t,Rd} > N_{fi.sd}$ = 34.1 kN, OK**

## 3. Modelling of Corner Columns

Section Classification

Web, d/s = 20.35 [Section is Class 1]

Flange, b/2t = 8.17 [Section is Class 1]    Therefore, the section is Class 1.

Ultimate Limit State Design at Ambient Temperature

Partial factor for permanent actions; $\gamma_G = 1.35$

Partial factor for variable actions;  $\gamma_{Q,1} = 1.5$

Floor area, $A_{floor}$ = 0.36 m$^2$

Design load for directly above:

Permanent action, $G_d = A_{floor} \times \gamma_G \times G_k = 3.62$ kN

Variable actions, $Q_d = A_{floor} \times \gamma_{Q,1} \times Q_{k,1} = 2.7$ kN

One floor total = 6.32 kN

Number of floors = 5

Design load from upper floors = 4 × 6.32 = 25.28 kN

Extra factored dead load (Cladding, walls) = 4,5 kN

**Total design axial compression load, $N_{sd}$ = (6.32 × 5) + 4,5 = 36.1 kN**

Design at normal temperature

Radius of gyration, $i = (I_y/A)^{0.5} = 0.0104$ m

Out of plane (minor axis) slenderness, $\lambda = L_{column} / i = 77.17$

$\lambda_1 = \pi\,[E/f_y]^{0.5} = 86.815$

Normalised slenderness, $\lambda/\lambda_1 = 0.8889$

Imperfection factor, $\alpha = 0.49$ (EC3, Part 1.1, Table 6.1 & 6.2)

$\Phi = 1.0639$ (EC3, Part 1.1, Section 6.3.1.2)

Reduction factor, $\chi = 0.6067$ (EC3, Part 1.1, Section 6.3.1.2) [but $\leq 1.0$]

**Buckling resistance, $N_{b,Rd} = \chi \times A \times f_y / \gamma_{M1}$ = 44.2435 kN**

**[$N_{b,Rd} > N_{sd}$ = 36.1 kN, (OK)]**

Design at fire situation

Combination factor, $\psi_{1,1} = 0.5$ $Q_{k,1}/ G_{k,1} = 1.3$

Reduction factor, $\eta_{fi} = \left( \dfrac{G_k + \psi_{fi}\, Q_{k,1}}{\gamma_G\, G_k + \gamma_{Q,1}\, Q_{k,1}} \right) = 0.504$

**Design loading in fire, $N_{fi,Sd} = \eta_{fi} \times N_{sd}$ = 18.19 kN**

Protection Material

Material, Box protection

**Thickness, $d_p$ = 25 mm**

Density, $\rho_p = 2100$ kg/m$^3$

Specific Heat, $c_p = 900$ J/kg$^o$K

Thermal Conductivity, $\lambda_p = 1.50$ W/m$^o$K

Design Resistance at Maximum Temperature

Effective length factor = 0.7

Slenderness, $\lambda = L_{cr}/i = (0.7 \times 4) / 0.066 = 54.0197$

Normalised slenderness, $\lambda/\lambda_1 = 42.42 / 86.815 = 0.6222$

Normalised slenderness at $\theta_a$, $\lambda_\theta = 0.489 \times ((1/0.653)^{0.5}) = 0.7410$

Imperfection factor, $\alpha = 0.601$ (EC3, Part 1.1, Table 6.1 & 6.2)

$\Phi_\theta = 0.9972$ (EC3, Part 1.1, Section 6.3.1.2)

Reduction factor, $\chi_{fi} = 0.6008$ (EC3, Part 1.1, Section 6.3.1.2) [but $\leq 1.0$]

Buckling resistance at time t with uniform $\theta_a$,

$k_{y,20} = 0.97$

$\mathbf{N_{b,fi,t,Rd} = (\chi_{fi} \times A_{section} \times 100 \times k_{y,20} \times f_y) / 1000 = 42.5022\ kN}$

$\mathbf{N_{b,fi,t,Rd} > N_{fi.sd} = 18.19\ kN}$**, OK**

## A.6 MATLAB Codes

MATLAB codes are used to work out the all complex calculations. "*column.m*" file is called for steel column design codes and "*beam.m*" file is called for composite beam design.

**Column Design Codes (column.m)**

```
clear all
clc

fyd = 275; % N/mm^2
fck = 30;  % N/mm^2

E = 210000; % N/mm^2
q = input('q=');  % kN/m^2..............(Dead load)
g = input('g=');  % kN/m^2..............(Imposed load)

B = input('B=');     % m
L = input('L=');     % m
h = input('h=');     % m
I = input('I=');     % mm^4
A = input('A=');     % mm^2
Af = input ('A_floor=');     % m^2

Qd = q*1.5*Af    % kN ................(Design load)
Gd = g*1.35*Af   % kN ................(Design Load)

% -------------------------------------------------------------------
Td_1 = Qd + Gd;    %kN
Nsd = 5*Td_1   %kN ................... Total design axial compression
% -------------------------------------------------------------------
i = ((I/A)^0.5)/1000  % m .............(Radius of gyration)
lamda = h/i    % ................. out-of-plane (minor axis)
slenderness
lamda1 = pi*(E/fyd)^0.5
r = lamda/lamda1   % ........... Normalised slenderness
alfa = 0.49    % ................ Imperfection factor
fi = 0.5*[1+alfa*(r-0.2)+r^2]
x = 1/(fi+(fi^2-r^2)^0.5)  % ........... Reduction factor (but < 1)
Nb_rd = x*A*fyd/1000    % ............... Buckling resistance
% -------------------------------------------------------------------
```

```
w11 = 0.5;  % ................ Combination factor
a = q/g;
nfi = 0.504;    % ............ Reduction factor
Nfi_sd = nfi*Nsd

% -----------------------------------------------------------------
b = 0.7;    % ................. Effective length factor
lamda2 = 0.7*(h/i) % ......... Slenderness
r2 = lamda2/lamda1
lamda_teta = r2*[(0.563/0.397)^0.5]    % .... Normalised slenderness
alfa2 = 0.65*(235/fyd)^0.5  % ... Imperfection factor
fi_teta = 0.5*[1+(alfa2*lamda_teta)+(lamda_teta^2)]
x_fi = 1/(fi_teta+(fi_teta^2-lamda_teta^2)^0.5)
N_bi_fi_rd = x_fi*A*0.97*fyd/1000
% -----------------------------------------------------------------
```

## Beam Design Codes (beam.m)

```
clear all
clc

fyd = 275; % N/mm^2
fck = 30;  % N/mm^2

B = input('B=');     % m
L = input('L=');     % m
q = input('q=');   % kN/m^2..............(Dead load)
g = input('g=');   % kN/m^2..............(Imposed load)

hc = input('hc=');     % mm .............(Thickness of concrete slab)
beff = input('beff='); % mm ......(Effective width of concrete slab)
Aa = input('Aa=');     % mm^2 ...........(Area of the section)
h = input('h=');   % mm ................(Section height)

xc = (Aa*fyd)/(0.85*fck/1.5*beff) % ...(neutral axis)
Qd = q*1.5*B;     % kN/m ................(Design load)
Gd = g*1.35*B;    % kN/m ................(Design Load)

%.................................................................
Msd = (Qd+Gd)*L^2/(8*10^9) % Design bending moment (kNm)
%.................................................................
MplRd= Aa*fyd*(h/2+hc-0.5*xc)/10^6 % Resistance bending moment (kNm)
%.................................................................

qfi = ((1*q*B) + (0.5*g*B))/10^3;     % Loading in fire (kN/m)
MfiSd = qfi* L^2/(8*10^6) % Action loads in fire (kNm)
nfit = MfiSd / MplRd % Load level < 1 OK !

% the critical temperature of the steel section is determined from
the load level and from the strength of the steel at elevated
temperature;

famaxcr = 0.9*nfit*fyd

% Strength reduction coefficient at time t is ;
kmax = famaxcr / fyd
```

# Appendix B

# Drawings

## B.1 Frame of the Full-Scaled Structure

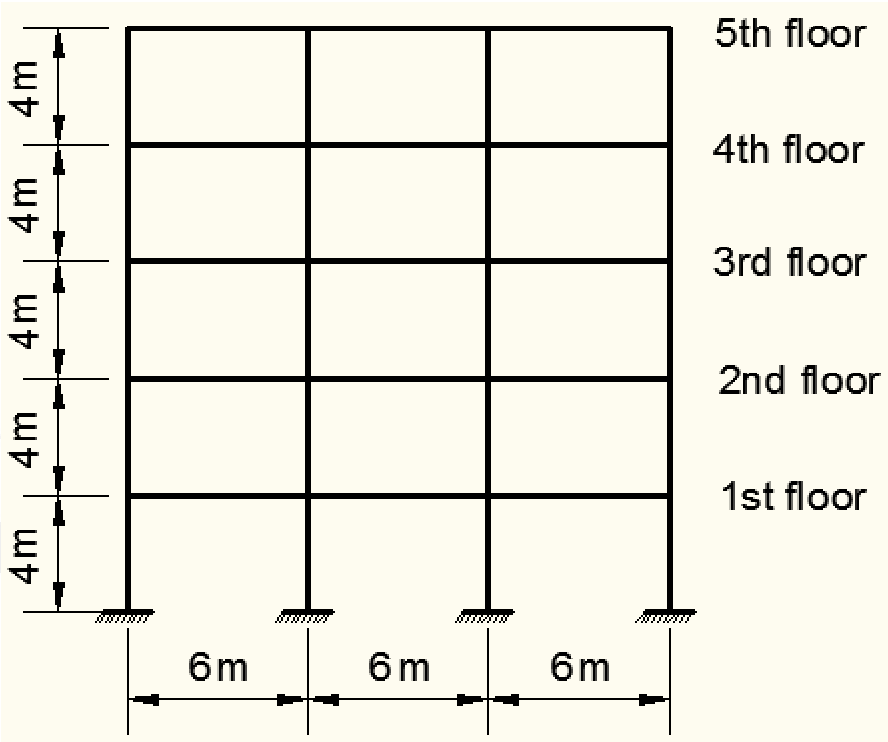


Figure B.1: Frame of the real structure

## B.2 Frame of the 1/5-Scaled Structure

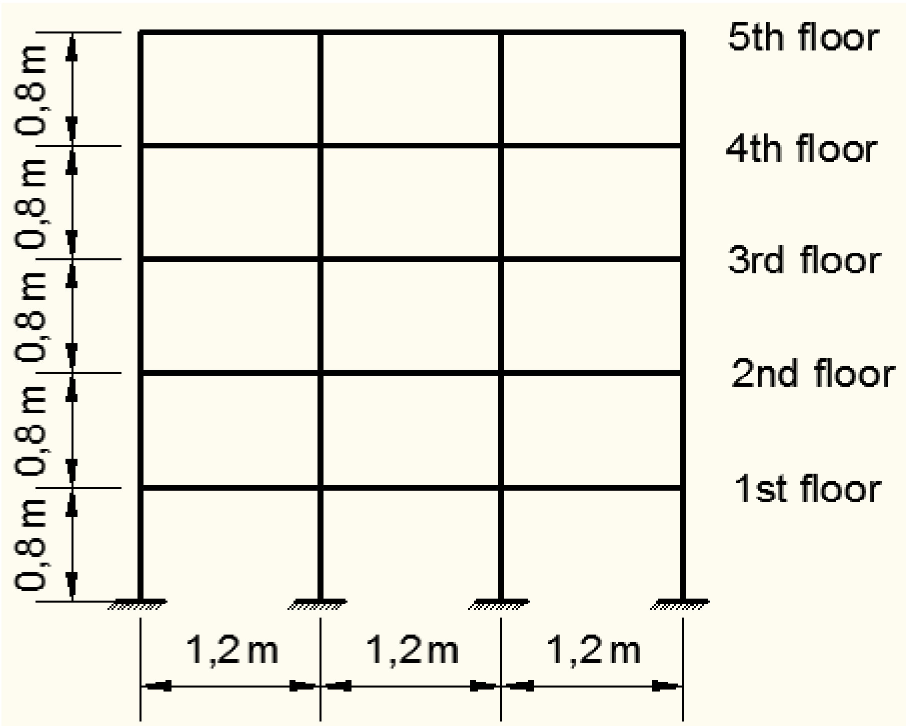


Figure B.2: Frame of the small-scaled structure

## B.3 Plan of Full-Scaled Structure

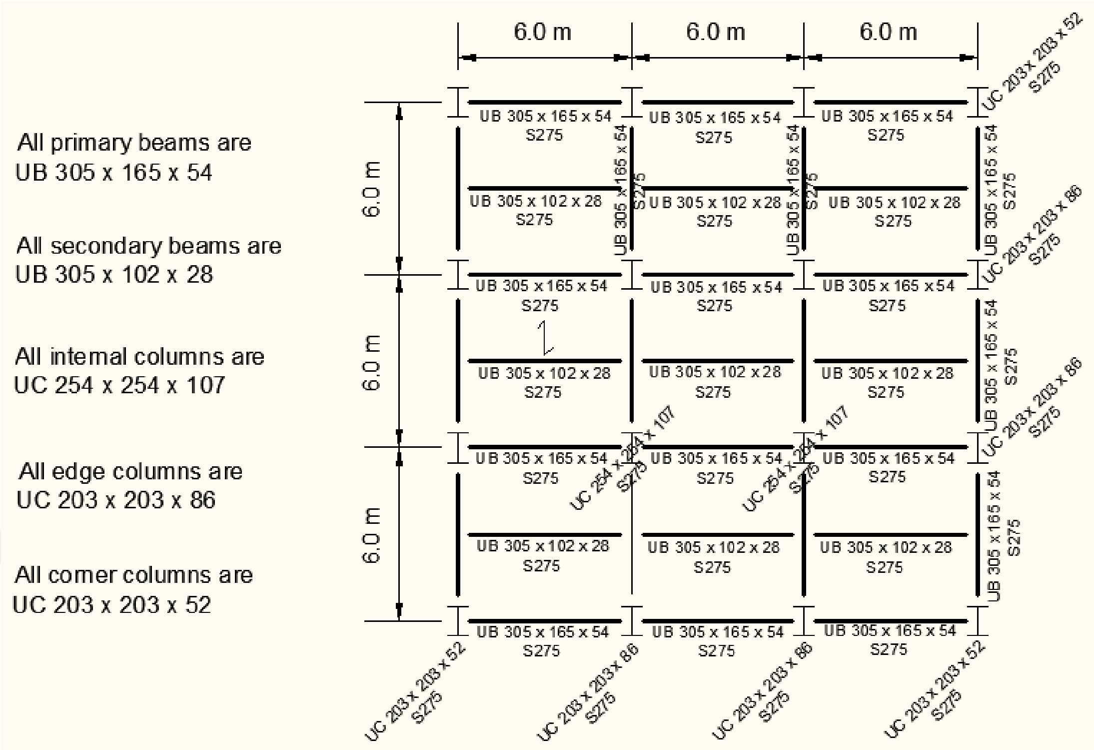


Figure B.3: Plan of real structure

## B.4 Plan of Small-Scaled Structure

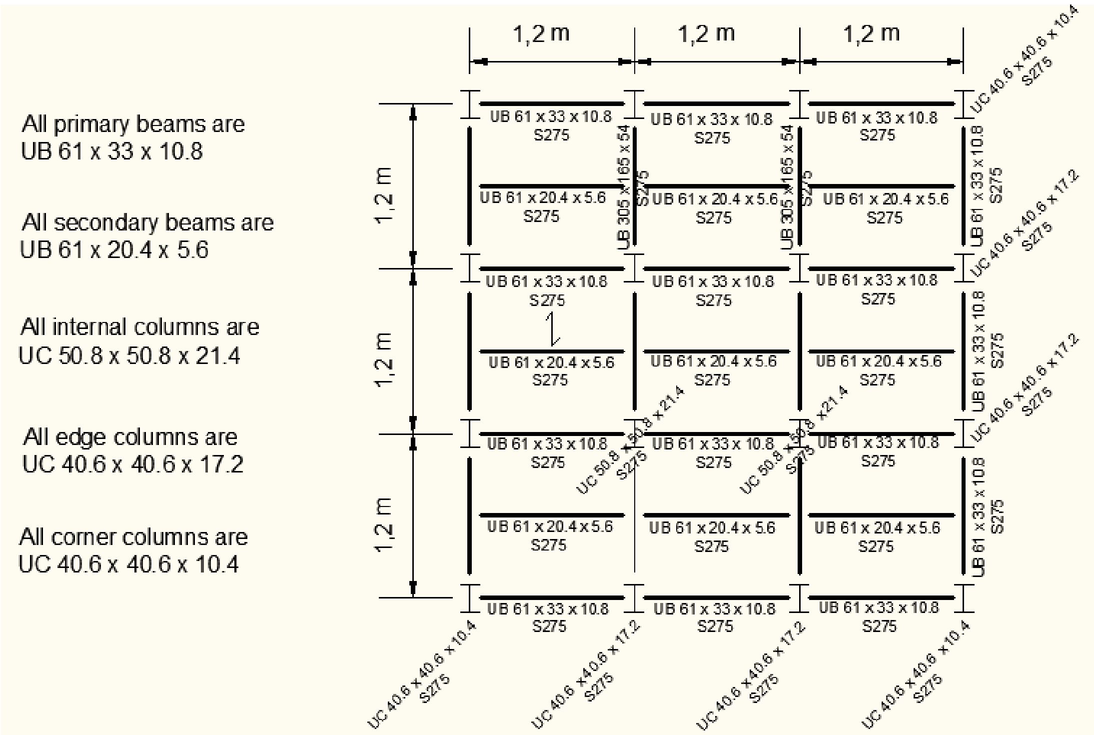


Figure B.4: Plan of reduced-scale structure

## B.5 Full-Scaled Composite Beam and Slab

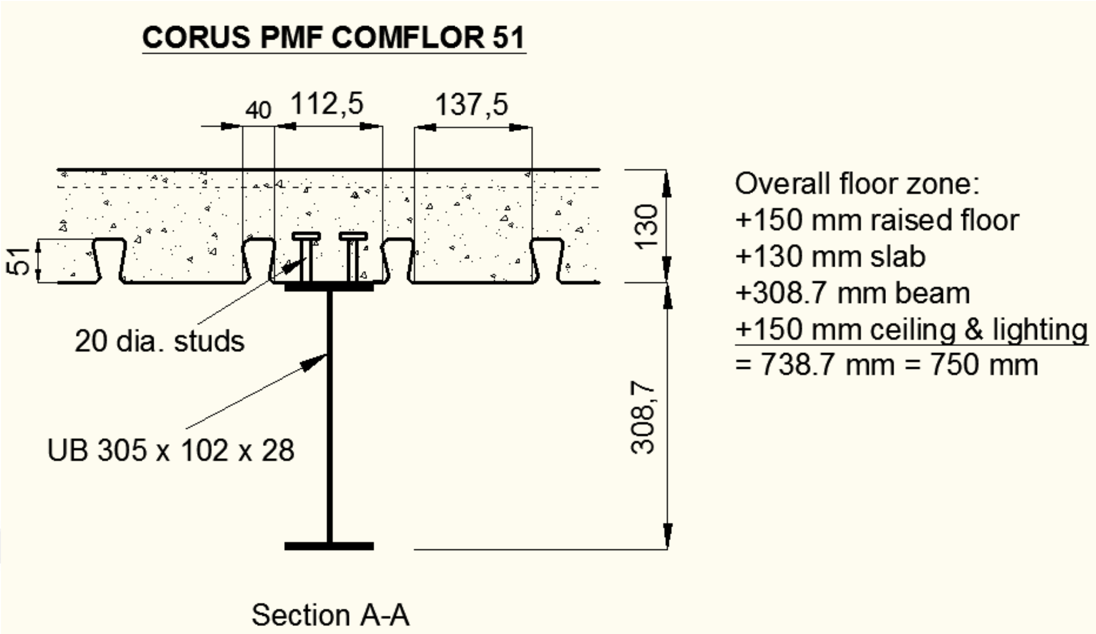


Figure B.5: Full-scaled composite beam and slab

## B.6 Small-Scaled Composite Beam and Slab

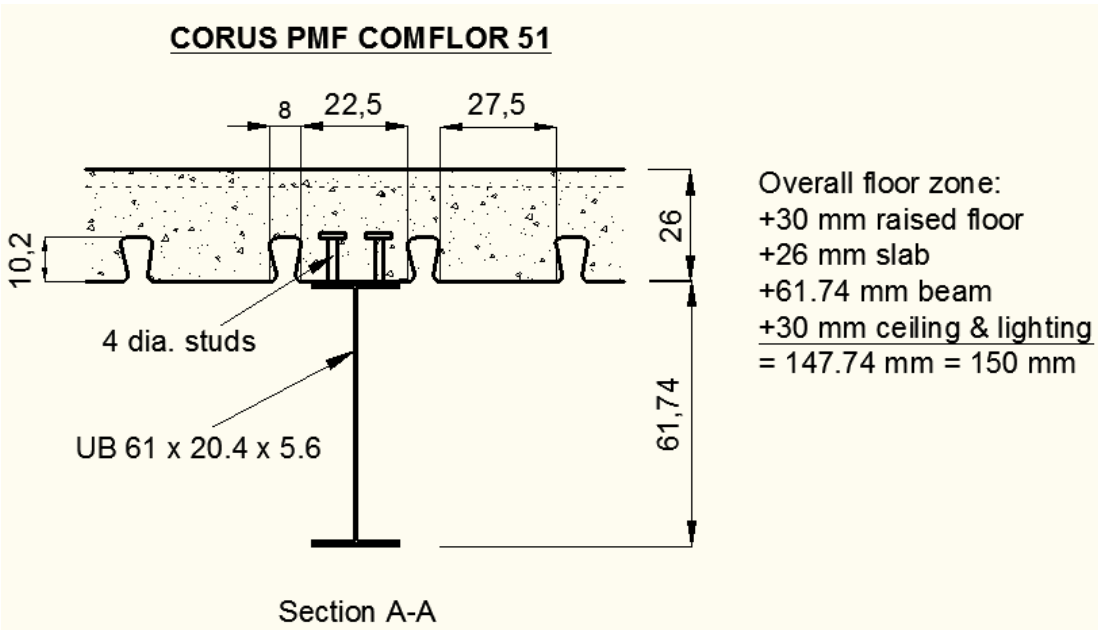


Figure B.6: Small-scaled composite beam and slab